Impurity-induced states in conventional and unconventional superconductors

A. V. Balatsky*

Theoretical Division, Los Alamos National Laboratory, Los Alamos, New Mexico 87545, USA

I. Vekhter†

Department of Physics and Astronomy, Louisiana State University, Baton Rouge, Louisiana 70803, USA

Jian-Xin Zhu‡

Theoretical Division, Los Alamos National Laboratory, Los Alamos, New Mexico 87545, USA

(Published 9 May 2006)

This review presents recent developments in the understanding of how impurities influence the electronic states in the bulk properties of superconductors. The focus is on quasilocalized states in the vicinity of impurity sites in conventional and unconventional superconductors and the goal is to provide a unified framework for their description. The nonmagnetic impurity resonances in unconventional superconductors are directly related to the Yu-Shiba-Rusinov states around magnetic impurities in conventional *s*-wave systems. The physics behind these states, including the quantum phase transition between screened and unscreened impurities, are reviewed and recent work on *d*-wave superconductors is emphasized. The bound states are seen in scanning-tunneling spectroscopy measurements on high-T_c cuprates, which are described in detail. This paper discusses very recent progress in our understanding of states coupled to impurity sites, which have their own dynamics. Also reviewed are inelastic electron-tunneling spectroscopy features that could be seen by scanning-tunneling microscopy in real space and their Fourier-transformed images and impurity resonances in the presence of an order competing with superconductivity. The last part of the review is devoted to the influence of local deviations of the impurity concentration from its average value on the density of states in *s*-wave superconductors. Discussed is how these fluctuations affect the density of states and it is shown that *s*-wave superconductors are, strictly speaking, gapless in the presence of an arbitrarily small concentration of magnetic impurities.

DOI: 10.1103/RevModPhys.78.373 PACS number(s): 73.20.Hb, 74.25.−q, 74.20.−z, 74.70.−b

CONTENTS

*Electronic address: avb@lanl.gov, http://theory.lanl.gov
†Electronic address: vekhter@phys.lsu.edu
‡Electronic address: jxzhu@lanl.gov

I. INTRODUCTION

A. Aim and scope

Real materials are not pure. Often, excessive impurities hinder observations of beautiful physics that exists in cleaner systems. For example, magnetic disorder destroys the coherence of the superconducting state. At the very least, in conventional metals impurities lead to higher resistivity. It is therefore very tempting to treat impurities as unfortunate obstacles to understanding the true underlying physics of the systems under consideration, to strive to make cleaner and better materials, and to ignore imperfections whenever possible.

Yet sometimes impurities lead directly to desired physical properties. They are crucial in achieving the functionality of doped semiconductors. Undoped semiconductors are just band insulators and not useful for applications in electronics. The entire multibillion-dollar semiconducting electronics industry is based on the precise control and manipulation of electronic states due to dopant (impurity) states.

Consequently, sensitivity of a physical system to disorder can be a blessing in disguise. It can lead not only to achieving new applications but also to uncovering the nature of exotic ground states, elucidating details of electronic correlations, and producing electronic states that are impossible in the bulk of a clean system. Until recently, this idea has not been emphasized in the study of correlated electron systems, but now more efforts are focused on understanding changes produced by disorder in a wide variety of strongly interacting electronic matter. One of the most promising directions is the study of disorder near quantum critical points, where several types of ordering compete and exist in a delicate balance that impurities have the power to tip in favor of one of the orders (Millis, 2003).

This is a review of the impurity effects on the electronic states in superconductors. The main purpose of our article is to give the reader an appreciation of recent developments, review the current understanding, and outline further questions on how impurities affect conventional, and especially unconventional, superconductors. Superconductors present probably the first example of a nontrivial many-electron system in which the consequences of disorder on the electronic states were studied experimentally and theoretically, and this review focuses on these effects.

The main classical results on impurity effects in superconductors, such as the Abrikosov-Gor'kov theory of pair breaking by magnetic impurities (Abrikosov and Gorkov, 1960) and the Anderson theorem (Anderson, 1959), are well covered in textbooks and reviews (Abrikosov *et al.*, 1963; Schrieffer, 1964; Fetter and Walecka, 1971; de Genmes, 1989; Annett, 1990; Sigrist and Ueda, 1991; Tinkham, 1996). The need to review the subject arises since (a) there are many new results, (b) the analyses of the classical papers have been substantially modified in applications to novel materials, and (c) the emphasis of the study of the impurity effects has shifted from macroscopic to atomic length scales.

From the early days, impurity doping was one of the most important tools for identifying the nature of the pairing state and microscopic properties. A classical experimental study of the role of magnetic impurities in conventional superconductors was carried out by Woolf and Reif (1965) and followed by many detailed investigations; see e.g., Edelstein (1967), Dumoulin *et al.* (1975, 1977), Bauriedl *et al.* (1981).

In the past two decades we have witnessed a tremendous growth in the number of novel superconductors.

Many of them belong to the general class of strongly correlated electron systems, and as a result of the Coulomb interaction the superconductivity is unconventional. Both magnetic and nonmagnetic impurities are pair breakers in unconventional superconductors, and often impurity suppression of superconductivity is an early hint of the unconventional pairing state. For example, rapid suppression of the transition temperature T_c in Al-doped $SrRuO_4$ was the first indication that it is a p-wave superconductor (Mackenzie *et al.*, 1998; Mackenzie and Maeno, 2003). The study of the effect of impurities on unconventional superconductors is still a developing field, yet it is mature enough to warrant an overview.

Sometimes a superconducting state emerges from competition between different phases, such as magnetically ordered and paramagnetic phases in high-temperature cuprates, organic materials, and heavy-fermion systems. Experimentally, superconductivity is often strongest when two competing states are nearly degenerate, near quantum critical points, as in Ce-based "115" heavy-fermion materials (Sidorov *et al.*, 2002) and UGe_2 (Saxena *et al.*, 2000). The study of impurity effects allows us (at least, in principle) to characterize the superconducting state and uncover competing electronic correlations.

The same reasoning has driven the study of impurity effects in high-T_c superconductors. Despite much progress, at present there is no complete microscopic description and certainly no consensus on the mechanism of superconductivity. The study of impurity-induced states has the potential to reveal the nature and origin of the superconducting state. Much of the recent experimental work has focused on high-T_c systems, and our comparison of theory and experiment inevitably emphasizes these materials. Nonetheless, this is emphatically not a comprehensive review of impurity effects in the cuprates. Their main properties are described in many excellent reviews, including those on scanning-tunneling microscopy (STM) (Fischer *et al.*, 2005), on angle-resolved photoemission spectroscopy (ARPES) (Damascelli *et al.*, 2003; Campuzano *et al.*, 2004), and on the pseudogap state (Timusk and Statt, 1999), to which we refer interested readers.

The new states and structures that appear due to disorder are often confined to microscopic or mesoscopic length scales. They would remain in the realm of academic discussion were it not for the development of new techniques and probes of disorder. At the time of the classical work, experimental interest was solely on macroscopic properties of materials: transition temperature T_c, specific heat, and the average density of states (DOS) (deduced from measuring the tunneling conductance of planar junctions). These were the experimentally measured quantities. With the perfection of more local probes such as nuclear magnetic resonance (NMR), and especially with the development of scanning-tunneling microscopy and spectroscopy (STM/STS), it became possible to experimentally determine the structures on atomic scales around impurity sites. Therefore the emphasis of theoretical work also shifted to the study of local properties. It is thus timely and useful to review new results and ideas about impurity-generated states in superconductors.

We had to be selective about the topics covered in this article. In the spirit of examining new approaches, our review primarily discusses the physics of the single-impurity bound or quasibound states at atomic scales and local electronic effects in the vicinity of defects. We also discuss mesoscopic effects and impurity effects in the presence of orders competing with superconductivity. The latter idea is applied to the pseudogap state of high-T_c materials.

We have restricted ourselves to the study of the density of states. A comprehensive review of the effects that have been studied experimentally and discussed theoretically is a much more difficult task that would take substantially more space. We do not analyze the behavior of transport coefficients. While this is a subject of intense current interest and many important results have been obtained, it is beyond the scope of this article.

To keep this review useful for people entering the field, we start with the Bardeen-Cooper-Schrieffer (BCS) model for superconductivity and use a modified version of this model throughout. In doing so, we neglect corrections due to strong coupling; in the known case of electron-phonon interactions these are quantitative rather than qualitative (Schachinger *et al.*, 1980; Schachinger, 1982; Schachinger and Carbotte, 1984; Carbotte, 1990). In many unconventional materials, such as cuprates, the dynamical glue in the self-consistent theory is not known. Yet most people agree that the superconducting state of cuprates is not very anomalous and has a d-wave symmetry superconducting gap. We take the view that in cuprates and other compounds at low energies, for the purposes of this review, superconductivity is adequately described by the BCS theory with an anisotropic gap.

B. Unconventional superconductivity

Examples of exotic superconductors discovered in the last two decades include high-T_c superconductors, heavy-fermion and organic superconductors, and $SrRuO_4$. A common feature of all is that the superconductivity is unconventional, i.e., the pairing symmetry is non-s-wave (in contrast to conventional materials, such as lead).

A superconducting order parameter describes the pairing of fermions with time-reversed momenta, $\mathbf{k}$ and $-\mathbf{k}$,

$$\Psi(\mathbf{k})_{\alpha,\beta} = \langle \psi_{\mathbf{k},\alpha}\psi_{-\mathbf{k},\beta}\rangle, \tag{1.1}$$

where α,β are the spin indices. If the order parameter transforms according to a nontrivial representation of the point group of the crystal, the superconductor is called unconventional. If it transforms according to a trivial representation of the group, it is a labeled s wave. We distinguish between the spin-singlet pairing (total

spin of the pair $S=0$), for which $\Psi(\mathbf{k})_{\alpha,\beta}=\Psi(\mathbf{k})(i\sigma_{y,\alpha\beta})$, where σ_y is the Pauli matrix in spin space, and the spin-triplet state ($S=1$), when $\Psi_{\alpha\beta}$ is a symmetric spinor in α,β. Since the order parameter has to be antisymmetric under permutation of the fermion operators in Eq. (1.1), the spatial part of $\Psi(\mathbf{k})_{\alpha,\beta}$ is even for spin-singlet superconductors and odd in the spin-triplet case. Expanding in eigenfunctions of orbital momentum, it follows that spin-singlet pairing corresponds to an even orbital function of momentum $\mathbf{k}$ and hence we call it an *s*-wave (for $l=0$), *d*-wave (for $l=2$), etc., superconductor in analogy with the notation for the atomic states. For a spin-triplet superconductor, the orbital part is an odd function of $\mathbf{k}$, and hence the spin-triplet superconductor can be *p* wave ($l=1$), *f* wave ($l=3$), etc. More rigorously, pairing states are characterized by the irreducible representation of the crystal lattice symmetry group, including the spin-orbit interaction (Volovik and Gor'kov, 1984; Blount, 1985; Sigrist and Ueda, 1991). Characterization in terms of orbital moment is an oversimplification, and we use this terminology with an understanding that the correct symmetries are implied for a given crystal structure. This classification is given for BCS-like or *even-frequency* superconductors. The classification is opposite for *odd-frequency* pairing, in which the spin-singlet state has odd parity because the pairing wave function is an odd function of time (Berezinskii, 1974; Balatsky and Abrahams 1992). We consider here only even-frequency superconductors.

We restrict ourselves to the most common examples of the unconventional pairing state, for which the order parameter averaged over the Fermi surface vanishes,

$$\sum_{\mathbf{k}} \Psi(\mathbf{k})_{\alpha\beta} = 0. \tag{1.2}$$

Hence superconductors with constant or nearly constant order parameter on the Fermi surface are *s* wave, while *p*-, *d*-, or higher-wave states, where Eq. (1.2) holds, are signatures of an unconventional superconductor. There are several excellent recent reviews that address the unconventional nature of superconducting pairing states in specific compounds, such as *p*-wave superconductivity in $SrRuO_4$ (Mackenzie and Maeno, 2003) and the *d*-wave state in high-T_c materials (Annett, 1990; Harlingen, 1995; Tsuei and Kirtley, 2000).

C. Outline

We start with a general overview of BCS-like superconductivity. To review effects of impurities, we discuss the properties of superconductors in general. In cuprates, as well as in some heavy-fermion systems and other novel superconductors, there is some evidence for the existence of an order competing with superconductivity on all or parts of the Fermi surface. The exact nature of the competing order parameter is only conjectured. A general feature of all such models is the enhancement of the competing order once superconductivity is destroyed, for example, in the vicinity of a scattering center. It has been suggested that the reaction of the system to the introduction of impurities can be an important test of the order, or even growing correlations towards such an order, in the superconducting state.

TABLE I. Effects of potential and magnetic impurity scattering on the *s*-, *p*-, and *d*-wave superconductors are shown qualitatively. "+" indicates that impurity scattering is a pair breaker and "−" indicates that impurity scattering is not a pair breaker. There is a qualitative difference between the potential scattering in *s*-wave superconductors and any other case. Potential scattering impurities are not pair breakers in the *s*-wave case due to the Anderson theorem. This is an exceptional case. For any other case impurity scattering, magnetic or nonmagnetic, suppresses superconductivity, although the details are model dependent. At high enough concentrations both magnetic and nonmagnetic impurities will suppress superconductivity regardless of symmetry.

	s wave	*p* wave	*d* wave
Potential scattering	−	+	+
Magnetic scattering	+	+	+

The prerequisite for such a test is the detailed understanding of the behavior of "simple" superconductors with impurities. Work aimed at developing this understanding spans a period of more than 40 years, and some of the very recent results continue to be fresh and unexpected. Therefore we devote a large fraction of this review to a discussion of the properties of superconductors with impurities in the absence of any competing order. In this case, from a theoretical standpoint, before discussing impurity effects we need to agree upon methods to describe the very phenomenon that makes the impurity effects so interesting: superconductivity. Even in the most exotic compounds investigated so far, the superconducting state itself is not anomalous in that it results from the pairing of fermionic quasiparticles, and these Cooper pairs may be broken by interaction with impurities or external fields.

Impurity effects in conventional superconductors were the subject of early studies by Anderson, who provided the Anderson theorem (Anderson, 1959) and by Abrikosov and Gor'kov (1960). This pioneering work laid the foundation for our understanding of impurity effects in conventional and unconventional superconductors, described in terms of electron lifetime due to scattering on an ensemble of impurities. Abrikosov and Gor'kov predicted the existence of gapless superconductivity that was subsequently observed in experiments (Woolf and Reif, 1965). A brief summary of the Abrikosov-Gor'kov (AG) theory and its extension to non-*s*-wave superconductivity is given in Table I, where the effect of impurities on the superconducting state on average or globally is listed.

After intense interest in early BCS theory, the subject was considered closed in the mid 1960s, with most experimentally relevant problems solved. Recently, however, there has been a revival of interest in the studies of "traditional" low-temperature *s*-wave superconductors

with magnetic and nonmagnetic impurities, with many new theoretical and experimental results changing our perspective on this classical problem.

A special place in this review is devoted to the study of impurity-induced local bound states or resonances. This is an old subject, going back to the 1960s when bound states near magnetic impurities in *s*-wave superconductors were predicted in the pioneering works of Yu (1965), Shiba (1968), and Rusinov (1969). They considered pair breaking by a single magnetic impurity in a superconductor and found that there are quasiparticle states inside the energy gap that are localized in the vicinity of the impurity atom. The corresponding gap suppression occurs locally and the concept of lifetime broadening is inapplicable. In general, in this situation it is more useful to focus on local quantities, such as local density of states (LDOS), local gap, etc., rather than on average impurity effects (which vanish for the single impurity in the thermodynamic limit). Yet it is clear that this local physics at some finite concentration of impurities suppresses superconductivity completely. This connection was discussed by Yu (1965), Shiba (1968), and Rusinov (1969). In particular, the formation of an intragap bound state and impurity bands due to magnetic impurities leads to filling of the superconducting gap and therefore connects to the Abrikosov-Gor'kov theory (Abrikosov and Gorkov, 1960).

At that time, there were no experimental techniques for directly observing single-impurity states. As a result, the entire subject was largely forgotten until STM was used by Yazdani *et al.* (1997) to study impurity states. This reinvigorated the field and led to a firm shift in interest from global to local properties. Soon afterwards, STM was used to observe local impurity states near vacancies and impurities in high-T_c cuprates (Hudson *et al.* 1999, 2001; Yazdani *et al.*, 1999; Pan, Hudson, Lang *et al.*, 2000). These discoveries led to a new field of research in which impurities opened a window into the electronic properties of exotic materials with atomic spatial resolution. As a first test of theories, this allowed a direct comparison of local electronic features in tunneling characteristics with the theoretical predictions for the density of states.

We start by briefly reviewing the BCS theory in Sec. II. Our main goal is to review three approaches used to analyze impurity effects: direct diagonalization of the Hamiltonian via the Bogoliubov-Valatin transformation, the variational wave function of the original BCS paper, and the Green's-function method which is well suited to the analysis of multiple impurity problems. Then we define different types of impurity scattering in Sec. III. We pay special attention to distinguishing between magnetic and nonmagnetic impurities and differentiating between static and dynamic scatterers. The basic features of nonmagnetic scattering in *s*-wave superconductors are outlined in Sec. IV.

To keep the review readable by graduate students and researchers entering the field, we begin the discussion of localized states by considering an example of an impurity bound state in a two-dimensional (2D) metal in Sec. V. Then we discuss the low-energy bound state in *s*- and *d*-wave superconductors in Secs. VI and VII, respectively. We briefly touch upon the possible existence of impurity resonances in different models of the pseudogap state of the cuprates in Sec. VIII. Recent STM measurements on both conventional and unconventional superconductors are discussed in Sec. IX. Changes in the ground state of a superconductor containing a classical spin as a function of the coupling strength between the spin and conduction electrons are discussed in Sec. X.

We proceed by considering situations when impurities have their own dynamics, so that their effect on electrons is more complicated, see Secs. XI and XII, and in Sec. XII.C we also study the combined influence of collective modes and impurities. The final two parts of our review are devoted to a discussion of the effects of impurities on the mesoscopic and macroscopic scale. For completeness, in Sec. XIII we briefly review the basic ideas of computing the average density of states for a macroscopic sample. Due to a lack of space, we cannot do justice to this rich subject and use it instead to discuss new results of the impurity effect on scales that are small compared to the sample size, but large relative to the superconducting coherence length. In that situation, there are dramatic consequences of local impurity realizations that may be different from the average, and we give an overview of the results for the density of states in Sec. XIV. We conclude with a summary in Sec. XV.

D. Other related work

In focusing largely on the properties of impurities on atomic or mesoscopic scales, we cannot give due attention, within the confines of this review, to several other questions that have been important in the studies of impurities. One of these is how exactly does the impurity band grow out of bound states on individual impurity sites, i.e., what is the effect of interference between such sites in real space? We briefly review some of the recent work in Sec. XIII but do not discuss the subject in depth, listing some recent work that addresses the issue.

The usual finite-lifetime diagrammatic approach, neglecting multiple impurity scattering (Gorkov and Kalugin, 1985; Ueda and Rice, 1985; Hirschfeld *et al.*, 1986; Schmitt-Rink *et al.*, 1986), yields a constant density of states at the Fermi level in a nodal superconductor with impurities. In three-dimensional systems, neglected contributions are smaller by either a factor $(k_F l)^{-1} \ll 1$, where k_F is the Fermi wave vector and l is the mean free path, or by an additional power of impurity concentration, $n_{\mathrm{imp}} \ll 1$. In two dimensions, and for *d*-wave superconductors, neglected diagrams contain a low-energy singularity, and therefore some of them contribute to the density of states at leading order (Nersesyan *et al.*, 1995). The result of Nersesyan *et al.* spawned a number of attempts to solve the problem of many impurities in a two-dimensional (2D) *d*-wave superconductor nonperturbatively. Some of the approaches and results are reviewed (from different standpoints) by Altland *et al.*

(2002) and Hirschfeld and Atkinson (2002).

Many of these nonperturbative solutions gave conflicting results for the residual density of states, including finite (Ziegler, 1996; Ziegler *et al.*, 1996), infinite (Pepin and Lee, 1998, 2001), and vanishing with different power laws in energy (Nersesyan *et al.*, 1995; Nersesyan and Tsvelik, 1997; Senthil and Fisher, 1999); see also Bhaseen *et al.* (2001). Further study demonstrated that different results are due to subtle differences in the symmetry of the model used (Altland and Zirnbauer, 1997; Altland *et al.*, 2000) and can be partly understood by analyzing the diffusion or Cooperon mode of near-nodal quasiparticles (Yashenkin *et al.*, 2001), in analogy to dirty metals (Altshuler, 1985; Lee and Ramakrishnan, 1985). Detailed self-consistent numerical studies confirm that the behavior of the DOS depends on the details of the impurity scattering and electronic structure (Atkinson *et al.*, 2000; Zhu, Sheng, and Ting, 2000). In particular, the divergence only occurs in perfectly particle-hole symmetric systems, and generically Atkinson *et al.* (2000) found that there is a nonuniversal suppression of the DOS over a small energy scale close to the Fermi level. Chamon and Mudry (2001) conjectured that the residual DOS always diverges when the single-impurity resonance is tuned to the Fermi level. This divergence was not found in numerical simulations of a model with large but finite on-site potential (Hirschfeld and Atkinson, 2002).

The interference between many impurities has been recently investigated (Zhu, Ting, and Hu, 2000, Zhu *et al.*, 2003; Zhu, Atkinson, and Hirschfield, 2004; Morr and Stavropoulos, 2002, 2003a; Atkinson *et al.*, 2003) with an eye on the importance of these effects for the interpretation of the features in the STM data on high-T_c cuprates collected over a large area of the sample. The interference is also responsible for the formation of impurity bands and therefore is crucial for determining transport properties, which we do not address in this review. Within the framework of the T-matrix approximation, transport properties of unconventional superconductors in general (Pethick and Pines 1986; Schmitt-Rink *et al.*, 1986; Arfi *et al.*, 1988; Hirschfeld *et al.*, 1986, 1988, 1989; Graf *et al.*, 1996) and high-T_c cuprates in particular (Hirschfeld and Goldenfeld, 1993; Hirschfeld *et al.*, 1994, 1997; Quinlan *et al.*, 1994, 1996; Graf *et al.*, 1995; Duffy *et al.*, 2001) have been extensively discussed. Experiments on microwave, optical, and thermal conductivity are used to extract properties of impurity scattering.[1]

The question of localization in both s wave (Ma and Lee, 1985) and d-wave superconductors (Lee, 1993; Senthil *et al.*, 1998; Senthil and Fisher, 2000; Vishveshwara *et al.*, 2000; Yashenkin *et al.*, 2001; Atkinson and Hirschfeld, 2002) continues to be investigated. Some of these results have been summarized in recent reviews on high-T_c systems (Timusk and Statt, 1999). We also do not touch upon the rich phenomena related to surfaces playing the role of extended impurities that can also lead to the formation of bound states (Buchholtz and Zwichnagl, 1981; Blonder *et al.*, 1982; Hu, 1994; Covington *et al.*, 1997; Fogelström *et al.*, 1997; Aprill *et al.*, 1998; Kashiwaya and Tanaka, 2000).

Now there are also a few reviews available on the subject of impurity states. Joynt (1997) reviewed early work on impurity states within the T-matrix theory focusing on anomalous transport due to the finite lifetime of quasibound states around impurities. Byers, Flatte, and Scalapino were among the pioneers of the detailed electronic structure studies of the resonance state and interference patterns (Byers *et al.*, 1993; Flatté and Byers, 1997a, 1997b; Flatte and Yers, 1998) and reviewed their and related work (Flatté and Byers, 1999). An excellent review of thermal and transport properties of low-energy quasiparticles in nodal superconductors was recently given by Hussey (2002).

The subject is so rich and well developed that it does not seem possible to do justice to both local quasiparticle properties around a single-impurity site and questions of interference and transport within the confines of a single paper. Therefore, in the following we focus primarily on the effect of impurities on the local density of states, rather than transport properties, and leave the discussion of nontrivial effects of interference effects in low dimensions to future reviewers.

II. A BCS THEORY PRIMER

We begin by reviewing the BCS theory. This section briefly summarizes results pertinent to our discussion; many textbooks provide an in-depth view of the theory (Schrieffer, 1964; de Gennes, 1989; Tinkham, 1996; Ketterson and Song, 1999). Consider a general Hamiltonian $\mathcal{H}_{\rm BCS}=\hat{H}_0(\mathbf{r})+H_{\rm int}$, where

$$\hat{H}_0(\mathbf{r})=\sum_\alpha \int d^dr\psi_\alpha^\dagger(\mathbf{r})[\epsilon(-i\nabla_{\mathbf{r}})-\mu]\psi_\alpha(\mathbf{r}) \tag{2.1}$$

is the band Hamiltonian of quasiparticles with dispersion $\epsilon(\mathbf{k})$, μ is the chemical potential, and the interaction part is given by

$$H_{\rm int}=-\frac{1}{2}\sum_{\substack{\alpha,\beta\\ \gamma,\delta}} \int d^dr d^dr' \psi_\alpha^\dagger(\mathbf{r})\psi_\beta^\dagger(\mathbf{r}')V_{\alpha\beta\gamma\delta}(\mathbf{r},\mathbf{r}') \times\psi_\gamma(\mathbf{r}')\psi_\delta(\mathbf{r}). \tag{2.2}$$

Here $\mathbf{r}$ is the real-space coordinate, α and β are spin indices, and $\psi^\dagger$ and ψ are fermionic creation and annihilation operators, respectively. The mean-field approximation consists of decoupling the four-fermion interaction into a sum of all possible bilinear terms, so that

[1]See Timusk and Statt (1999) for a review. For very recent results in experiment, see Hosseini *et al.*, 1999; Carr *et al.*, 2000; Chiao *et al.*, 2000; Corson *et al.*, 2000; Segre *et al.*, 2002; Tu *et al.*, 2002; Turner *et al.*, 2003; Hill *et al.*, 2004; Lee *et al.*, 2004 and in theory, see Hettler and Hirschfeld, 1999; Berlinsky *et al.*, 2000; Chubukov *et al.*, 2003; Nicol and Carbotte, 2003; Howell *et al.*, 2004.

$$H_{\rm int} = \sum_{\alpha,\beta} \int d^d r d^d r' \{ \tilde{V}_{\alpha\beta}(\mathbf{r},\mathbf{r}') \psi^\dagger_\alpha(\mathbf{r}) \psi_\beta(\mathbf{r}') + \Delta_{\alpha\beta}(\mathbf{r},\mathbf{r}') \psi^\dagger_\alpha(\mathbf{r}) \psi^\dagger_\beta(\mathbf{r}') + \Delta^\star_{\alpha\beta}(\mathbf{r},\mathbf{r}') \psi_\beta(\mathbf{r}) \psi_\alpha(\mathbf{r}') \}. \tag{2.3}$$

The effective potential $\tilde{V}_{\alpha\beta}(\mathbf{r},\mathbf{r}')$ is the sum of the Hartree and Fock (exchange) terms, and the last two terms account for superconducting pairing. The pairing field Δ is determined self-consistently from

$$\Delta_{\alpha\beta}(\mathbf{r},\mathbf{r}') = -\frac{1}{2} \sum_{\gamma,\delta} V_{\alpha\beta\gamma\delta}(\mathbf{r},\mathbf{r}') \langle \psi_\gamma(\mathbf{r}') \psi_\delta(\mathbf{r}) \rangle. \tag{2.4}$$

The pairing occurs only for positive $V_{\alpha\beta\gamma\delta}$ and only below the transition temperature T_c; above T_c, $\Delta_{\alpha\beta}=0$. In contrast, Hartree and Fock terms are finite at all temperatures and can be incorporated into the quasiparticle dispersion $\epsilon(\mathbf{k})$. These terms do change upon entering the superconducting state, but their relative change is on the order of a fraction of electrons participating in superconductivity and therefore is small for weak-coupling superconductors ($\sim \Delta/W \ll 1$, where W is the electron bandwidth). Therefore, the effective potential $\tilde{V}$ is not explicitly included in the following discussion except where specified.

We consider a reduced mean-field BCS Hamiltonian,

$$\mathcal{H}_{\rm BCS} = \sum_\alpha \int d^d r \psi^\dagger_\alpha(\mathbf{r}) \hat{H}_0(\mathbf{r}) \psi_\alpha(\mathbf{r}) + \sum_{\alpha,\beta} \int d^d r d^d r' \{ \Delta_{\alpha\beta}(\mathbf{r},\mathbf{r}') \psi^\dagger_\alpha(\mathbf{r}) \psi^\dagger_\beta(\mathbf{r}') + \text{H.c.} \}. \tag{2.5}$$

The spatial and spin structure of $\Delta_{\alpha\beta}(\mathbf{r},\mathbf{r}')$ determines the type of superconducting pairing. In most of this review, we consider singlet pairing, $\Delta_{\alpha\beta}(\mathbf{r},\mathbf{r}') = (i\sigma_y)_{\alpha\beta} \Delta(\mathbf{r},\mathbf{r}')$, where Δ is a scalar function; see Sec. I.B.

In a uniform superconductor, the interaction depends only on the relative position of electrons, so that $V(\mathbf{r},\mathbf{r}')=V(\boldsymbol{\rho})$ with $\boldsymbol{\rho} \equiv \mathbf{r}-\mathbf{r}'$. Therefore in the absence of impurities, the structure of the order parameter in real space depends on the symmetry properties of $V(\boldsymbol{\rho})$. These are easier to consider in momentum rather than coordinate space. In models with local attraction, when $V(\boldsymbol{\rho})=V_0\delta(\boldsymbol{\rho})$, the Fourier transform of the interaction is featureless, and $\Delta(\mathbf{k})=\Delta_0$—an example of an isotropic or *s*-wave superconductor.

In the remainder of this section, we give an overview of the main methods for solving the BCS Hamiltonian since similar methods are commonly applied to impurity effect studies in superconductors. The approaches that we consider are (a) direct diagonalization via the Bogoliubov-Valatin transformation, (b) variational determination of the ground-state energy from the trial wave function, and (c) the Green's-function formalism.

A. Bogoliubov transformation

Since the effective Hamiltonian of Eq. (2.5) is bilinear in fermion operators ψ and $\psi^\dagger$, it can be diagonalized by a canonical transformation of the form

$$\psi_\alpha(\mathbf{r}) = \sum_n [u_{n\alpha}(\mathbf{r}) \gamma_n - \alpha v^*_{n\alpha}(\mathbf{r}) \gamma^\dagger_n], \tag{2.6}$$

subject to the condition $|u_{n\alpha}(\mathbf{r})|^2 + |v_{n\alpha}(\mathbf{r})|^2 = 1$. The coefficients u and v are determined by solving the Bogoliubov–de Gennes equations (de Gennes, 1989),

$$E u_\alpha(\mathbf{r}) = H_0(\mathbf{r}) u_\alpha(\mathbf{r}) + \int d^d\mathbf{r}' \Delta_{\alpha\beta}(\mathbf{r},\mathbf{r}') v_\beta(\mathbf{r}'), \tag{2.7}$$

$$E v_\alpha(\mathbf{r}) = -H^\star_0(\mathbf{r}) v_\alpha(\mathbf{r}) + \int d^d\mathbf{r}' \Delta^\star_{\alpha\beta}(\mathbf{r},\mathbf{r}') u_\beta(\mathbf{r}'). \tag{2.8}$$

Here we have suppressed the label n for brevity. Clearly, when $\Delta=0$, the coefficients u and v do not couple and there is no particle-hole mixing.

For each n there are four functions, $u_\uparrow(\mathbf{r}), u_\downarrow(\mathbf{r}), v_\uparrow(\mathbf{r}), u_\downarrow(\mathbf{r})$, that need to be determined. However, for a singlet superconductor the matrix $\Delta_{\alpha\beta}$ is off-diagonal in the spin indices, so that $u_\uparrow$ ($u_\downarrow$) couples only to $v_\downarrow$ ($v_\uparrow$), and hence only two of the equations are coupled. In the presence of the general impurity potential, however, all four components are interdependent.

Equations (2.7) and (2.8) are coupled integro-differential equations for the functions $u_{n\alpha}(\mathbf{r})$ and $v_{n\alpha}(\mathbf{r})$. They have to be complemented by the self-consistency equations on $\Delta_{\alpha\beta}$, which can be obtained directly from Eq. (2.4),

$$\Delta_{\alpha\beta}(\mathbf{r},\mathbf{r}') = \frac{1}{2} V_{\alpha\beta\gamma\delta}(\mathbf{r},\mathbf{r}') \sum_n [\delta u_{n\gamma}(\mathbf{r}') v^\star_{n\delta}(\mathbf{r}) f(-E_n) + \gamma v^\star_{n\gamma}(\mathbf{r}') u_{n\delta}(\mathbf{r}) f(E_n)]. \tag{2.9}$$

Here the Fermi function is given by $f(E)=[\exp(E/T)+1]^{-1}$.

In a uniform superconductor, the Fourier transform of the Bogoliubov–de Gennes equations (2.7) and (2.8) into momentum space gives

$$(\xi_\mathbf{k} - E_\mathbf{k}) u_{\mathbf{k}\alpha} + \Delta_{\alpha\beta}(\mathbf{k}) v_{\mathbf{k}\beta} = 0, \tag{2.10}$$

$$(\xi_\mathbf{k} + E_\mathbf{k}) v_{\mathbf{k}\alpha} + \Delta^\star_{\alpha\beta}(-\mathbf{k}) u_{\mathbf{k}\beta} = 0, \tag{2.11}$$

where $\xi_\mathbf{k}$ is the bare quasiparticle energy measured with respect to the chemical potential $\xi_\mathbf{k}=\epsilon(\mathbf{k})-\mu$. In a singlet superconductor,

$$(\xi_\mathbf{k} - E_\mathbf{k}) u_{\mathbf{k}\uparrow} + \Delta(\mathbf{k}) v_{\mathbf{k}\downarrow} = 0, \tag{2.12}$$

$$(\xi_\mathbf{k} + E_\mathbf{k}) v_{\mathbf{k}\downarrow} + \Delta^\star(\mathbf{k}) u_{\mathbf{k}\uparrow} = 0, \tag{2.13}$$

and we recover the familiar energy spectrum $E_\mathbf{k} = \sqrt{\xi^2_\mathbf{k} + |\Delta(\mathbf{k})|^2}$, with the coefficients u and v given by

$$\begin{pmatrix} u^2_\mathbf{k} \\ v^2_\mathbf{k} \end{pmatrix} = \frac{1}{2} \left[1 \pm \frac{\xi_\mathbf{k}}{E_\mathbf{k}} \right]. \tag{2.14}$$

B. BCS variational wave function

Superconductivity originates from the instability of the Fermi sea towards the pairing of time-reversed quasiparticle states. The variational wave-function approach, originating with the BCS paper, is to restrict the trial wave function to the subspace of either empty or doubly occupied states,

$$|\Psi_{\mathrm{BCS}}(\mathbf{r})\rangle = \prod_n (a_n + b_n c_{n\uparrow}^\dagger c_{\bar{n}\downarrow}^\dagger)|0\rangle, \tag{2.15}$$

and to minimize the energy, $E_{\mathrm{BCS}}=\langle\Psi|H|\Psi\rangle$. This is an excellent approximation at low temperatures. In Eq. (2.15), the vacuum state $|0\rangle$ denotes the filled Fermi sea, and $c_{n\uparrow}^\dagger$ creates a quasiparticle with spin up, $c_{\bar{n}\downarrow}^\dagger$ creates a quasiparticle with spin down, and with the wave function $\phi_n(\mathbf{r})$ $[\phi_n^*(\mathbf{r})]$ that is the eigenfunction of the single-particle Hamiltonian. Normalization requires that $|a_n|^2+|b_n|^2=1$.

In the absence of impurities, the eigenfunctions ϕ_n can be labeled by the same indices, $\mathbf{k}$ and α, as in the previous section. Consequently, the variational approach is equivalent to the Bogoliubov analysis with the choice $u_n(\mathbf{r})=a_n\phi_n(\mathbf{r})$ and $v_n(\mathbf{r})=b_n\phi_n(\mathbf{r})$. In general, however, an interaction with impurities may lead to the appearance of single-particle states in the ground-state wave function; see Sec. X. It is worth reminding that the energy of the BCS state is greater than or equal to that of the exact ground state.

C. Green's functions

The third approach used is the Green's-function method, which originates with the work of Gor'kov. Following Nambu, we introduce a four-component vector that is a spinor representation of particle and hole states,

$$\Psi^\dagger(\mathbf{r}) = (\psi_\uparrow^\dagger, \psi_\downarrow^\dagger, \psi_\uparrow, \psi_\downarrow). \tag{2.16}$$

The matrix Green's function is defined as the ordered average (a hat denotes a matrix in Nambu space)

$$\hat{G}(x,x') = -\langle T_\tau \Psi(x)\Psi^\dagger(x')\rangle, \tag{2.17}$$

where the four-component vector $x=(\mathbf{r},\tau)$ combines the real-space coordinate $\mathbf{r}$ and imaginary time τ. The time evolution of operators in the Heisenberg approach is given by $\partial\psi/\partial\tau=[\mathcal{H}_{\mathrm{BCS}},\psi]$.

For a singlet homogeneous superconductor, the Hamiltonian of Eq. (2.5) in Nambu notation takes the form

$$\mathcal{H}_{\mathrm{BCS}} = \int d\mathbf{r}\Psi^\dagger(\mathbf{r})[\xi(-i\nabla)\tau_3 + \Delta\tau_1\sigma_2]\Psi(\mathbf{r}), \tag{2.18}$$

and we find (Maki, 1969)

$$\hat{G}_0^{-1}(\mathbf{k},\omega) = i\omega_n - \xi(\mathbf{k})\tau_3 - \Delta(\mathbf{k})\sigma_2\tau_1. \tag{2.19}$$

Here $\omega_n=\pi T(2n+1)$ is the Matsubara frequency, σ_i are Pauli matrices acting in spin space, τ_i are Pauli matrices in particle-hole space, and $\tau_i\sigma_j$ denotes a direct product of matrices operating in four-dimensional Nambu space. The Fourier transform in τ is defined as

$$\hat{G}(\mathbf{k};\tau) = k_B T\sum_{\omega_n} \hat{G}(\mathbf{k},\omega_n)e^{-i\omega_n\tau}. \tag{2.20}$$

The self-consistency equation for a single superconductor takes the form

$$\Delta(\mathbf{k}) = -\frac{T}{4}\sum_{\omega_n}\int d\mathbf{k}' V(\mathbf{k},\mathbf{k}')\mathrm{Tr}[\tau_1\sigma_2 G_0]. \tag{2.21}$$

In BCS, the interaction is restricted to a thin shell of electrons near the Fermi surface, and therefore

$$\Delta(\hat{\Omega}) = -\frac{T}{4}N_0\sum_{\omega_n}\int d\hat{\Omega}' V(\hat{\Omega},\hat{\Omega}')\mathrm{Tr}\left[\tau_1\sigma_2\int d\xi_{\mathbf{k}} G_0\right], \tag{2.22}$$

where $\hat{\Omega}$ denotes a direction on the Fermi surface and N_0 is the normal-state density of states.

The off-diagonal component $(\hat{G}_0)_{12}=F$ is often called the Gor'kov anomalous Green's function since it describes the pairing average

$$F_{\alpha\beta}(x,x') = -\langle T_\tau \psi_\alpha(x)\psi_\beta(x')\rangle. \tag{2.23}$$

In general $F_{\alpha\beta}(x,x')=g_{\alpha\beta}F(x,x')$, where the matrix g describes the spin structure of the superconducting order. For singlet pairing $g=i\sigma_y$, and in a spatially uniform superconductor,

$$G(\omega_n,\mathbf{k}) = \frac{i\omega_n + \xi_{\mathbf{k}}}{(i\omega_n)^2 - \xi_{\mathbf{k}}^2 - |\Delta(\mathbf{k})|^2}, \tag{2.24}$$

$$F(\omega_n,\mathbf{k}) = \frac{\Delta(\mathbf{k})}{(i\omega_n)^2 - \xi_{\mathbf{k}}^2 - |\Delta(\mathbf{k})|^2}. \tag{2.25}$$

The connection with Bogoliubov's transformation is obtained by rewriting the Green's functions as

$$G(\omega_n,\mathbf{k}) = \frac{u_{\mathbf{k}}^2}{i\omega_n - E_{\mathbf{k}}} + \frac{v_{\mathbf{k}}^2}{i\omega_n + E_{\mathbf{k}}}, \tag{2.26}$$

$$F(\omega_n,\mathbf{k}) = u_{\mathbf{k}}v_{\mathbf{k}}^\star\left(\frac{1}{i\omega_n - E_{\mathbf{k}}} - \frac{1}{i\omega_n + E_{\mathbf{k}}}\right), \tag{2.27}$$

where $u_{\mathbf{k}}$ and $v_{\mathbf{k}}$ are given by Eq. (2.14).

The three approaches discussed above are complementary and equivalent in the case of homogeneous superconductors. However, some of them are better suited for addressing specific questions in the presence of impurities. In particular, the Green's-function method is advantageous for determining thermodynamic properties of a material and averaging over many impurity configurations. For inhomogeneous problems, in which we are interested in spatial variations of the superconducting order and electron density, both the Bogoliubov–de Gennes equations and Green's functions are often used. The choice of method depends on the type of question asked, and we describe the basic models and issues related to impurity scattering in superconductors below.

III. IMPURITIES IN SUPERCONDUCTORS

A. Single-impurity potential

Grain and surface boundaries, twinning planes, and other structural inhomogeneities scatter conduction electrons and therefore affect order parameters. Here we focus on only one type of imperfection: impurity atoms.

1. Potential scattering

First and foremost, an impurity atom has a different electronic configuration than the host solid and therefore interacts with the density of conduction electrons via a Coulomb potential,

$$H_{\rm imp} = \sum_{\alpha} \int d\mathbf{r} \psi_{\alpha}^{\dagger}(\mathbf{r}) U_{\rm pot}(\mathbf{r}) \psi_{\alpha}(\mathbf{r}). \tag{3.1}$$

In good metals the Coulomb interaction is screened at length scales comparable to the lattice spacing, and therefore the scattering potential is often assumed to be completely local, $U_{\rm pot}(\mathbf{r}) = U_0 \delta(\mathbf{r} - \mathbf{r}_0)$, with the impurity at $\mathbf{r}_0$. The resulting scattering occurs only in the isotropic, *s*-wave, angular momentum channel. If the finite range of the interaction is relevant, scattering in $l \neq 0$ channels needs to be considered. In that case, the treatment is similar to that of magnetic scattering in conventional superconductors, see Sec. VI, and was applied to unconventional superconductors in, for example, Balatsky *et al.* (1994) and Kampf and Devereaux (1997).

In the four-component vector notation of the previous section, the potential scattering has the same matrix structure as the chemical potential, or $\xi(\mathbf{k})$ in Eq. (2.19), so that

$$H_{\rm imp} = \int d\mathbf{r} \Psi^{\dagger}(\mathbf{r}) \hat{U}_{\rm pot}(\mathbf{r}) \Psi(\mathbf{r}), \tag{3.2}$$

$$\hat{U}_{\rm pot} = U_0 \tau_3 \delta(\mathbf{r} - \mathbf{r}_0). \tag{3.3}$$

2. Magnetic scattering

In addition to electrostatic interactions, if the impurity atom has a magnetic moment, there is an exchange interaction between the local spin on the impurity site and conduction electrons,

$$H_{\rm imp} = \sum_{\alpha\beta} \int d\mathbf{r} J(\mathbf{r}) \psi_{\alpha}^{\dagger}(\mathbf{r}) \mathbf{S} \cdot \boldsymbol{\sigma}_{\alpha\beta} \psi_{\beta}(\mathbf{r}). \tag{3.4}$$

The range of interaction is determined by the quantum-mechanical structure of the electron cloud associated with the localized spin. Again, in reality we often consider a simplified exchange Hamiltonian with $J(\mathbf{r}) = J_0 \delta(\mathbf{r} - \mathbf{r}_0)$, which captures the essential physics of the problem. In four-component vector notations, the electron-spin operator becomes (Maki, 1969)

$$\boldsymbol{\alpha} = \frac{1}{2}[(1 + \tau_3)\boldsymbol{\sigma} + (1 - \tau_3)\sigma_3 \boldsymbol{\sigma} \sigma_3]. \tag{3.5}$$

Therefore

$$H_{\rm imp} = \int d\mathbf{r} \Psi^{\dagger}(\mathbf{r}) \hat{U}_{\rm mag}(\mathbf{r}) \Psi(\mathbf{r}), \tag{3.6}$$

$$\hat{U}_{\rm mag} = J(\mathbf{r}) \mathbf{S} \cdot \boldsymbol{\alpha}. \tag{3.7}$$

3. Anderson impurity

However, even if the ground state of an isolated atom has a spin, putting such an impurity into a host matrix may modify the spin configuration as impurity electrons couple to the conduction band. Therefore a more realistic model for an impurity site is the Anderson model, with the Hamiltonian

$$H_A = \sum_{\alpha} E_0 d_{\alpha}^{\dagger} d_{\alpha} + U n_{d\uparrow} n_{d\downarrow} + H_{\rm sd}, \tag{3.8}$$

$$H_{\rm sd} = \sum_{\mathbf{k},\alpha} V_{\rm sd} c_{\mathbf{k},\alpha}^{\dagger} d_{\alpha} + \text{H.c.} \tag{3.9}$$

Here E_0 is the position of the impurity level relative to the Fermi energy, $d^{\dagger}$ and d operate on the impurity site, U is the Coulomb repulsion for the electrons localized on the impurity site, and $c_{\mathbf{k}}^{\dagger}, c_{\mathbf{k}}$ create and annihilate conduction electrons. This Hamiltonian allows electrons to hop on and off the impurity site, resulting in a finite width of the impurity level $\Gamma = \pi |V_{\rm sd}|^2 N_0$; see, e.g., Hewson (1993) for a detailed analysis in a host normal metal. The model describes potential scattering when $U \ll \Gamma$. On the other hand, when $E_0 \ll E_F$, $E_0 + U \gg E_F$, and $U \gg \Gamma$, the local levels remain split so that the impurity state is singly occupied and has a local spin. Therefore the model allows a natural interpolation between potential and magnetic scattering. The price to pay for such rich behavior is the difficulty of studying the model analytically, and in practice many results have been obtained in the simplified treatments of 1 and 2 above, although a number of very thorough numerical renormalization-group studies of Anderson impurities in superconductors exist. We review some of them, but do not focus extensively on those.

B. Scanning-tunneling microscopy as a tool to measure local density of states

STM/STS is a powerful and versatile tool for studying electronic properties of solids. Its remarkable energy and spatial resolution are particularly well suited for characterization of materials at small energy and short length scales. STS measures the tunneling current between the metallic tip and sample as a function of voltage bias, and the tip position is controlled with atomic resolution (Yazdani *et al.*, 1997; Pan *et al.*, 1998; Suderow *et al.*, 2001; Martinez-Samper *et al.*, 2003). From the tunneling Hamiltonian, the differential conductance—the

derivative of the current with respect to the bias—is related to the electron spectral function of the sample, $A_\sigma(\lambda,\omega)=-(1/\pi)\mathrm{Im}\, G_\sigma(\lambda,\omega+i\delta)$, with $\delta\to 0^+$, by

$$\frac{dI}{dV}\propto -\int d\omega\sum_{\lambda,\sigma}|T_\lambda|^2 A_\sigma(\lambda,\omega)f'_{\mathrm{FD}}(\omega-eV). \tag{3.10}$$

Here f_{FD} is the Fermi distribution function and λ is the electronic eigenstate for states in the sample (for a translationally invariant system, λ is often chosen to be a momentum index $\mathbf{k}$). The tunneling matrix element is $|T_\lambda|^2=\Sigma_\rho|M_{\lambda\rho}|^2A_{\mathrm{tip}}(\rho,\omega)$, where $M_{\lambda\rho}$ is the matrix element for the overlap of electronic states in the tip and sample. If the DOS of the tip is featureless around the Fermi energy, $|T_\lambda|^2$ is nearly energy independent. If we assume a λ-independent tunneling matrix element and consider low temperatures ($T\to 0$), the tunneling conductance is proportional to the local density of state (LDOS) at the bias energy at the tip position, $dI/dV(\mathbf{r})\propto\rho(eV,\mathbf{r})=\Sigma_{\lambda,\sigma}\mathbf{A}_\sigma(\lambda,\omega=eV)|\langle\lambda|\mathbf{r}\rangle|^2$. This in turn is related to the electronic Green's function via $\rho(\mathbf{r},eV)=-\pi^{-1}\Sigma_\sigma\,\mathrm{Im}\,G_\sigma(\mathbf{r},\mathbf{r};eV+i\delta)$. Therefore tunneling spectroscopy provides a real-space image of the local density of states computed theoretically. For more details, see Fischer *et al.* (2005).

C. Many impurities

In our discussions we assume noninteracting impurities[2] so that the net impurity potential is

$$\hat{U}_{\mathrm{imp}}(\mathbf{r})=\sum_i \hat{U}_{\mathrm{imp}}(\mathbf{r}-\mathbf{r}_i) \tag{3.11}$$

$$=\int d\mathbf{r}'\rho_i(\mathbf{r}')\hat{U}_{\mathrm{imp}}(\mathbf{r}-\mathbf{r}'). \tag{3.12}$$

Here $\hat{U}$ is a matrix in both spin- and particle-hole space, and we introduce the impurity density

$$\rho_i(\mathbf{r})=\sum_i \delta(\mathbf{r}-\mathbf{r}_i). \tag{3.13}$$

We also work in the dilute limit, where the average impurity concentration $n_i=\int d\mathbf{r}\rho(\mathbf{r})/\mathcal{V}\ll 1$, with $\mathcal{V}$ the system volume.

A local physical quantity, such as the LDOS at the position $\mathbf{r}$ measured by STM, depends on the distance to nearby impurities and therefore is different for different impurity distributions. In contrast, thermodynamic quantities such as T_c or the density of states measured in planar junctions are averaged over the sample and hence over many random local configurations of impurities. Therefore in computing their values we average over all impurity configurations (Abrikosov *et al.*, 1963) so that (the bar denotes impurity average)

[2]For magnetic scatterers, the effect of the RKKY interaction between impurities on superconducting properties is small (Larkin *et al.*, 1971; Galitskii and Larkin, 2002).

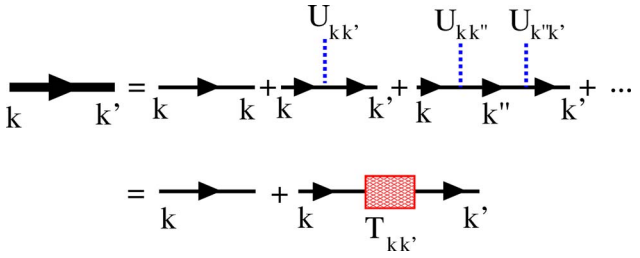

FIG. 1. (Color online) Multiple scattering on a single impurity. The thick line denotes the full Green's function, the thin line the bare Green's function, and the dashed line denotes the scattering process. The second line defines the T matrix according to Eq. (3.18).

$$\bar{G}(\omega_n,\mathbf{k})=\prod_{i=1}^{N_i}\left[\frac{1}{\mathcal{V}}\int d\mathbf{r}_i G(\omega_n,\mathbf{k},\mathbf{r}_1,\ldots,\mathbf{r}_{N_i})\right]. \tag{3.14}$$

By definition, $\bar{\rho}_{\mathrm{imp}}=n_i$. We also assume an uncorrelated, or random, impurity distribution, which means

$$\overline{\rho(\mathbf{r})\rho(\mathbf{r}')}=n_i\delta(\mathbf{r}-\mathbf{r}')+n_i^2.$$

For dilute impurities, $n_i^2\ll n_i$, and we neglect the second term compared to the first. In Sec. XIII we implement this procedure to determine the impurity-averaged DOS.

D. The self-energy and *T*-matrix approximation

To compute the Green's function in the presence of impurities, we employ the T-matrix approximation. This method is described elsewhere (Hirschfeld *et al.*, 1986, 1988; Hirschfeld and Goldenfeld, 1993; Hotta, 1993; Mahan, 2000; Hussey, 2002) and we only summarize it.

For a single impurity with scattering potential $\hat{U}_{\mathbf{k},\mathbf{k}'}$ in momentum space, the T matrix exactly accounts for multiple scattering off that impurity. In the language of Feynman diagrams, the corresponding process is shown in Fig. 1. Since translational invariance is broken by the impurity, the Green's function depends on two momenta, $\mathbf{k}$ and $\mathbf{k}'$,

$$\hat{G}(\mathbf{k},\mathbf{k}')=\hat{G}_0(\mathbf{k})+\hat{G}_0(\mathbf{k})\hat{U}_{\mathbf{k},\mathbf{k}'}\hat{G}_0(\mathbf{k}')+\sum_{\mathbf{k}''}\hat{G}_0(\mathbf{k})\hat{U}_{\mathbf{k},\mathbf{k}''}\hat{G}_0(\mathbf{k}'')\hat{U}_{\mathbf{k}'',\mathbf{k}'}\hat{G}_0(\mathbf{k}')+\cdots, \tag{3.15}$$

where $\hat{G}_0$ is given by Eq. (2.19). We have suppressed the frequency index as the scattering is elastic. The series can be summed to write (see Fig. 1)

$$\hat{G}(\mathbf{k},\mathbf{k}')=\hat{G}_0(\mathbf{k})+\hat{G}_0(\mathbf{k})\hat{T}_{\mathbf{k},\mathbf{k}'}\hat{G}_0(\mathbf{k}'), \tag{3.16}$$

where the T matrix is given by an infinite series,

$$\hat{T}_{\mathbf{k},\mathbf{k}'} = \hat{U}_{\mathbf{k},\mathbf{k}'} + \sum_{\mathbf{k}''} \hat{U}_{\mathbf{k},\mathbf{k}''}\hat{G}_0(\mathbf{k}'')\hat{U}_{\mathbf{k}'',\mathbf{k}'} + \cdots \tag{3.17}$$

$$= \hat{U}_{\mathbf{k},\mathbf{k}'} + \sum_{\mathbf{k}''} \hat{U}_{\mathbf{k},\mathbf{k}''}\hat{G}_0(\mathbf{k}'')\hat{T}_{\mathbf{k}'',\mathbf{k}'}. \tag{3.18}$$

This equation needs to be solved for $\hat{T}$. If the impurity scattering is purely local, the scattering is isotropic, $\hat{U}_{\mathbf{k},\mathbf{k}'} = \hat{U}$, greatly simplifying the equation as $\hat{T}$ depends only on energy and not on momentum.

Note that we can draw the set of diagrams in Fig. 1 in real space and write the corresponding set of equations for the T matrix and Green's function $\hat{G}(\mathbf{r},\mathbf{r}')$,

$$\hat{G}(\mathbf{r},\mathbf{r}';\omega) = \hat{G}_0(\mathbf{r},\mathbf{r}';\omega) + \hat{G}_0(\mathbf{r},\mathbf{r}_0;\omega)\hat{T}(\omega)\hat{G}_0(\mathbf{r}_0,\mathbf{r}';\omega). \tag{3.19}$$

The T matrix lends itself easily to describing the effect of an ensemble of impurities. In the context of unconventional superconductors, the first such treatment of transport properties was done by Pethick and Pines (1986). The so-called self-consistent T-matrix approach considers multiple scattering on a single site of electron that has already been scattered on other impurity sites (Hirschfeld *et al.*, 1986, 1988; Schmitt-Rink *et al.*, 1986). This results in replacing the bare Green's function in Eq. (3.18) by its impurity-averaged counterpart $\hat{G}(\mathbf{k},\omega)$. After averaging over the random impurity distribution, translational invariance is restored, and the Green's function depends on a single momentum $\mathbf{k}$. The combined effect of impurities is given by the self-energy, $\hat{\Sigma}(\mathbf{k},\omega) = n_i\hat{T}_{\mathbf{k},\mathbf{k}}$, namely,

$$\hat{G}^{-1}(\mathbf{k},\omega) = \hat{G}_0^{-1}(\mathbf{k},\omega) - \hat{\Sigma}(\mathbf{k},\omega). \tag{3.20}$$

In contrast to the single-impurity case, where Eq. (3.16) with the T matrix given by Eq. (3.18) is the exact solution of the problem, the Green's function given above is an approximation, and much recent research is motivated by questions about how accurately it describes properties of nodal superconductors with impurities.

E. Static and dynamic impurities

So far we have only considered static impurities. However, for potential scattering it is possible that a vibrational mode modulates the charge on the impurity site and U_{pot} acquires a characteristic frequency. Such a mode can be extended, such as a phonon, or local. The influence of the dynamical impurity on the local properties of a superconductor is a relatively new subject discussed in Sec. XII; see however, Brandt (1970).

For magnetic scattering, the situation is more complex. Degeneracy between spin-up and spin-down states on the impurity site and nontrivial commutation relations between different spin components ensure that quantum dynamics of the impurity is relevant. The dynamics of the local spin flips leads to the screening of the impurity spin by conduction electrons in a metal below the Kondo temperature T_K; see Hewson (1993) for a review. In Sec. XI, we review the current status of Kondo effect studies in superconductors.

Impurity spin dynamics does not play a major role: (a) for large spins $S \gg 1$ (except in a magnetic field), or (b) when the Kondo temperature is low and measurements are done at $T \gg T_K$. In these limits, the approximation of classical spin suffices and the corresponding local and global density of states are analyzed in Secs. VI and XIII, respectively.

IV. NONMAGNETIC IMPURITIES AND ANDERSON'S THEOREM

One important early experimental result was the robustness of conventional superconductivity to small concentrations of nonmagnetic impurities. The theoretical underpinning of this result is known as Anderson's theorem (Anderson, 1959). Anderson noticed that since superconductivity is due to the instability of the Fermi surface to pairing of time-reversed quasiparticle states, any perturbation that does not lift the Kramers degeneracy of these states does not affect the mean-field superconducting transition temperature.

This is most clearly seen from the BCS analysis, which we carry out following Ma and Lee (1985), for an isotropic pairing potential $V_{\alpha\beta\gamma\delta}(\mathbf{r},\mathbf{r}') = V\delta(\mathbf{r}-\mathbf{r}')\delta_{\alpha\delta}\delta_{\beta\gamma}$. In the absence of a magnetic field, the coefficients $a_n = \sin\theta_n$ and $b_n = \cos\theta_n$ in Eq. (2.15) can be taken as real, without loss of generality, so that the self-consistency condition, Eq. (2.9), reads

$$\Delta_n = V\sum_{m\neq n} \frac{\Delta_m}{\sqrt{\epsilon_m^2 + \Delta_m^2}} \int d^d\mathbf{r}\,\phi_n^2(\mathbf{r})\phi_m^2(\mathbf{r}). \tag{4.1}$$

Here ϵ_m are the energies of the eigenstates and

$$\Delta_n = \int d^d\mathbf{r}\,\Delta(\mathbf{r})\phi_n^2(\mathbf{r}). \tag{4.2}$$

As noted above, in the BCS approach the ϕ's are eigenfunctions of the single-particle Hamiltonian. In a pure system, $\Delta(\mathbf{r}) = \Delta_n = \Delta_0$. The most important assumption underlying Anderson's theorem is that in the presence of impurities, when $\phi_n(\mathbf{r})$ are rather complicated functions, the superconducting order parameter can still be taken to be uniform, $\Delta(\mathbf{r}) = \Delta_1$. Then the gap equation, Eq. (4.1), takes the form

$$\frac{1}{V} = \int d^d\mathbf{r}\,d\epsilon\,\phi_n^2(\mathbf{r})\frac{N(\epsilon,\mathbf{r})}{\sqrt{\epsilon^2 + \Delta_1^2}}. \tag{4.3}$$

If the density of states of the system with impurities,

$$N(\epsilon,\mathbf{r}) = \sum_m \phi_m^2(\mathbf{r})\delta(\epsilon - \epsilon_m), \tag{4.4}$$

is unchanged compared to that of the pure metal, $N(\epsilon,\mathbf{r}) \approx \rho_0$, the solution of the gap equation, Eq. (4.3), is $\Delta_1 = \Delta_0$. Therefore, the transition temperature and gap are insensitive to impurity scattering at the mean-field level.

The Anderson theorem explained why superconductivity was robust to disorder in early experiments. It is important to realize, however, that it is an approximate statement about thermodynamic averages of the system. In the next section we analyze changes that impurities create in superconductors. We shall see that even purely potential scattering does induce changes in local properties of superconductors, although the corresponding change in the transition temperature remains minimal. The Anderson theorem suggests the separation of the studies of impurity effects on different length scales, from lattice spacing to the coherence length to sample size.

Before proceeding, we discuss extensions of Anderson's treatment of impurities. In weakly disordered systems, $N(\epsilon,\mathbf{r})\approx\rho_0$. Ma and Lee (1985) argued that Anderson's theorem remains valid even in strongly disordered systems provided the localization length $L\gg(\rho_0\Delta_0)^{1/d}$. In that case, a large number of states localized within energy Δ_0 of the Fermi surface form a local superconducting patch. The Josephson interaction between patches then leads to global phase coherence at $T=0$. Ma and Lee also argued that the theorem holds to the limit of site localization.

At the same time, the superfluid stiffness, i.e., the ability to carry supercurrent, is affected by disorder: When the quasiparticle lifetime τ becomes sufficiently short, $\Delta_0\tau\ll1$, the superfluid density $\rho_s\approx\Delta_0\tau$. Consequently, the local phase fluctuations of the order parameter are strong, and the experimentally observed transition temperature is severely suppressed compared to the mean field T_c. Studies of such granular superconductors are outside the scope of this review.

For dilute impurities, Anderson's theorem is valid provided the superconducting order parameter is nearly uniform. The "healing length" of $\Delta(\mathbf{r})$ over which it can change appreciably is the coherence length $\xi_0\simeq v_F/\Delta_0$, where v_F is the Fermi velocity, while the Coulomb screening length for the charged impurities in metals is of the order of the lattice spacing a. Hence for $\xi_0\gg a$, the order parameter remains essentially uniform and Anderson's theorem holds. Recent studies considered impurity scattering in superconductors with ultrashort coherence length, and found that when the pairing range is of the order of the electron bandwidth, Anderson's theorem is violated (Ghosal *et al.*, 1988; Tanaka and Marsiglio, 2000; Moradian *et al.*, 2001).

Xiang and Wheatley (1995) and Ghosal *et al.* (1998) explored the difference between the single-particle excitation gap and superconducting order parameter as a function of disorder. When disorder depletes the density of states, both quantities at first decrease simultaneously. However, the spectral gap persists even when superconducting off-diagonal long-range order vanishes. This may be related to the formation of local pairs without phase coherence (Ma and Lee, 1985).

In most experimentally relevant situations, however, corrections to the main statement of Anderson's theorem are quantitative rather than qualitative. Therefore, it is generally sufficient to consider impurity effects in BCS-like superconductors.

V. SINGLE-IMPURITY BOUND STATE IN TWO-DIMENSIONAL METALS

Before we proceed to discuss superconductors, it is very instructive to review the simpler problem of an impurity in a metal. We show here a T-matrix calculation for finding bound states due to a single impurity in d dimensions with an on-site attractive potential $U(\mathbf{r})=U_0\delta(\mathbf{r})$, where $U_0\leqslant0$. The Hamiltonian is

$$\mathcal{H}=\sum_{\mathbf{k}}[\epsilon(\mathbf{k})-\mu]c^{\dagger}_{\mathbf{k},\sigma}c_{\mathbf{k},\sigma}+\sum_{\mathbf{k},\mathbf{k}'}U_0c^{\dagger}_{\mathbf{k},\sigma}c_{\mathbf{k}',\sigma}. \tag{5.1}$$

We consider, for simplicity, the single-particle case ($\mu=0$), although the results for a normal metal follow by replacing $\epsilon(\mathbf{k})$ with $\xi(\mathbf{k})=\epsilon_{\mathbf{k}}-\mu$ below.

The bare Green's function for a free particle is

$$G_0(\omega,\mathbf{k})=[\omega-\epsilon(\mathbf{k})]^{-1}. \tag{5.2}$$

Since the vertex of the impurity interaction U_0 is momentum independent, the equation for the T matrix is particularly simple and follows from Eq. (3.18),

$$T(\omega)=U_0+U_0\sum_{\mathbf{k}}G_0(\omega,\mathbf{k})T(\omega),$$

$$T(\omega)=\frac{U_0}{1-U_0\sum_{\mathbf{k}}G_0(\omega,\mathbf{k})}. \tag{5.3}$$

Summation over $\mathbf{k}$ is performed using the DOS

$$N(\epsilon)=\sum_{\mathbf{k}}\delta(\epsilon-\epsilon(\mathbf{k}))=\Gamma_d\epsilon^{(d/2)-1}, \tag{5.4}$$

where Γ_d is a constant dependent on dimension. As an example for $d=3$ we find

$$\begin{aligned}g_0(\omega)&=\frac{1}{N}\sum_{\mathbf{k}}G_0(\omega,\mathbf{k})\\&=\int_0^W\frac{d\epsilon N(\epsilon)}{\omega-\epsilon}\\&\simeq-2\Gamma_3\sqrt{W}+2\Gamma_3\omega\sqrt{W},\end{aligned} \tag{5.5}$$

where W is the bandwidth. Here N represents the system size. Consequently, the T matrix for $d=3$ is given by

$$T(\omega)=\frac{1}{1/U_0+2\Gamma_3\sqrt{W}-2\Gamma_3\omega\sqrt{W}}. \tag{5.6}$$

A similar expression can be obtained for $d=2$ by substituting $g_d(\omega)=-\Gamma_2\ln[|W/\omega-1|]$.

The poles of the Green's function give the energy spectrum of single-particle excitations. The poles of the Green's function in the presence of impurity scattering, $G=G_0+G_0TG_0$, see Eq. (3.16), consist of the poles of the original $\hat{G}_0$ and poles of the T matrix. The latter signify the appearance of new states. We find the energy

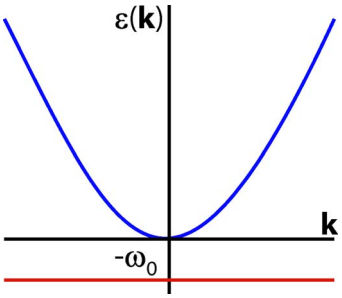

FIG. 2. (Color online) Impurity bound state in a metal at energy ω_0 formed as a result of multiple scattering.

of this state ω_0 from Eq. (5.6). The bound state ($\omega_0<0$, see Fig. 2) is formed for an arbitrarily small potential $|U_0|$ in $d=1,2$, but requires a critical coupling for $d=3$. The energy of this state is given by

$$\omega_0 \sim (g_1)^2 \quad \text{if } d=1, \tag{5.7}$$

$$\omega_0 = W\exp\left(-\frac{1}{g_2}\right) \quad \text{if } d=2, \tag{5.8}$$

$$\omega_0 \sim [g_3 - g_{3c}] \quad \text{if } d=3, \tag{5.9}$$

where for $d=3$ the critical coupling is given by $g_{3c} \sim W/2|U_0|$ and $g_3=1$.

We focus on the two-dimensional case, when $g_2 = \Gamma_2|U_0|$ and $\Gamma_2=m/2\pi$ is the electron density of states. The bandwidth, $W\simeq\hbar^2/2ma^2$, is the ultraviolet cutoff corresponding to the lattice parameter a for a free particle. This result can be compared to the solution of Schrödinger's equation for a particle in the 2D attractive potential U_0 (Landau and Lifshitz, 2000, Chap. 45). For an arbitrary potential $U(\mathbf{r})$, the solution obtained using the T matrix is asymptotically correct if the scattering length is greater than a. For a shallow potential, the bound-state energy $-\omega_0$ is exponentially small, and the characteristic extent of the bound-state wave function is $l_0=(\hbar^2/2m\omega_0)^{1/2}\gg a$. Therefore in this limit we can safely approximate $U(\mathbf{r})=U_0\delta(\mathbf{r})$, where $U_0=\int U(\mathbf{r})d\mathbf{r}$.

Finding the energy of the bound state, Eq. (5.8), is only one part of the solution. We also want to determine corrections to the local density of states due to the bound state. We write the equation for the Green's function in real space, Eq. (3.19),

$$G(\mathbf{r},\mathbf{r}';\omega) = G_0(\mathbf{r},\mathbf{r}';\omega) + G_0(\mathbf{r},0;\omega)T(\omega)G_0(0,\mathbf{r}';\omega),$$

and read off the position-dependent DOS,

$$N(\mathbf{r},\omega) = -\frac{1}{\pi}\,\mathrm{Im}\,G(\mathbf{r},\mathbf{r};\omega) = N_0(\mathbf{r},\omega) + \delta N(\mathbf{r},\omega). \tag{5.10}$$

The first term is the DOS of a clean system and the second is the correction due to the bound state. Consider $\omega\approx\omega_0$. Since the bound state is below the bottom of the band, the unperturbed Green's function G^0 has no imaginary part in this range. Therefore, the only contribution to Im $G(\mathbf{r},\mathbf{r};\omega)$ in Eq. (5.10) is from the T matrix,

$$\mathrm{Im}\,T(\omega) = \mathrm{Im}\,\frac{1}{1/g_2 - \ln[W/(-\omega)]} = \mathrm{Im}\,\ln^{-1}\left[\frac{\omega+i\delta}{\omega_0}\right] = \pi\delta(\omega-\omega_0), \tag{5.11}$$

and the correction to the DOS of a clean system is

$$\delta N(\mathbf{r},\omega) = |G_0(\mathbf{r},\omega_0)|^2\delta(\omega-\omega_0), \tag{5.12}$$

where $G_0(\mathbf{r},\omega)=N_0J_0(k_Fr)\ln[W/\omega]$ is the real part of the Green's function in 2D systems. Equations (5.9) and (5.12) are the main results of this section. They establish the strategy to which we adhere in finding the impurity-induced bound states: (a) find the poles of the T matrix and the new poles of the full Green's function and (b) compute the inhomogeneous DOS due to the impurity-induced state. There are other approaches to searching for scattering-induced bound states. For example, the exact numerical solution for a finite system is the only approach available for calculations accounting for the self-consistent suppression of the superconducting order.

VI. LOW-ENERGY STATES IN *s*-WAVE SUPERCONDUCTORS

A. Potential scattering

Even though potential scattering does not change the bulk properties of isotropic superconductors, it may affect the local density of states. The first analysis of conditions for the existence of the bound state and the structure of Friedel oscillations around a spherically symmetric impurity in an s-wave superconductor was carried out by Fetter (1965). Here we follow Machida and Shibata (1972) and Shiba (1973) and consider the Anderson impurity model, Eqs. (3.8) and (3.9), in the limit $U=0$ (resonance scattering). As discussed above, the localized state acquires a finite width, $\Gamma=\pi|V_{\mathrm{sd}}|^2N_0$, due to hybridization with the conduction band. Consequently, the effective scattering potential varies significantly over the bandwidth energy, violating provisions of Anderson's theorem. The T-matrix approach gives (Machida and Shibata, 1972; Shiba, 1973)

$$\hat{T}(\omega) = |V_{\mathrm{sd}}|^2\tau_3\left[\omega - E_0\tau_3 - |V_{\mathrm{sd}}|^2\tau_3\sum_{\mathbf{k}}\hat{G}_0(\mathbf{k},\omega)\tau_3\right]^{-1}\tau_3. \tag{6.1}$$

The poles ω_0 of the T matrix determine the location of bound states,

$$\omega^2\left[1+\frac{2\Gamma}{\sqrt{\Delta^2-\omega^2}}\right] = E_0^2+\Gamma^2. \tag{6.2}$$

In most physical situations $\Gamma\gg\Delta$, so that

$$\omega_0 = \pm\Delta\{1-2\pi^2[\Delta N_d(0)]^2\}, \tag{6.3}$$

where $N_d(0)=\pi^{-1}\Gamma/(\Gamma^2+E_0^2)$ is the density of states of the resonant impurity level. Typically $\Delta N_d(0)\sim10^{-3}$, so that the bound state lies essentially at the gap edge. Shiba (1973) considered a finite but small value of the

Coulomb repulsion and allowed for induced pairing on the impurity site. He concluded that even though the bound state may be shifted to lower energies, it still lies within $10^{-3}\Delta$ of the gap edge and therefore can be neglected in discussions of physical properties.

B. Classical spins

If impurities are magnetic, time-reversal symmetry is violated and superconductivity is thus suppressed. We consider a combination of the scattering potential $\hat{U}_{\rm pot}(\mathbf{r})=V(\mathbf{r})\tau_3$ and the magnetic scattering, Eq. (3.6), written in momentum space,

$$H_{\rm ex}=\frac{1}{2N}\sum_{\substack{\mathbf{k},\mathbf{k}'\\ \alpha\beta}} J(\mathbf{k}-\mathbf{k}')c^{\dagger}_{\mathbf{k},\alpha}\boldsymbol{\sigma}_{\alpha\beta}\cdot\mathbf{S}c_{\mathbf{k}'\beta}. \tag{6.4}$$

As discussed in Sec. III.E, for $S\gg 1$ or $T\gg T_K$, we ignore Kondo screening and consider the scattering on classical spins first studied by Shiba, Rusinov, and Yu (Yu, 1965; Rusinov, 1968, 1969; Shiba, 1968). Technically this is achieved by taking $S\to\infty$, while simultaneously $J\to 0$ so that $JS=$const. In this limit the localized spin acts as a local magnetic field.

The impurity location is chosen at the origin for a BCS s-wave superconductor with the unperturbed Hamiltonian of the form

$$\mathcal{H}_0=\sum_{\mathbf{k}\alpha}\varepsilon_{\mathbf{k}}c^{\dagger}_{\mathbf{k},\alpha}c_{\mathbf{k}\alpha}+\Delta_0\sum_{\mathbf{k}}\{c^{\dagger}_{\mathbf{k}\uparrow}c^{\dagger}_{-\mathbf{k}\downarrow}+c_{-\mathbf{k}\downarrow}c_{\mathbf{k}\uparrow}\}. \tag{6.5}$$

This problem serves as a starting point for all subsequent analysis of resonance states in superconductors.

To find a localized state with energy $0<E<\Delta_0$ near a single paramagnetic impurity, we perform a Bogoliubov transformation (Yu, 1965; Rusinov, 1968) to find

$$Eu_{\alpha}(\mathbf{r})=\varepsilon(\mathbf{k})u_{\alpha}(\mathbf{r})+i\Delta\sigma^{y}_{\alpha\beta}v_{\beta}(\mathbf{r})+U_{\alpha\beta}(\mathbf{r})u_{\beta}(\mathbf{r}), \tag{6.6}$$

$$Ev_{\alpha}(\mathbf{r})=-\varepsilon(\mathbf{k})v_{\alpha}(\mathbf{r})-i\Delta\sigma^{y}_{\alpha\beta}u_{\beta}(\mathbf{r})-U_{\alpha\beta}(\mathbf{r})v_{\beta}(\mathbf{r}). \tag{6.7}$$

This system is solved by Fourier transforming the equations and expanding the impurity potentials in spherical harmonics in $\mathbf{k}$ space, J_l and V_l, and has solutions at

$$\frac{E_l}{\Delta_0}=\frac{1+(\pi N_0V_l)^2-(\pi N_0J_lS/2)^2}{\sqrt{[1+(\pi N_0V_l)^2-(\pi N_0J_lS/2)^2]^2+4(\pi N_0J_lS/2)^2}}, \tag{6.8}$$

where N_0 is the normal-state DOS at the Fermi energy. This result can be written in a more elegant form using the phase shifts δ_l of scattering for up (+) and down (−) electrons in each angular channel,

$$\tan\delta_l^{\pm}=(\pi N_0)(V_l\pm J_lS/2). \tag{6.9}$$

Then the energies of the states in the gap become

$$\epsilon_l=\frac{E_l}{\Delta_0}=\cos(\delta_l^{+}-\delta_l^{-}). \tag{6.10}$$

Clearly, for purely potential scattering ($\delta_l^{+}=\delta_l^{-}$) the spectrum begins at the gap edge, and there are no intragap states. However, as magnetic scattering increases, low-energy states appear below the gap edge. Purely magnetic scattering corresponds to $\delta_l^{+}=-\delta_l^{-}$, and strong scattering (unitarity limit, $\delta\sim\pi/2$) yields a localized state deep in the gap, while weak scattering ($\delta\ll 1$) results in a bound state close to the gap edge.

The same result can be obtained using the Green's-function formulation (Shiba, 1968; Rusinov, 1969) and solving the single-impurity problem via the T matrix. In Nambu notation

$$\hat{G}(\mathbf{k},\mathbf{k}';\omega)=\hat{G}_0(\mathbf{k},\omega)\delta(\mathbf{k}-\mathbf{k}')+\hat{G}_0(\mathbf{k},\omega)\hat{T}(\mathbf{k},\mathbf{k}')\hat{G}_0(\mathbf{k}',\omega). \tag{6.11}$$

Here the T matrix is computed as in Sec. III.D for a matrix Hamiltonian of Sec. III.A, and we sum over indices of the matrix α in each vertex. The lth angular component $\hat{T}_l$ satisfies (for a spherical Fermi surface and isotropic gap)

$$\hat{T}_l(\omega)=\hat{U}_l+\hat{U}_l\int d\varepsilon\hat{G}_0(\mathbf{k},\omega)\hat{T}_l(\omega). \tag{6.12}$$

The full expression for T_l is straightforward to obtain (Rusinov, 1969) but is rather cumbersome, so that we do not give it here. Even for spherically symmetric scattering ($l=0$ only) with both $V_0\neq 0$ and $J\neq 0$, the T matrix is simple yet lengthy (Okabe and Nagi, 1983). The bound-state energy is, of course, still given by Eq. (6.10).

For a purely magnetic spherically symmetric exchange, $J(\mathbf{k}-\mathbf{k}')=J$, the T matrix has a particularly simple form (Shiba, 1968), with the diagonal (in spin indices) component

$$T^{(1)}(\omega)=\frac{1}{N}\frac{(JS/2)^2\hat{g}_0(\omega)}{I-[JS\hat{g}_0(\omega)/2]^2}. \tag{6.13}$$

Here $\hat{g}_0$ is the local matrix Green's function,

$$\hat{g}_0(\omega)=\frac{1}{N}\sum_{\mathbf{k}}\hat{G}_0(\mathbf{k},\omega)=-\pi N_0\frac{\omega+\Delta_0\sigma_2\tau_2}{\sqrt{\Delta_0^2-\omega^2}}. \tag{6.14}$$

The bound-state energy is

$$\epsilon_0=\frac{E_0}{\Delta_0}=\frac{1-(JS\pi N_0/2)^2}{1+(JS\pi N_0/2)^2}. \tag{6.15}$$

The wave functions of bound states at E_l can be computed using the Bogoliubov equations above. In the simplest case of isotropic scattering at distances $r\gg p_F^{-1}$, both $u(\mathbf{r})$ and $v(\mathbf{r})$ vary as (Fetter, 1965; Rusinov, 1969)

$$\frac{\sin(p_Fr-\delta_0^{\pm})}{p_Fr}\exp[-r|\sin(\delta_0^{+}-\delta_0^{-})|/\xi_0], \tag{6.16}$$

that is, the state is localized near the impurity site at distances

$$r_0 \sim \frac{\xi_0}{|\sin(\delta_0^+ - \delta_0^-)|} = \frac{\xi_0}{\sqrt{1-\epsilon_0^2}}. \quad (6.17)$$

The square of these coefficients gives the spatial dependence of the particle and hole components of the density of states at a given position $\mathbf{r}$ (Yazdani *et al.*, 1997).

The analysis above was carried out under the assumption that the variation of the order parameter Δ around the impurity site does not change the position of the resonance state. There are several characteristic length scales for this variation, $\delta\Delta(\mathbf{r})$. Far from the impurity $r \gg \xi_0$, at temperatures close to T_c, where this variation can be determined perturbatively, $\delta\Delta(\mathbf{r})/\Delta_0 \simeq 1/p_F r$ (Heinrichs, 1968; Rusinov, 1968). This power law is insensitive to phase shifts of scattering on the impurity. At low temperatures, a fully self-consistent treatment is required, which leads to $\delta\Delta(\mathbf{r})$ decaying as $(p_F r)^{-3}$ and oscillating on the scale of $\xi_0\Delta_0/\omega_D$, where the Debye temperature ω_D sets the scale for the interaction between electrons (Schlottmann, 1976).

In the immediate vicinity of impurity $v_F/\omega_D \ll r \ll \xi_0$ the variation of the order parameter is $\delta\Delta(\mathbf{r})/\Delta_0 \simeq 1/(p_F r)^2$ in the linear-response approximation (Rusinov, 1968). In the fully self-consistent treatment at distances $r \ll \xi_0\omega_D/E_F$, this dependence was found to acquire an oscillating factor $\sin^2 p_F r$ (Schlottmann, 1976).

In the Anderson model the local change $\Delta(\mathbf{r})$ is related to the impurity T matrix (Kim and Muzikar, 1993) and can be determined if a reliable approximation for the T matrix exists for the given parameter range. In principle, the method of Kim and Muzikar covers both Kondo and mixed-valence regimes and is useful in determining local structures of the order parameter.

In all cases, the suppression of the order parameter is determined by the Fermi wavelength and does not affect the position of the bound state.

VII. IMPURITY-INDUCED VIRTUAL BOUND STATES IN *d*-WAVE SUPERCONDUCTORS

We now extend our discussion to impurity-induced states in *d*-wave superconductors. Scalar (nonmagnetic) impurities are pair breakers for higher-orbital-momentum states, such as *d*-wave states. The change of the quasiparticle momentum upon scattering disrupts the phase assignment for particular directions of the momenta in a nontrivial pairing state (Anderson, 1959; Tsuneto, 1962; Markowitz and Kadanoff, 1963). This also follows from the analysis of the self-energy in the Abrikosov-Gorkov theory (Abrikosov *et al.*, 1963). An early argument about pair-breaking effects of potential scattering was put forth by Larkin (1965).

As emphasized above, for pair-breaking impurities local properties of the superconductor near the impurity site, such as the LDOS and gap amplitude, are modified dramatically. To capture these modifications, we use a variation of the Yu-Shiba-Rusinov approach (Yu, 1965; Rusinov, 1968; Shiba, 1968); see Sec. VI. We restrict our consideration to *s*-wave scatterers ($l=0$) close to the unitarity limit, $\delta_0 \simeq \pi/2$, when the bound-state energy is far from the gap edge. In contrast to *s*-wave superconductors, in *d*-wave systems the density of states below the gap maximum Δ_0 is nonzero and varies linearly with energy in a pure system, $N(\omega)/N_0 \simeq \omega/\Delta_0$. Consequently, the overlap with the particle-hole continuum only allows the formation of resonance, or *virtual bound* states, with a finite lifetime.

We focus on pointlike defects and use the T-matrix approach. A closely related method uses the quasiclassical approximation and the ideas of Andreev scattering to reproduce the same results (Choi and Muzikar, 1990; Chen, Rainer, and Sauls, 1998; Shnirman *et al.*, 1999). Interesting extensions are obtained within the quasiclassical formalism for extended defects: for example, the index theorem dictates the existence of a low-energy quasibound state in unconventional superconductors (Adagideli *et al.*, 1999).

High-T_c cuprates with Zn substitution for in-plane Cu are a well-studied example of an impurity system. Zn ions have a full *d* shell and are nominally nonmagnetic. The high stability of this configuration and the rapid suppression of T_c by Zn doping (Ishida *et al.*, 1991; Hotta, 1993) support the view that Zn ions are strong nonmagnetic scatterers. Another point of view, that Zn induces a localized moment on neighboring Cu sites (Bobroff *et al.*, 2001; Polkovnikov *et al.*, 2001) leads naturally to the Kondo problem in gapless superconductors, and is discussed in Sec. XI.

Based on strong anisotropy of the electronic transport, we model cuprates as 2D *d*-wave superconductors and analyze virtual impurity-induced bound states, closely following Buchholtz and Zwicknagl (1981), Stamp (1987), Balatsky *et al.* (1995), and Salkola *et al.* (1996, 1997). Our results are easily extended to any nontrivial pairing state and to higher dimensions and are relevant, for example, for heavy-fermion superconductors with impurities.

The main results of this section are as follows. (i) A strongly scattering scalar impurity produces a localized, virtual, or virtually bound state (or resonance) in a *d*-wave superconductor. It is intuitively obvious that any strong pair-breaking impurity—magnetic or nonmagnetic—will induce such a state. Indeed, low-lying quasiparticle states close to nodes in the energy gap will be influenced even by a nonmagnetic impurity potential, resulting in a virtual bound state in the unitary limit. (ii) This should be compared to the fact that in *s*-wave superconductors magnetic impurities produce bound states inside the energy gap (Machida and Shibata, 1972). The energy Ω' and decay rate Ω'' of this state are given by

$$\Omega \equiv \Omega' + i\Omega'' = -\Delta_0 \frac{\pi c/2}{\ln(8/\pi c)}\left[1 + \frac{i\pi}{2}\frac{1}{\ln(8/\pi c)}\right], \quad (7.1)$$

where $c = \cot\delta_0$. These results are valid provided $\ln(8/\pi c) \gg 1$ and assuming band particle-hole symmetry. The impurity breaks local particle-hole symmetry, however, since Ω' has a definite sign. In the unitary limit c

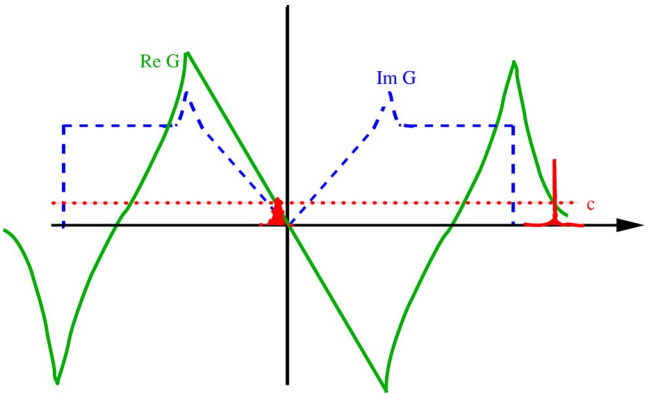

FIG. 3. (Color online) Real and imaginary parts of the Green's function. Graphic solution of Eq. (7.5) for $U_0>0$. We show a physically relevant solution with $\Omega_0''\ll\Omega_0'$. If $\mathrm{Im}\, g_0(\Omega_0) \gg \mathrm{Re}\, g_0(\Omega_0)$, the resonance is broadened and merges with the continuum. Resonances below (or above, for $U_0<0$) the band are sharp, with most of the spectral weight. The virtual bound state inside the gap is well resolved for large U_0 (small c).

$\to 0$ the virtual bound state is a sharp resonance at $\Omega \to 0$ with $\Omega''/\Omega' \to 0$. In the opposite case of weak scattering, $c \lesssim 1$, the energy of the state formally approaches $\Omega' \sim \Delta_0$ and the state is ill defined since $\Omega'' \sim \Omega'$ (see Fig. 10 in Sec. VIII). The wave function of the bound state decays as a power law, $\Psi(r) \sim 1/r$, and is not normalizable. The wave function is localized along the directions where the gap vanishes (nodal directions).

A. Single potential impurity problem

Consider a potential impurity at $\mathbf{r}=\mathbf{0}$ described by

$$H_{\mathrm{int}} = \sum_{\mathbf{k}\mathbf{k}'\sigma} U_0 c^\dagger_{\mathbf{k}\sigma} c_{\mathbf{k}'\sigma}, \tag{7.2}$$

where U_0 is the strength of the isotropic scattering, resulting in phase shift δ_0. The T matrix is independent of the wave vector, and the Green's function is given by

$$\hat{G}(\mathbf{k},\mathbf{k}';\omega) = \hat{G}_0(\mathbf{k},\omega)\delta_{\mathbf{k}\mathbf{k}'} + \hat{G}_0(\mathbf{k},\omega)\hat{T}(\omega)\hat{G}_0(\mathbf{k}',\omega), \tag{7.3}$$

where in $\hat{G}_0$ we choose the $d_{x^2-y^2}$ gap $\Delta_{\mathbf{k}}=\Delta_0\cos 2\varphi$.

For s-wave scattering, the matrix $\hat{T}=T_0\hat{\tau}_0+T_3\hat{\tau}_3$ (Shiba, 1968; Pethick and Pines, 1986; Schmitt-Rink *et al.*, 1986; Stamp, 1987; Hirschfeld *et al.*, 1988; Hirschfeld and Goldenfeld, 1993; Lee, 1993; Balatsky *et al.*, 1994; Pogorelov, 1994; Loktev and Pogorelov, 2002) and its diagonal element is

$$T(\omega)_{11} = 1/[c - g_{11}(\omega)], \tag{7.4}$$

where $g_{11}(\omega)=(1/2\pi N_0)\Sigma_{\mathbf{k}}[\hat{G}^{(0)}(\mathbf{k},\omega)(\hat{\tau}_0+\hat{\tau}_3)]_{11}$. Quasibound states are given by the poles of the T matrix,

$$c = g_{11}(\Omega), \tag{7.5}$$

which is an implicit equation for the energy of the impurity resonance Ω_0 as a function of $c=\cot\delta_0$.

For the particle-hole symmetric case, $g_{11}=g_0(\omega) = \langle \omega/\sqrt{\Delta(\varphi)^2-\omega^2}\rangle_{\mathrm{FS}}$, where the angular brackets denote an average over the Fermi surface; for simplicity, we take $\langle\cdot\rangle_{\mathrm{FS}}=\int\cdot\, d\varphi/2\pi$.[3] For $|\omega|\ll\Delta_0$, we find

$$g_0(\omega) = -\frac{2\omega}{\pi\Delta_0}\left(\ln\frac{4\Delta_0}{\omega} - \frac{i\pi}{2}\right). \tag{7.6}$$

Using its solution in Eq. (7.5), Eq. (7.1) follows immediately. In Fig. 3 we illustrate a solution of Eq. (7.5) for fermions with a finite bandwith.

The solution of Eq. (7.5) is complex, indicating a resonant nature of the quasiparticle state, better described as a virtual state. This is easily seen from Eq. (7.1), which solves Eq. (7.5) to logarithmic accuracy. However, as $c \to 0$, the resonance can be made arbitrarily sharp. For $c=0$, the virtual state becomes a sharp resonance state bound to the impurity (Balatsky *et al.*, 1995). As $c\to 1^-$, Ω' and Ω'' increase without bound so that $\Omega''/\Omega' \to 1^-$, and the solution becomes unphysical. For $c>1$, no solution has been found for Ω.[4]

To solve the single-impurity problem, one has to retain both the T_0 and T_3 components of the T matrix,

$$T_0 = \frac{g_0(\omega)}{c^2 - g_0^2(\omega)}, \quad T_3 = \frac{c}{c^2 - g_0^2(\omega)}. \tag{7.7}$$

Each of them has two poles at $c=\pm g_0(\omega)$, however, $T_{11} = T_0+T_3$ has only one pole; see Eq. (7.4). The sign of the resonance energy reflects a particle-hole asymmetry introduced by the on-site impurity potential U_0.

Now we turn to the physical implications of these virtual bound states in a d-wave superconductor and consider the most interesting case of unitary impurities in the dilute limit, separated by a distance $l \gg \xi_0$. These bound states are nearly localized close to the impurity sites (see below) and substantially modify the local characteristics of the superconductor, such as the density of tunneling states, observed in STM, and the local NMR relaxation rate close to the impurity site.

Consider a local density of electronic states,

$$N(\mathbf{r},\omega) = -\frac{1}{\pi}\,\mathrm{Im}\, g_{11}(\mathbf{r},\mathbf{r};\omega+i0^+), \tag{7.8}$$

with the Green's function in real space,

[3]We assume that the energy gap has line nodes in three dimensions with weak quasiparticle dispersion along the z axis; an extension to a general three-dimensional case is straightforward.

[4]A related model of the Anderson impurity model in an unconventional superconductor was considered by L. Borkowskii and P. Hirschfeld, Phys. Rev. B **46**, 9274 (1992). The results found here for pure potential scattering require generalization of the Anderson model to include the impurity-potential phase shift, independent of the Kondo temperature. This aspect of impurity scattering has not been addressed previously.

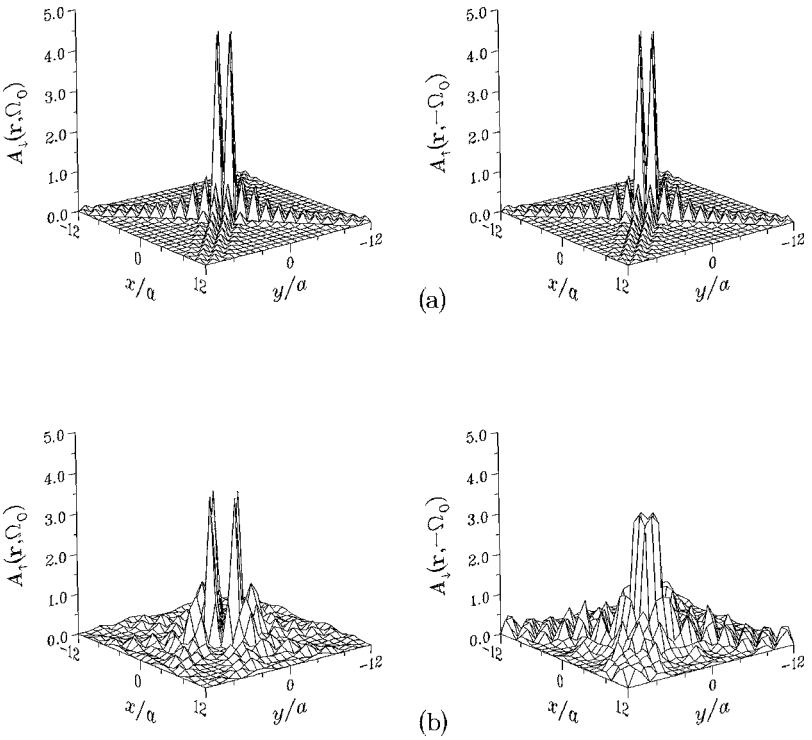

FIG. 4. The cross-shaped nature of the impurity state. The spectral density $A_\sigma(\mathbf{r},\pm\Omega_0)$ is shown as a function of position and spin in units of $N_0\Delta_0$ for (a) $\mu=0$ and (b) $\mu=-W$; $2W$ is the bandwidth in a two-dimensional d-wave superconductor as a function of position around a classical magnetic moment ($N_0J_0=10$ and $U_0=0$) located at $\mathbf{r}=\mathbf{0}$; a is the lattice spacing. These results are computed self-consistently with $\xi=10a$. At half-filling, the spectral density obeys particle-hole symmetry: $A_\uparrow(\mathbf{r},\Omega_0)=A_\downarrow(\mathbf{r},-\Omega_0)$. The energies of the shown virtual-bound states are (a) $\Omega_0=0.05\Delta_0$ and (b) $\Omega_0=0.5\Delta_0$. From Salkola *et al.*, 1997.

$$\hat{G}(\mathbf{r},\mathbf{r}';\omega)=\hat{G}_0(\mathbf{r}-\mathbf{r}',\omega)+\hat{G}_0(\mathbf{r},\omega)\hat{T}(\omega)\hat{G}_0(\mathbf{r}',\omega).$$

The local density of states $N(\mathbf{r},\omega)=N(\omega)+N_{\rm imp}(\mathbf{r},\omega)$ has two contributions. The first, position independent, is due to bulk delocalized quasiparticles with $E_\mathbf{k}=\sqrt{\xi_\mathbf{k}^2+\Delta_\mathbf{k}^2}$. Using $g^{(0)}(0,\omega)=\Sigma_\mathbf{k}[u_\mathbf{k}^2/(\omega-E_\mathbf{k})+v_\mathbf{k}^2/(\omega+E_\mathbf{k})]$, where $u_\mathbf{k}$ and $v_\mathbf{k}$ are Bogoliubov factors, we find for a superconductor with line nodes, $N(\omega)/N_0=\omega/\Delta_0$, at $\omega\ll\Delta_0$. The second term,

$$N_{\rm imp}(\mathbf{r},\omega)=-\frac{1}{\pi}\,{\rm Im}[\hat{G}_0(\mathbf{r},\omega)\hat{T}(\omega)\hat{G}_0(\mathbf{r},\omega)]_{11}, \qquad (7.9)$$

describes a local change in the DOS due to the virtual bound state created around the impurity site.

In a 2D d-wave superconductor, this impurity state is cross shaped in real space, with long tails extending along the gap nodes as shown in Fig. 4. Consider unitary scattering, for which the resonance is at $E_{{\rm imp},n}\equiv\Omega\to 0$; see Sec. V. As ${\rm Im}\,G^{(0)}(\mathbf{r},\omega=0)=-\pi N(\omega=0)=0$ for bulk quasiparticles, only the imaginary part of the T matrix contributes to $N_{\rm imp}$. The probability density for the bound state decays quadratically in distance from the impurity. Along the gap nodes

$$N_{\rm imp}(\mathbf{r},\omega=0)={\rm Re}[\hat{G}^{(0)}(\mathbf{r},\omega=0)]^2\propto r^{-2}, \qquad (7.10)$$

while in the direction of the maximal gap

$$N_{\rm imp}(\vec{r},\omega=0)\propto\frac{\Delta_0^2}{E_F^2}r^{-2}. \qquad (7.11)$$

In addition to the power-law asymptotic decay at large distances, there is an additional contribution that decays exponentially with the angle-dependent coherence length of the superconductor $\xi(\varphi)=\hbar v_F/|\Delta(\varphi)|$. This contribution is important for the detailed comparison of the induced LDOS to that measured by STM near the impurity site, since the intensity near the impurity is mapped out only within a few lattice spacings. For resonance energy away from the Fermi energy, the wave functions of the resonance decay exponentially with the characteristic length scale $\hbar v_F/|\Omega_0|$. A detailed discussion of this decay and the particle-hole asymmetry due to the impurity potential is given by Aristov and Yashenkin (1998) and Balatsky and Salkola (1998).

Gap nodes lead to the power-law decay of the wave function along all directions at large distances $r\gg\xi$. This follows from the power counting of the d-wave propagator:

$$G(\mathbf{r},\omega\to 0)\sim\int d^2k\,\exp(i\mathbf{k}\cdot\mathbf{r})G(\mathbf{k},\omega\to 0)$$
$$\sim\int kdk\,\exp(i\mathbf{k}\cdot\mathbf{r})\frac{v_Fk}{k^2}\sim 1/r.$$

The logarithmically divergent normalization reflects the fact that the impurity state is virtually bound. At a finite impurity concentration, the divergence is cut off at the average distance between impurities. For an arbitrary position of the resonance, taking into account that only one state has been produced with $E_{{\rm imp},n}=\Omega'+i\Omega''$, we find

$$N_{\rm imp}(\mathbf{r},\omega)=\frac{\Omega_i''}{\pi}\sum_i\left[\frac{|u(\mathbf{r}-\mathbf{r}_i)|^2}{(\omega-\Omega_i')^2+\Omega_i''^2}-\frac{|v(\mathbf{r}-\mathbf{r}_i)|^2}{(\omega+\Omega_i')^2+\Omega_i''^2}\right]. \qquad (7.12)$$

Here the sum is over impurity positions $\mathbf{r}_i$ and $u(\mathbf{r}$

$-\mathbf{r}_i), v(\mathbf{r}-\mathbf{r}_i)$ are the eigenfunction of the Bogoliubov–de Gennes equation with an impurity.

Local effects of impurities are best revealed by local probes. NMR experiments on Cu in Zn-doped cuprates are quite useful in this regard. From Eq. (7.10) and below, one concludes immediately that the NMR signal shows two distinct relaxation rates (or even a hierarchy of rates) depending on the distance of the Cu sites from the impurity location. The Cu sites near the impurities couple to the higher LDOS and have a faster relaxation rate at low T. At a finite impurity concentration ($\sim 2\%$), the volume-averaged density of states is finite as $\omega \to 0$, and therefore the relaxation rate of Cu atoms close to and away from an impurity has the same temperature dependence, $(T_1 T)^{-1} = \text{const}$, but is of a different magnitude. Precisely this behavior has been observed experimentally. Ishida *et al.* (1991) measured two NMR relaxation rates for Cu in Zn-doped $YBa_2Cu_3O_{7-\delta}$. The second NMR signal with faster relaxation was inferred to arise from sites near the impurities. Alloul and collaborators (1991) pointed out that the NMR signal from sites close to impurities shows a distribution of relaxation rates, which reflects local electronic and magnetic distortions produced by the impurity in the host system; see Bobroff *et al.* (2001), and references therein.

More direct evidence for impurity-induced resonances in high-T_c superconductors came from scanning-tunneling microscopy. These experiments were crucial in establishing the existence of the impurity-induced resonances in cuprates and their anisotropic nature (Hudson *et al.*, 1999; Pan, Hudson, Lang, *et al.*, 2000) and are discussed in Sec. IX.

We contrast our picture of the dilute limit of strongly scattering centers with the usual approach of averaging over a finite concentration of impurities. In the latter approach, two distinct NMR relaxation rates, arising from inequivalent sites, cannot be resolved. Similarly, the inhomogeneous LDOS due to localized states is lost after averaging over impurity positions.

The distinction between true bound states and the continuum in nodal superconductors is not as well defined as in s-wave systems. Any finite temperature leads to a finite lifetime for bound states, and they hybridize with the continuum of low-energy extended quasiparticles since the two are not separated by an energy gap.

B. Single magnetic impurity problem

A full analysis for magnetic impurity is more involved. For a quantum spin one needs to address the Kondo effect, which is discussed in Sec. XI. In the simplified treatment of a classical spin ($S \gg 1$ or $T \gg T_K$) the mean-field analysis is similar to that in the previous section (Salkola *et al.*, 1997). In that case the main effect of the exchange coupling between the local moment S and electron spin is the renormalization of the effective scattering potential for electrons of two different spin orientations: they see a net impurity potential $U_0 \pm J$, where

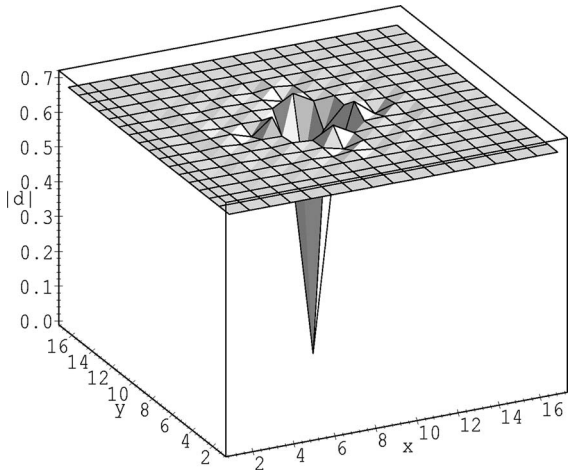

FIG. 5. Self-consistently determined gap function near the scalar impurity in a 2D d-wave superconductor. The gap suppression is strongly localized near the impurity site aside from weak oscillating tails. From Franz *et al.*, 1996.

U_0 is the potential scattering strength and J is the exchange coupling to the impurity spin. There are two virtual bound states, one for each electron-spin orientation, with energies

$$\Omega_{1,2} = -\frac{\Delta_0}{2N_0(U_0 \pm J)\ln|8N_0(U_0 \pm J)|}. \tag{7.13}$$

STM data on the Ni-doped high-T_c cuprate $Bi_2Sr_2CaCu_2O_{8+\delta}$ are fit well using this simple formula; see Sec. IX. Even in the classical limit the spin S may have its own dynamics, which was omitted in the mean-field approach of Salkola *et al.* (1997). Further studies are certainly desirable.

C. Self-consistent gap solution near impurity

Impurity scattering locally modifies the order parameter, and we discuss the self-consistent gap in 2D d-wave systems. To address these effects, one has to use the (numerically determined) exact electron spectra near the impurity and solve the self-consistent equation on the d-wave gap, defined on the bonds of a square lattice,

$$\Delta(i, i+\delta) = \frac{V_{i,i+\delta}}{2}\sum_n [u_n(i+\delta)v_n^*(i) + u_n^*(i)v_n(i+\delta)] \times \tanh\left(\frac{E_n}{2k_B T}\right). \tag{7.14}$$

Such numerical solutions were presented by Franz *et al.* (1996), Salkola *et al.* (1997), Tsuchiura *et al.* (2000), and Zhu, Lee, *et al.* (2000). Impurity scattering clearly suppresses the gap magnitude, and the suppression is the strongest at the impurity site. The gap quickly recovers to a bulk value, although there are oscillating tails at long distances due to $2k_F$ oscillations, as shown in Fig. 5.

Realistically the difference between the self-consistent and non-self-consistent solutions is not important be-

yond a few lattice spacings from the impurity site. Near such a site local gap suppression is clearly seen in the STM data; see Sec. IX.

For superconducting order parameters with complex internal structure there is a possibility that impurity couples to a soft mode other than the amplitude mode (Rainer and Vuorio, 1997). This was investigated for the nonunitary A-phase superconductor by Choi and Muzikar (1990), who concluded that an indirect coupling to the rotational mode may produce a local magnetic moment around the impurity site.

D. Spin-orbit scattering impurities

Spin-orbit coupling in impurity scattering in superconductors is much less thoroughly investigated than purely magnetic or potential scattering. The standard form of the spin-orbit-scattering equation due to Elliott (1954) and Yafet (1963) is

$$H_{\mathrm{SO,imp}} = \sum_{\mathbf{k},\mathbf{k}'} \lambda_{\mathrm{SO}} c^{\dagger}_{\mathbf{k},\alpha} \vec{\sigma}_{\alpha\beta} \cdot (\mathbf{k} \times \mathbf{k}') c_{\mathbf{k}'\beta}, \tag{7.15}$$

where λ_{SO} is the scattering strength. This coupling is present even for nonmagnetic impurities, provides pair breaking, and produces additional quasibound states inside the gap. The structure of these additional resonances and their response to a Zeeman magnetic field were studied by Grimaldi (1999, 2002), who concluded that in the limit of strong spin-orbit scattering the local DOS exhibits off-site particle-hole symmetric resonance (in contrast to potential scatterers), which is not split by the field.

In a different type of spin-orbit scattering from a magnetic impurity, the impurity spin is coupled to the orbital motion of conduction electrons. For 2D d-wave systems, this was investigated by experiments on Ni-doped Bi2212 (Movshovich *et al.*, 1998; Neils and Harlingen, 2002) and studied by Barash *et al.* (1997), Balatsky *et al.* (1998), and Graf *et al.* (2000). We write the Hamiltonian, $H_{\mathrm{SO,imp}} = \gamma_{\mathrm{SO}} \hat{\mathbf{L}} \cdot \mathbf{S}$, in second quantized notation,

$$H_{\mathrm{SO,imp}} = \sum_{\mathbf{k},\mathbf{k}'} \gamma_{\mathrm{SO}} c^{\dagger}_{\mathbf{k},\sigma} \mathbf{S} \cdot (\mathbf{k} \times \mathbf{k}') c_{\mathbf{k}'\sigma}, \tag{7.16}$$

where γ_{SO} is the strength of coupling and $\mathbf{S}$ is the impurity spin. Predominantly in-plane motion of electrons (as is the case in Bi2212) couples the angular momentum L_z with respect to the impurity site $\hat{\mathbf{L}}_z = i\hbar\partial_\phi$ to S_z. The net effect of this term is twofold. First, it is pair breaking, so that the gap is locally suppressed, and a resonance is formed. Even more interesting is the distortion of the $d_{x^2-y^2}$-wave order parameter in the vicinity of an impurity, which results from the nontrivial orbital structure of the d-wave order. This state is a linear combination of the state with $l_z = 2$ and $l_z = -2$, $\Delta(\phi) = \Delta_0 \cos(2\phi) \propto \exp(2i\phi) + \exp(-2i\phi) \sim x^2 - y^2$. The two orbital components are affected differently by scattering. Treating $H_{\mathrm{SO,imp}}$ perturbatively, one generates in first order the correction to the order parameter $\Delta' = i\Delta_0 \gamma_{\mathrm{SO}} \sin(2\phi) \sim xy$. There is a finite amplitude for the incoming d-wave pair $|\mathrm{in}\rangle \propto |x^2 - y^2\rangle$ to scatter into the $|\mathrm{out}\rangle \propto i|xy\rangle$ channel,

$$|\mathrm{out}\rangle = i\gamma_{\mathrm{SO}} \Delta_0 \hat{\mathbf{L}} \cdot \mathbf{S} |\mathrm{in}\rangle = i\hbar \gamma_{\mathrm{SO}} \Delta_0 \sin(2\phi), \tag{7.17}$$

generating an out-of-phase component of the order parameter near a spin-orbit impurity, coexisting with and induced by the original $d_{x^2-y^2}$ symmetry.

This illustrates nontrivial effects of impurity scattering in superconductors with orbital structure to the Cooper-pair wave function. For more details, see Balatsky (1998), Graf *et al.* (2000), and Zhu and Balatsky (2002). An applied magnetic field [which couples to L_z similarly to the S_z term in Eq. (7.17)] not only suppresses the d-wave order parameter but also produces the secondary d_{xy} component; see Franz and Tešanović (1998), Kuboki and Sigrist (1998), Laughlin (1998), Tanuma *et al.* (1998), and Balatsky (2000).

E. Effect of Doppler shift and magnetic field

The main effect of the Zeeman field is to split impurity-induced resonances (Grimaldi, 1999, 2002). The orbital effect of a magnetic field can be analyzed by considering the Doppler shift of the quasiparticle energy.

In the simplest approach, due to Galilean invariance, in the presence of a superflow with velocity $\mathbf{v}_S(\mathbf{r})$ electron propagators are modified by $G(\mathbf{k},\omega) \to G(\mathbf{k},\omega - \mathbf{k}\cdot\mathbf{v}_S)$ for a planar wave state at $\mathbf{k}$. The rest of the calculation for the impurity state follows exactly the previous analysis. The local scattering potential of the impurity requires summing over momenta to obtain the local Green's function $G_0(\omega)$, and only this local propagator enters the solution for the resonance, Eq. (7.1). Therefore changes in the resonance state are due to an increase in the density of states arising from the Doppler shift.

The effect of superflow produced by screening currents on the impurity resonance was studied by Samokhin and Walker (2001), who pointed out that the Doppler shift leads to broadening of the resonance. The scale of the effect is set by the ratio of the typical Doppler shift $v_S k_F$ at the impurity site to the resonance energy Ω'. If the Doppler shift is small, the effect is negligible, while in the opposite limit $v_S k_f \gg \Omega'$, superflow broadens the resonance significantly. Superflow does not shift the resonance energy.

Tsai and Hirschfeld (2002) analyzed the effect of an isolated impurity on the penetration depth of a d-wave superconductor. They concluded that the effect leads to a divergent $1/T$ contribution at finite temperatures, in close analogy with Andreev bound states (Walter *et al.*, 1998; Barash *et al.*, 2000).

F. Sensitivity of impurity state to details of band structure

Above we used a single-band model with particle-hole symmetry to prove the existence and explore the basic

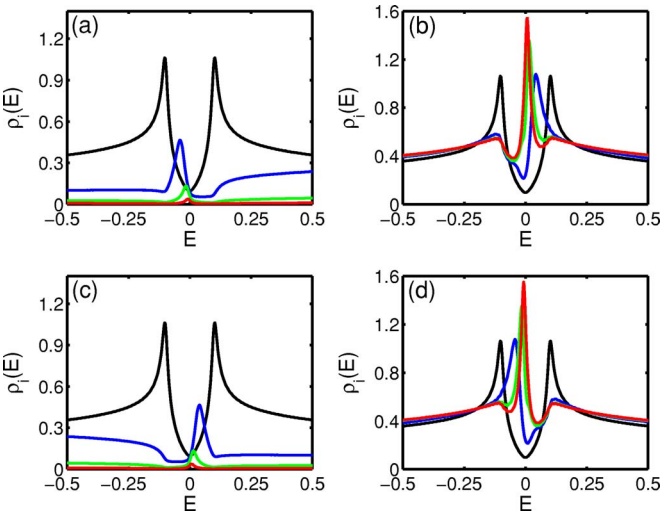

FIG. 6. (Color online) The LDOS as a function of energy at the impurity site (left panels) and at one of its nearest neighbors (right panels) in a 2D lattice. The upper panels are for the repulsive potential, $U_0=0,2,5,10$, while the lower panels are for the attractive potential, $U_0=0,-2,-5,-10$. Note that the resonance peak is pushed toward the Fermi energy as the potential strength is increased.

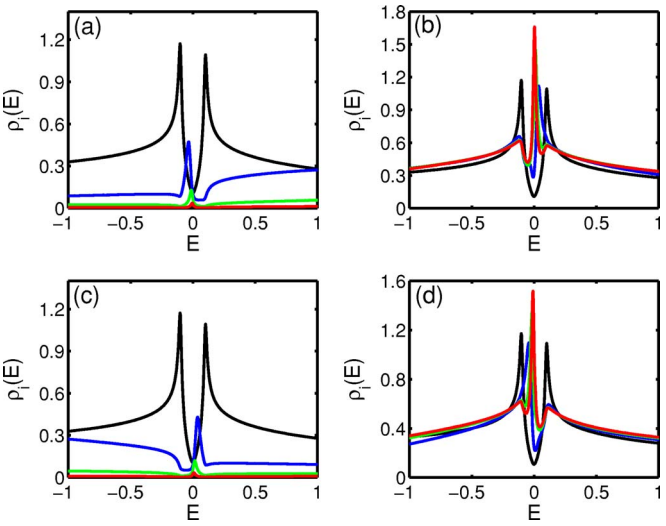

FIG. 7. (Color online) Same as Fig. 6 for $t=1$, $t'=-0.2$, and $\mu=-0.784$.

features of impurity-induced resonances. Real bands are asymmetric, and the effect of asymmetry was considered by Joynt (1997), who modeled it by a constant DOS with different energy cutoffs at the upper and lower limits. To make a quantitative comparison with the experimental data on impurity resonances (see Sec. IX), we have to understand the details of the band structure. For example, in cuprates in-plane Cu $d_{x^2-y^2}$ and O $p_{x,y}$ bands are relevant. Above we assumed that by reducing the complicated band structure of a high-T_c (or another) material to a single-band model, one can describe the nonmagnetic impurity by a single parameter, the on-site potential U_0. Reality is more complex.

Even within the one-band approach one can still explore the change in the position of the impurity-induced resonance beyond the simplest assumptions. The resonance position depends on the sign of the impurity potential, electron occupation numbers, and band structure. To illustrate the sensitivity to the latter we performed an exact diagonalization for the t-t'-V model with nearest-neighbor hopping t, next-nearest-neighbor hopping t', and a negative V that describes the nearest-neighbor attraction and produces d-wave pairing. The single-particle energy dispersion in the normal state is

$$\xi_k = -2t(\cos k_x + \cos k_y) - 4t' \cos k_x \cos k_y - \mu, \tag{7.18}$$

and μ is the chemical potential. The impurity was modeled by an on-site potential U_0. We considered three possibilities: (i) $t=1$, $t'=0$, $\mu=0$ (the filling factor $n=1.0$), with band particle-hole symmetry present, see Fig. 6; (ii) $t=1$, $t'=-0.2$, $\mu=-0.784$ ($n=0.84$), with no band particle-hole symmetry, see Fig. 7; and (iii) $t=1$, $t'=-0.3$, $\mu=-1.0$ ($n=0.85$), again with band particle-hole symmetry absent, see Fig. 8. We consider the band particle-hole symmetry because the local particle-hole symmetry is broken by the potential U_0.

As shown in Figs. 6–8, for (i) and (ii), the band DOS has two coherent peaks. Also for (ii), the DOS is asymmetric with respect to the zero energy. In these two situations, a repulsive potential $U_0>0$ leads to an impurity state at $\Omega_0'<0$, manifested by a peak in the LDOS below the Fermi energy at the impurity site. In contrast, the peaks are above the Fermi energy at the four nearest-neighbor sites. Correspondingly, an attractive impurity potential $U_0<0$ induces a state at $\Omega_0'>0$ at the impurity site, but below the Fermi energy at its nearest neighbors.

For (iii), in addition to two coherent peaks, there are also two Van Hove singularity peaks (more pronounced on the negative-energy side and faint at the positive side). For a repulsive impurity, the on-site resonance peak does shift from the negative-energy side slightly above the zero energy. This phenomenon is absent for (i)

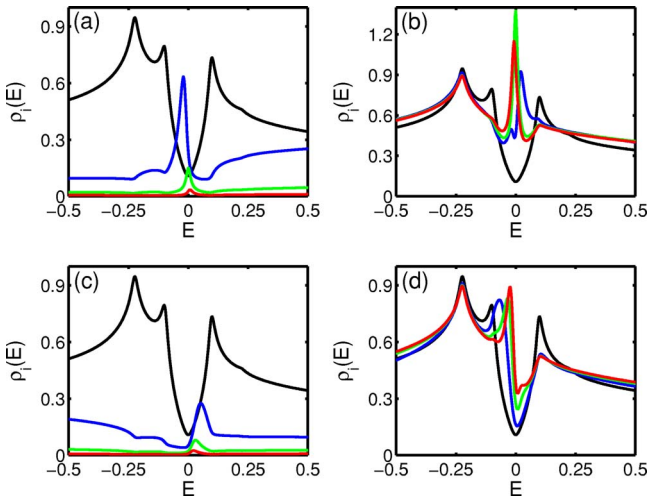

FIG. 8. (Color online) Same as Fig. 6 for $t=1$, $t'=-0.3$, and $\mu=-1.0$.

and (ii). For $U_0<0$, the result is similar to (i) and (ii). Here we consider the optimal doping regime for (ii) and (iii). At other dopings all possibilities discussed above could occur depending on band structure.

The sign of the impurity potential for Zn and Ni atoms in cuprates is still an unsettled issue. It is believed that these atoms substitute Cu in the Cu-O plane and do not change the hole doping. Then Zn^{2+} is in the d^{10} configuration, and the third ionization energy is a rough measure of the impurity potential U_0 (even though the Cu d orbitals form a band). By comparing the energies of the Cu atom $E_{Cu^{2+}}=-36.83$ eV and the Zn atom $E_{Zn^{2+}}=-39.722$ eV, we estimate $U_0\simeq-2.89$ eV. Therefore the Zn atom plays the role of a strong attractive potential in the Cu-O lattice. The location of the level at negative energy is consistent with the d^{10} configuration.

Ni^{2+} has a $3d^8$ shell and a spin $S=1$ ground state. Therefore to describe the effect of the Ni impurity we need to account for both potential (U_0) and magnetic (J) scattering. We estimate the energy U_0 by taking the difference between atomic energies using $E_{Ni^{2+}}=-35.17$ eV to find $U_0\simeq1.66$ eV for Ni. Compared to Zn, its potential is weaker and repulsive. Similar conclusions about the sign and strength of Zn and Ni impurities were reached recently in a more sophisticated three-band model (Xiang *et al.*, 2002).

For a detailed comparison of the results from model calculations with the experimental data, the band-structure effects need to be well understood. Ultimately we need realistic band-structure calculations with impurities for these complex materials.

VIII. SINGLE-IMPURITY BOUND STATE IN A PSEUDOGAP STATE OF TWO-DIMENSIONAL METALS

A. General remarks on impurities in a pseudogap state

A natural question to address is whether superconductivity, or even any off-diagonal long-range order, is required for a resonance state, and we address this in the experimentally relevant context of cuprates. Many experiments (Norman *et al.*, 1998; Renner *et al.*, 1998; Loram *et al.*, 2000) show that in high-T_c systems the electronic density of states near the Fermi surface is suppressed above the superconducting transition temperature T_c, but below a characteristic temperature T^*. The energy range of this suppression, Δ_{PG}, is known as the pseudogap, and its origin has been hotly debated; see Timusk and Statt (1999) and Timusk (2003). Scenarios for this anomalous phenomenon include precursors to superconductivity, such as a preformed pair with phase fluctuations (Emery abd Kivelson, 1995), Bose-Einstein condensation of Cooper pairs (Chen *et al.*, 1998), as well as various competing orders not related to superconductivity, such as the time-reversal–symmetry-breaking circulating current (Varma, 1999) and the unconventional d-density wave (Chakravarty *et al.* 2001). The latter is a variant of the staggered flux state (Affleck and Marston, 1988; Marston and Affleck, 1989; Hsu *et al.*, 1991). In the first scenario, the "normal" state contains preformed Cooper pairs, but phase fluctuations of the pairing field destroy the long-range order, that is, the bulk superconductivity. Since at the onset the pairing field has d-wave symmetry in the momentum space, a d-wave pseudogap follows.

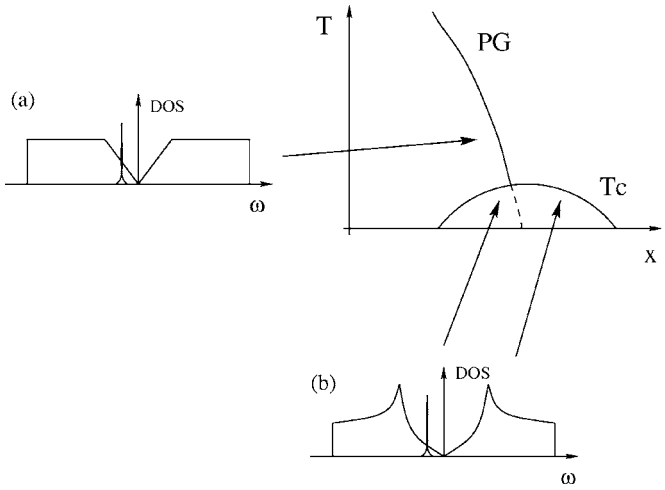

FIG. 9. An impurity state in a high-T_c superconductor: (a) The DOS in the pseudogap regime used here [see also Altland and Zirnbauer (1997)] and (b) the DOS in the superconducting state as used by Abanov and Chubukov (2000). In both phases there is a resonant state.

Here, instead of discussing the origin of the pseudogap, we model it phenomenologically in some of these scenarios and study electronic properties around a single impurity. If a STM measurement is done at different temperatures, there are two possibilities for the evolution of an impurity resonance at $T>T_c$: (a) it gradually broadens and disappears when the superconductivity vanishes, as in a conventional superconductor; and (b) the resonance broadens but survives above in the pseudogap state. It was argued experimentally (Krasnov *et al.*, 2000; Loram *et al.*, 2000) that in underdoped cuprates the superconducting gap and pseudogap are separate phenomena, and we show below that the resonance survives above T_c. We find that its position and width depend on both the impurity scattering strength and the pseudogap energy scale.

Our simplest model of the (unrelated to superconductivity) pseudogap is a metallic state with linearly vanishing DOS around the Fermi energy, but no off-diagonal order; see Fig. 9. This simplification allows analytical calculations and provides a "reference point" for the impurity state in the pseudogap regime. Once again we focus on the Zn substitution for Cu and use the T-matrix approach. We find that the depletion of the DOS alone is sufficient to produce a resonance near a nonmagnetic impurity.

The analysis is quite general and similar to that of Sec. V and Balatsky *et al.* (1995). The states generated by the impurity are given by the poles Ω of the T matrix,

$$g_0(\Omega) = \frac{1}{U_0}. \tag{8.1}$$

This is an implicit equation for $\Omega(U_0)$, and complex solutions indicate the resonant nature of the state. To solve it, we need the unperturbed local Green's function on the impurity site, $g_0(E)=g_0'+ig_0''$, where the imaginary part is given by $g_0''(\omega)=-\pi N_0(\omega)$ and $N_0(\omega)$ is the bulk DOS.

Measurements of the electronic specific heat by Loram *et al.* (2000) showed that the pseudogap opens below hole doping $p_{\rm crit}\sim 0.19$ hole/CuO_2 and has a V-shaped energy profile. Guided by these data, we assume that low-energy electronic states are partially depleted, so that $N_0(\omega)=N_0|\omega|/\Delta_{\rm PG}$ for $|\omega|\leqslant\Delta_{\rm PG}$ and $N_0(\omega)=N_0$ for $\Delta_{\rm PG}<|\omega|<W/2$ with W the bandwidth; see Fig. 10(a). We use this DOS to generate solutions of Eq. (8.1). Clearly, the precise position and width of the resonance depend on the specific form chosen for $N(\omega)$ (in our case linear). Results for other forms of $N(\omega)$ are very similar.[5]

Using this DOS for g_0'' and invoking the Kramers-Kronig relation (see, e.g., Mahan 2000),

$$g_0'(\omega) = \frac{1}{\pi}\int_{-\infty}^{\infty} d\omega' g_0''(\omega') P\left(\frac{1}{\omega'-\omega}\right), \tag{8.2}$$

with P the Cauchy principal value, we find

$$g_0'(\omega) = -N_0 \ln\left|\frac{\frac{W}{2}-\omega}{\frac{W}{2}+\omega}\right| + N_0 \ln\left|\frac{\Delta_{\rm PG}-\omega}{\Delta_{\rm PG}+\omega}\right| - N_0\frac{\omega}{\Delta_{\rm PG}}\ln\left|\frac{\Delta_{\rm PG}^2-\omega^2}{\omega^2}\right|. \tag{8.3}$$

Figure 10(b) shows $g_0'(\omega)$ together with $1/U_0$ to obtain a graphical solution as in Fig. 3. For $2U_0N_0>1$, Eq. (8.1) has four solutions. Since the width of the resonance is proportional to $|\Omega|$, only solutions with $|\Omega|$ close to zero are sharp. Expanding in ω in Eq. (8.3) we find

[5]We argue that the appearance of the ingragap impurity state is a robust feature of any depleted DOS around the Fermi surface. We have considered a model with $N_0(\omega)=N_0[a+(1-a)\omega^2/\Delta_{\rm PG}^2]$, which is similar to a resonant state at

$$\Omega = -\Delta_{\rm PG}(1+i\pi a N_0U_0)/[4N_0U_0(1-a\Delta_{\rm PG}/W)]$$
$$\approx -\Delta_{\rm PG}(1+i\pi a N_0U_0)/[4N_0U_0(1-a)]$$

when $\Delta_{\rm PG}/W\ll 1$. For a fully gapped DOS, $N(\omega)=N_0$ for $|\omega|\in[\Delta_{\rm PG},W/2]$ and zero otherwise. The resonant state is at $\Omega=-\Delta_{\rm PG}/(2U_0N_0)$.

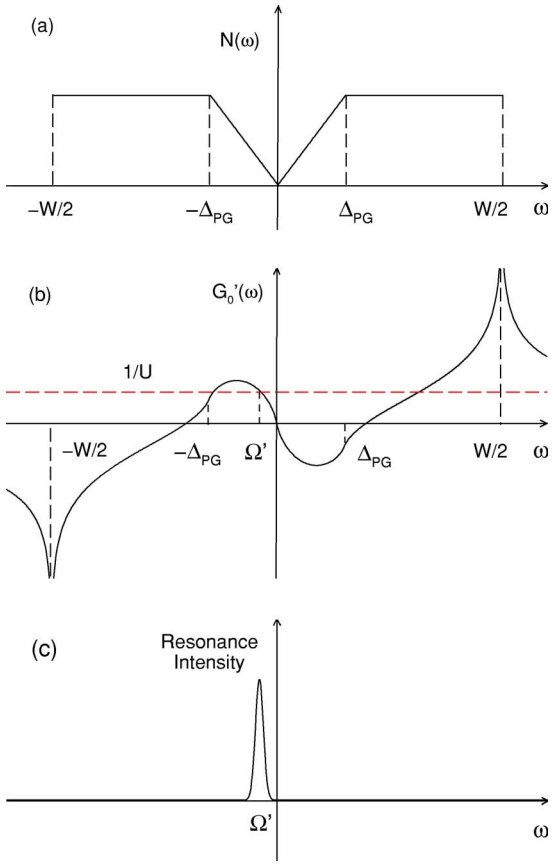

FIG. 10. (Color online) Impurity-induced resonance states. (a) The density of states $N(\omega)=-g_0''(\omega)/\pi$ for the model discussed in the text. (b) The real part $g_0'(\omega)$ of the Green's function together with $1/U_0$ and U_0 positive. Ω' is the real part of the solution of $g_0(\Omega)=1/U_0$. (c) The impurity-induced resonance at $\Omega'=-\Delta_{\rm PG}/2U_0N_0\ln(2U_0N_0)$. The other three solutions of Eq. (8.1) are much broader and are not depicted. All plots are at the impurity site. From Kruis, Martin, and Balatsky (2001).

$$g_0(\Omega) = -\frac{2\Omega N_0}{\Delta_{\rm PG}}\left[\ln\left|\frac{\Delta_{\rm PG}}{\Omega}\right| + 1 - \frac{i\pi\,\mathrm{sgn}(U_0)}{2}\right] = \frac{1}{U_0}. \tag{8.4}$$

This equation can be solved exactly in terms of Lambert's W functions,[6] which to logarithmic accuracy in $\ln|2U_0N_0|>1$, gives $\Omega=\Omega'+i\Omega''$ with[7]

$$\Omega' = -\frac{\Delta_{\rm PG}}{2U_0N_0}\frac{1}{\ln|2U_0N_0|}\left[1-\frac{1}{\ln|2U_0N_0|}\right], \tag{8.5}$$

[6]The exact solution in terms of Lambert's W function, $Lw(-1,x)$, defined from $Lw(x)\exp[Lw(x)]=x$, is $\Omega=-\Delta_{\rm PG}\mathrm{sgn}(U_0)\exp\{Lw[-1,-\mathrm{sgn}(U_0)\exp(i\pi/2-1)/(2N_0U_0)]+1-i\pi/2\}$.

[7]The simplest model for thermal broadening is to assign the temperature-dependent width. Thermal broadening at high temperatures $T>T_c$ substantially broadens the impurity resonance peak $\Omega''(T)=\sqrt{[\Omega''(T=0)]^2+T^2}$.

$$\Omega'' = -\frac{\pi\Delta_{\rm PG}\,\mathrm{sgn}(U_0)}{4U_0N_0\ln^2|2U_0N_0|}. \tag{8.6}$$

Here Ω' is the energy position and Ω'' is the decay rate.

Using Eq. (8.5) for Zn doping in cuprates and setting $N_0=1$ state/eV, $\Delta_{\rm PG}\sim 300$ K ~ 30 meV, and the scattering potential $U_0\approx\pm 2$ eV, we estimate $\Omega\sim\pm 2$ meV $\sim\pm 20$ K as found by Loram *et al.* (2000). This value is close to the Zn resonance energy $\omega_0=-16$ K, seen in the superconducting state (Pan, Hudson, Lang *et al.*, 2000). By combining these results with band-structure arguments (Martin *et al.*, 2002), we conclude that the Zn impurity in Bi2212 is strongly attractive, with $U_0\sim -2$ eV. This value, as we show below, is modified due to the particle-hole asymmetry expected in doped cuprates.

A similar calculation can be done in the absence of particle-hole symmetry. The simplest way to introduce the asymmetry is by making the upper and lower cutoffs in the DOS different, i.e., keep the bare density of states featureless, but move the chemical potential μ away from the middle of the band. The pseudogap is still centered at the chemical potential. Therefore the calculation proceeds as above with the sole change being in the first logarithmic term of Eq. (8.3),

$$-N_0\ln\left|\frac{W/2-\mu-\omega}{W/2+\mu+\omega}\right|. \tag{8.7}$$

Neglecting the frequency ω relative to the chemical potential μ and assuming that μ is small relative to the bandwidth, we find that the asymmetric case can be mapped onto the symmetric situation by the substitution

$$\frac{1}{U^0}\to\frac{1}{U^0}-\frac{4N_0\mu}{W}. \tag{8.8}$$

The effect of the asymmetry can be estimated. In cuprates, for 20% hole doping, $\mu\sim -(1/5)W/2=-W/10$. Hence the modified value for the Zn impurity strength in Bi2212 can be obtained from the symmetric result, $1/U^*=1/U_0+4N_0\mu/W$. The new value is $U^*\sim -1$ eV, which is a strongly attractive potential, as is expected from band-structure arguments.

The solution for the resonance state involves determining the energy position and width of the resonance, as well as the real-space shape of the impurity state. The energy of the resonance for a local impurity potential U_0 depends only on the local propagator $g_0(\omega)$. Hence knowledge of the DOS (related to the imaginary part of the on-site propagator) is sufficient to determine (via Kramers-Kronig relations) the real part of g_0 and to find the energy of the impurity state. On the other hand, to determine the real-space image of the resonance, one requires more knowledge of the state and its Green's function. Quite generally, for a *d*-wave-like pseudogap with nearly nodal points along the $(\pm\pi/2,\pm\pi/2)$ directions, the impurity resonance is fourfold symmetric, similar to superconducting solutions (Balatsky *et al.*, 1995). However, any detailed calculation requires a more specific model for the pseudogap state. Some of these are considered below.

B. Impurity state in pseudogap models

1. *d*-density wave

This model postulates the mean-field Hamiltonian (Chakravarty *et al.*, 2001)

$$H_0=\sum_{ij,\sigma}[-t_{ij}+(-1)^i iW_{ij}]c^\dagger_{i\sigma}c_{j\sigma}-\mu\sum_{i,\sigma}c^\dagger_{i\sigma}c_{i\sigma}, \tag{8.9}$$

with the order parameter W_{ij} defined at the bonds of a square lattice, $W_{i,i\pm\hat{x}}=W_{\pm\hat{x}}=W_0/4$ and $W_{i,i\pm\hat{y}}=W_{\pm\hat{y}}=-W_0/4$, and zero otherwise. The prefactor $i=\sqrt{-1}$ indicates that the *d*-density-wave state breaks the time-reversal symmetry. In momentum space,

$$H_0=\sum_{k,\sigma}\xi_k c^\dagger_{k\sigma}c_{k\sigma}+\sum_{k,\sigma}iW_k[c^\dagger_{k\sigma}c_{k+Q,\sigma}-c^\dagger_{k+Q,\sigma}c_{k\sigma}]. \tag{8.10}$$

We take the single-particle energy $\xi_{\mathbf{k}}$ from Eq. (7.18), with $t'=0$ for simplicity. For k_x and k_y in the first Brillouin zone, the *d*-density-wave gap is *d*-wave-like,

$$W_k=\frac{W_0}{2}(\cos k_x-\cos k_y). \tag{8.11}$$

d-density-wave order breaks the symmetry with respect to translations by a lattice constant a along x or y, but preserves translations by $\sqrt{2}a$ along the diagonals of the square lattice. Therefore it is convenient to rewrite the Hamiltonian in the reduced Brillouin zone. Introducing a two-component operator $\Psi^\dagger_{k\sigma}=(c^\dagger_{k\sigma},c^\dagger_{k+Q,\sigma})$ with $\mathbf{Q}=(\pi,\pi)$, we find

$$H_0=\sum_{k\in\mathrm{rBZ},\sigma}\Psi^\dagger_{k\sigma}\begin{pmatrix}\xi_k & i2W_k\\ -2iW_k & \xi_{k+Q}\end{pmatrix}\Psi_{k\sigma}, \tag{8.12}$$

where rBZ denotes the reduced Brillouin zone.

In analogy with Gor'kov-Nambu notation, we introduce the matrix Green's functions (cf. Sec. II.C)

$$\hat{\mathcal{G}}^{(0)}(k;\tau)=\begin{pmatrix}\mathcal{G}^{(0)}_{11} & \mathcal{G}^{(0)}_{12}\\ \mathcal{G}^{(0)}_{21} & \mathcal{G}^{(0)}_{22}\end{pmatrix}, \tag{8.13}$$

where

$$\mathcal{G}^{(0)}_{11}(k;\tau)=-\langle T_\tau[c_{k\sigma}(\tau)c^\dagger_{k\sigma}(0)]\rangle, \tag{8.14a}$$

$$\mathcal{G}^{(0)}_{12}(k;\tau)=-\langle T_\tau[c_{k\sigma}(\tau)c^\dagger_{k+Q,\sigma}(0)]\rangle, \tag{8.14b}$$

$$\mathcal{G}^{(0)}_{21}(k;\tau)=-\langle T_\tau[c_{k+Q,\sigma}(\tau)c^\dagger_{k\sigma}(0)]\rangle, \tag{8.14c}$$

$$\mathcal{G}^{(0)}_{22}(k;\tau)=-\langle T_\tau[c_{k+Q,\sigma}(\tau)c^\dagger_{k+Q,\sigma}(0)]\rangle. \tag{8.14d}$$

From the Hamiltonian Eq. (8.12), using an equation of motion for the operators $c_{k\sigma}$ and $c^\dagger_{k\sigma}$, and by performing a Fourier transform with respect to τ, we find

$$\hat{\mathcal{G}}^{(0)}(k;i\omega_n)=\begin{pmatrix}i\omega_n-\xi_k & -2iW_k\\ 2iW_k & i\omega_n-\xi_{k+Q}\end{pmatrix}^{-1}. \tag{8.15}$$

To solve for the bound state we need the Green's function in real space,

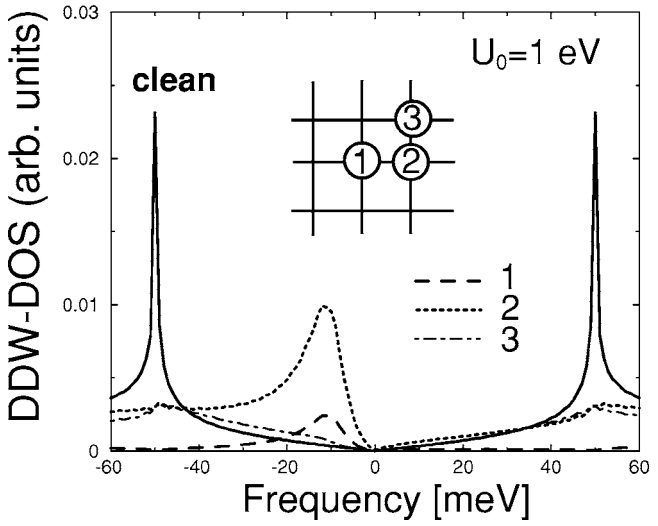

FIG. 11. d-density wave (DDW) DOS for the clean case (solid line) and in the presence of a nonmagnetic impurity with U_0 =1 eV: (1) DOS on the impurity site, (2) DOS on the nearest-neighbor site, and (3) DOS on the next-nearest-neighbor site. The other parameter values are t=300 meV, W_0=25 meV, t' =0, and μ=0. From Morr, 2002.

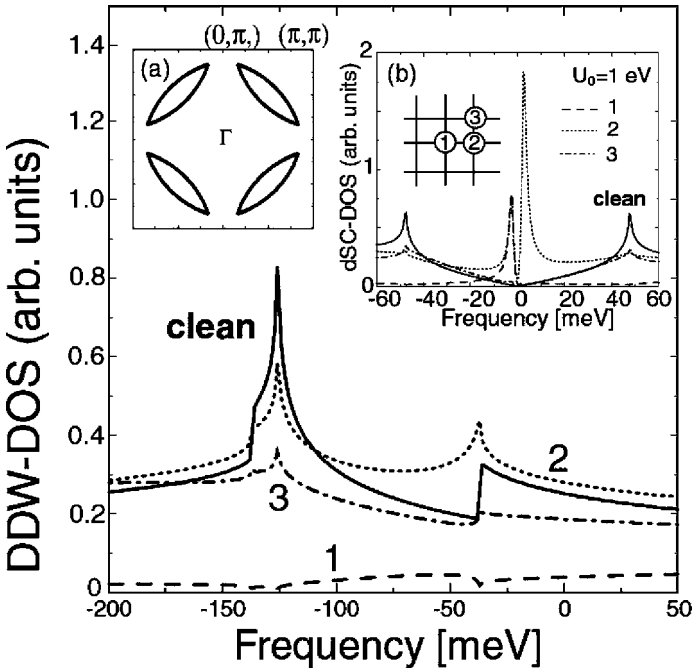

FIG. 12. DDW-DOS for the clean and iimpure cases. (a) Fermi surface in the DDW state with $t'=-0.3t$, $\mu=-0.91t$ (hole doping of 10%), and W_0=25 meV. The hole pockets are centered around $(\pm\pi/2,\pm\pi/2)$. (b) DOS in the DDW state with the same band parameters as in (a), for the clean case (solid line) and in the presence of a nonmagnetic impurity with U_0 =1 eV: (1) DOS on the impurity site, (2) DOS on the nearest-neighbor site, and (3) DOS on the next-nearest-neighbor site. Inset: Superconducting DOS for the same band parameters as in (a). From Morr, 2002.

$$\mathcal{G}^{(0)}(i,j;i\omega_n)=\frac{1}{N}\sum_{k\in \mathrm{rBZ}} e^{i\mathbf{k}\cdot\mathbf{R}_{ij}}[\mathcal{G}_{11}^{(0)}(k;i\omega_n)+\mathcal{G}_{22}^{(0)}(k;i\omega_n) + e^{-i\mathbf{Q}\cdot\mathbf{R}_j}\mathcal{G}_{12}^{(0)}(k;i\omega_n)+e^{i\mathbf{Q}\cdot\mathbf{R}_i}\mathcal{G}_{21}^{(0)}(k;i\omega_n)], \tag{8.16}$$

where $\mathbf{R}_i$ are lattice vectors and $\mathbf{R}_{ij}=\mathbf{R}_i-\mathbf{R}_j$. From Eqs. (8.15) and (8.16), the local Green's function is

$$\mathcal{G}^{(0)}=\frac{1}{N}\sum_{k\in \mathrm{rBZ}}\frac{2i\omega_n-\xi_{k+Q}-\xi_k}{(i\omega_n-\xi_k)(i\omega_n-\xi_{k+Q})-4W_k^2}. \tag{8.17}$$

We now analyze the scattering on a single nonmagnetic impurity in the d-density-wave state. Without loss of generality, hereafter we assume that the impurity is located at the origin. The poles of the T matrix give the energy of the resonance state, i.e., once again

$$\mathcal{G}^{(0)}(0,0;\omega+i0^+)=\frac{1}{U_0}. \tag{8.18}$$

The real-space map of resonant states is manifested in the local density of states,

$$N_i(\omega)=-\frac{2}{\pi}\,\mathrm{Im}\,\mathcal{G}(i,i;\omega+i\delta). \tag{8.19}$$

Numerical results are displayed in Figs. 11 and 12. It is clear that the electronic excitation spectrum around the impurity in the d-density-wave state is very sensitive to the band structure. For $t'=0$ and at half-filling ($\mu=0$), the electron density of states of a pure d-density-wave system vanishes at the Fermi energy. Therefore in the presence of an impurity resonance states appear at low energies. With $t'=0$ and with the system doped away from half-filling, the resonant peak in the LDOS is shifted away from the Fermi energy. This is because the energy at which the band DOS vanishes no longer coincides with the Fermi energy. For more realistic parameter values, the density of states in the clean limit shows essentially no reduction at low energies, and the LDOS near the impurity does not exhibit any signature of a resonance state. These results were independently obtained by Zhu *et al.* (2001), Morr (2002), and Wang (2002). The quasiparticle states in the d-density-wave state with a finite concentration of nonmagnetic impurities have been investigated by Ghosal and Kee (2004).

2. Phase-fluctuation scenario

We now discuss the impurity state in a phase-fluctuating superconductor; see Wang (2002) for details. The mean-field Hamiltonian for a d-wave superconductor on a square lattice is

$$H=\sum_{ij}\Psi_i^\dagger\begin{pmatrix}-t_{ij}-\mu\delta_{ij} & -\Delta_{ij}\\ -\Delta_{ij}^* & -(-t_{ji}-\mu\delta_{ij})\end{pmatrix}\Psi_j, \tag{8.20}$$

where $\Psi_i^\dagger=(c_{i\uparrow}^\dagger,c_{i\downarrow})$ is the Nambu spinor, Δ_{ij} is defined on the bonds in analogy to Sec. VII.C, and its phase is allowed to fluctuate, while its amplitude is fixed,

$$\Delta_{ij} = \frac{\Delta_0 \eta_{ij}}{4} e^{i\varphi_{ij}} = \tilde{\Delta}_{ij} e^{i\varphi_{ij}}. \tag{8.21}$$

For d-wave pairing, $\eta_{ij}=1$ (-1) for x (y) direction bonds and phase $\varphi_{ij}=(\varphi_i+\varphi_j)/2$. Spatial variation of the phase gives rise to superfluid flow of the Cooper pairs. By performing a gauge transformation,

$$\tilde{\Psi}_i = e^{-i\varphi_i \sigma_3/2} \Psi_i, \tag{8.22}$$

where σ_3 is the Pauli matrix, we transfer the phase from the pairing field to the hopping t, so that

$$\tilde{H} = \sum_{ij} \tilde{\Psi}_i^{\dagger} \begin{pmatrix} -\tilde{t}_{ij} - \mu\delta_{ij} & -\tilde{\Delta}_{ij} \\ -\tilde{\Delta}_{ij}^{*} & -(-\tilde{t}_{ji} - \mu\delta_{ij}) \end{pmatrix} \tilde{\Psi}_j, \tag{8.23}$$

where $\tilde{t}_{ij}=t_{ij}e^{-i(\varphi_i-\varphi_j)/2}$. Assuming that the length scale of the phase variation (the London penetration depth) is much greater than the Fermi wavelength, we can define the phase for the Cooper pair $\varphi_i=2\mathbf{q}_s\cdot\mathbf{R}_i$, where $\mathbf{q}_s$ is the average momentum per electron in the superfluid state. This ansatz gives the Green's function

$$\hat{\mathcal{G}}^{(0)}(k;q_s;i\omega_n) = \begin{pmatrix} i\omega_n - \xi_{k+q_s} & -\Delta_k \\ -\Delta_k^{*} & i\omega_n + \xi_{k-q_s} \end{pmatrix}^{-1}, \tag{8.24}$$

for pure systems, where $\Delta_k=(\Delta_0/2)(\cos k_x-\cos k_y)$ and the $\xi_{\mathbf{k}}$ is given by Eq. (7.18).

In the presence of a nonmagnetic impurity at site $i=(0,0)$, the Green's function becomes

$$\hat{\mathcal{G}}(i,j;q_s;i\omega_n) = \hat{\mathcal{G}}^{(0)}(i,j;q_s;i\omega_n) + \hat{\mathcal{G}}^{(0)}(i,0;q_s;i\omega_n) \times \hat{T}(q_s;i\omega_n)\hat{\mathcal{G}}^{(0)}(0,j;q_s;i\omega_n), \tag{8.25}$$

$$\hat{T}^{-1}(i\omega_n;\mathbf{q}_s) = \hat{\tau}_3/U_0 - \hat{\mathcal{G}}^{(0)}(0,0;q_s;i\omega_n). \tag{8.26}$$

For fixed $\mathbf{q}_s$, the LDOS at site i is given by

$$N(i;q_s;\omega) = -(2/\pi)\mathrm{Im}\,\mathcal{G}_{11}(i,i;q_s;\omega+i0^{+}). \tag{8.27}$$

Averaging over fluctuating phases in Δ_{ij} is equivalent to averaging over $\mathbf{q}_s$. If the fluctuations are thermal, the statistical distribution of $\mathbf{q}_s$ is Gaussian, $\rho(q_s)=e^{-q_s^2/2n_v}/\Sigma_{q_s}e^{-q_s^2/2n_v}$, where $n_v=\exp[-\sqrt{aT_c/(T-T_c)}]$ is the vortex concentration, as in the Kosterlitz-Thouless theory (Kosterlitz and Thouless, 1973, 1974; Sheehy *et al.*, 2001). In the continuum limit, $\sqrt{\langle q_s^2\rangle}=\sqrt{n_v}$. The averaged LDOS is caculated as $N(i;\omega)=\langle N(i;q_s;\omega)\rangle$.

The results are shown in Fig. 13. For small n_v, the resonance peak is sharp and similar to that in the superconducting state ($n_v=0$). As n_v is increased, the peak is broadened and its height is reduced until the spectrum at low energies becomes featureless.

We can therefore compare the predictions of different models. In the phase-fluctuation scenario, the electron excitation spectrum around the impurity is very sensitive to how far the temperature is from the actual T_c. In contrast, in the normal-state ordering scenario, resonance states are not sensitive to the temperature up to the closing of the pseudogap. Notice that the energy of the resonance state in the phase-fluctuation scenario is not sensitive to doping while in the state with normal (particle-hole) ordering it shifts with doping. Generally, if superconducting fluctuations are present, a satellite peak appears at the opposite bias due to the particle-hole nature of Bogoliubov quasiparticles. The relative magnitude of the particle and hole parts of the impurity spectrum can be used to determine the extent to which the pseudogap is governed by superconducting fluctuations. For a fully nonsuperconducting pseudogap (e.g., the d-density-wave state), there is no counterpart state. Together with other proposals (Janko *et al.*, 1999; Martin and Balatsky, 2000), the study of impurity resonances can help to better understand the mysterious pseudogap state.

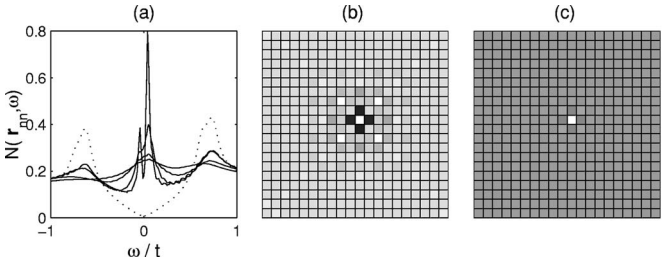

FIG. 13. Local density of states with $\Delta_0=0.68t$, $\mu=-0.3t$, $t'=0$, and $U_0=100t$. (a) $N(\mathbf{r}_{nn},\omega)$ vs ω. Solid lines: $n_v=10^{-6}$, 10^{-4}, 10^{-3}, and 5×10^{-3} with decreasing peaks. The dotted line is the LDOS at $n_v=0$ and $U_0=0$ for comparison. (b) $N(\mathbf{r},0.05t)$ at $n_v=0$. The impurity is at the center. (c) The same as (b) for $n_v=5\times10^{-3}$. The gray scale is the same in (b) and (c). From Wang, 2002.

IX. SCANNING-TUNNELING MICROSCOPY RESULTS

A. STM results around a single impurity

Experimental attempts to detect and accurately resolve subgap features in the density of states in superconductors with impurities have a long history. Their signatures were found early in planar junctions doped with magnetic impurities (Dumoulin *et al.*, 1975, 1977), but a direct observation using scanning-tunneling spectroscopy (STS) only became possible in the late 1990s. Yazdani *et al.* (1997) deposited adatoms, Mn, Gd, and Ag, on the (110)-oriented surface of a superconducting Nb sample and examined the electronic structure around them. Figure 14 shows the tunneling spectra. The main findings are as follows: (i) The local density of states is essentially identical in the vicinity of Ag impurity atoms and far away from them. This is consistent with the belief that Ag is nonmagnetic. (ii) Near magnetic Mn and Gd atoms the LDOS is enhanced at the length scale of 10 Å, at energies below the Nb superconducting gap, indicating that the impurity states are bound. (iii) The LDOS spectra are asymmetric about the Fermi energy. Within the Bogoliubov–de Gennes theory, a two-parameter magnetic impurity model was used, in which electrons are coupled with the impurity through both a magnetic exchange interaction J and a nonmag-

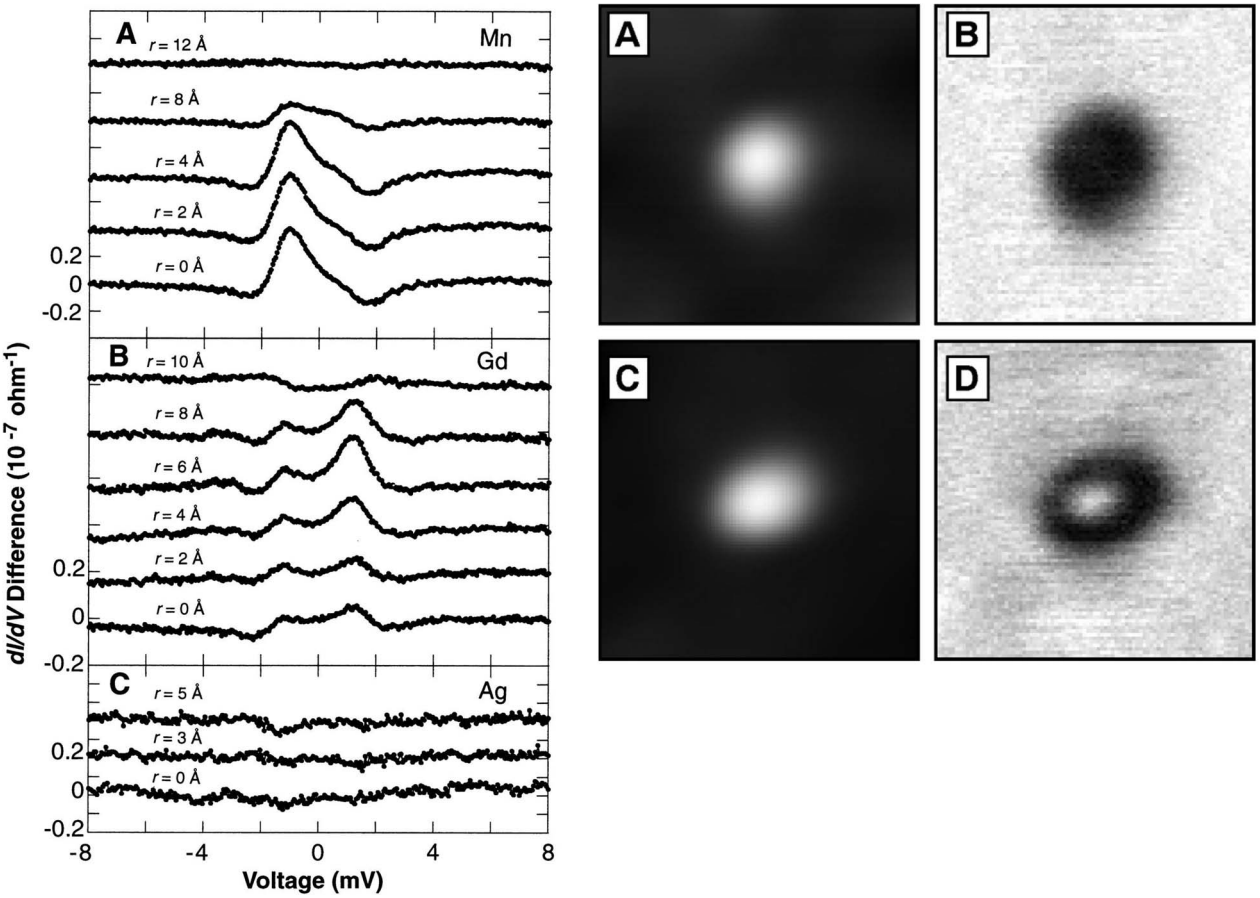

FIG. 14. Differential local tunneling conductance in the vicinity of single impurity in *s*-wave superconductor. Left panel: The dI/dV spectra measured near (a) Mn, (b) Gd, and (c) Ag atoms and far away from the impurity. Right panel: Constant-current topographs and simultaneously acquired dI/dV images show the spatial extent of the bound state near Mn and Gd adatoms. (a) Constant-current (32 Å by 32 Å) topograph of a Mn adatom. (b) Image of dI/dV near the Mn adatom acquired simultaneously with the topograph in (a). Reduced dI/dV (dark areas) marks the bound state. The contrast is reversed because dc bias voltage was chosen well above the energy of the bound state, and the resonance affects dI/dV only indirectly. (c) Constant-current (32 Å by 32 Å) topograph of a Gd adatom. (d) Image of dI/dV near the Gd adatom acquired simultaneously with the topograph in (c). From Yazdani *et al.*, 1997.

netic potential scattering U. The results obtained were consistent with the Yu-Shiba-Rusinov prediction and more recent theories (Yazdani *et al.*, 1997) and fit the experimental data. However, the model calculation required the value of J of the order of 4 eV in the strong coupling limit and failed to capture the detailed spatial dependence of the spectra around the Gd site.

Byers, Flatte, and Scalapino (1993) were the first to suggest the use of STM to study local effects of impurities in the superconducting state. Balatsky and coworkers (Balatsky *et al.*, 1995; Salkola *et al.*, 1996) predicted that quasiparticle resonance states are induced around a nonmagnetic impurity in a *d*-wave superconductor, in striking contrast to *s*-wave systems. The pioneering STM experiments which tested these predictions were carried out in nominally pure samples of the high-T_c cuprate $Bi_2Sr_2CaCu_2O_{8+\delta}$ (BSCCO) by Eigler (Yazdani *et al.*, 1999) and Davis (Hudson *et al.*, 1999). The STM spectra clearly showed enhancement of the local density of states close to zero bias near chemically induced defects. These experiments provided strong evidence for the existence of low-energy quasiparticle resonance states around single nonmagnetic impurities, as predicted theoretically. The asymmetry or splitting of the measured resonance was conjectured to be the result of the breaking of the particle-hole symmetry by local defects or from the asymmetry of the underlying realistic band structure of BSCCO (Flatte and Byers, 1998; Zhu, Lee, *et al.*, 2000). However, in these experiments the location in the crystal and identity of these scattering centers were unknown. Moreover, since enhancement of the LDOS at these scattering centers is not large, and since the coherence of high-T_c superconductors is short, it was difficult to investigate in detail the LDOS at the atomic scale.

STM studies on $Bi_2Sr_2Ca(Cu_{1-x}Zn_x)_2O_{8+\delta}$ single crystals intentionally doped with $x=0.6\%$ Zn were reported by Pan, Hudson, Lang, *et al.* (2000). Zn^{2+} has a filled d shell and hence acts as a strong potential scatterer for holes in the CuO_2 plane. Therefore, according to the predictions of Balatsky *et al.*, the quasiparticle resonance is expected close to the Fermi energy. To search for it,

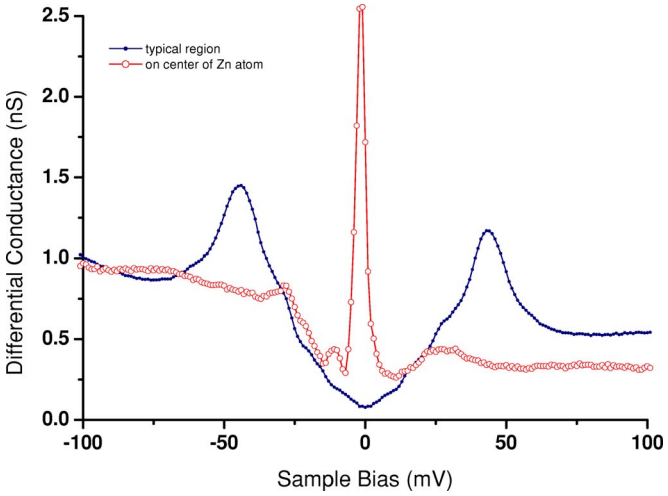

FIG. 15. (Color online) Differential tunneling spectra taken at the Zn-atom site (open circles) and a location far away from the impurity (filled circles). Note that on the impurity site one has peaks at both positive and negative bias albeit of very different magnitude that are a reflection of the particle-hole character of the impurity resonance. To fit the data use a simple potential scattering model with an essentially unitary scattering phase shift $\theta=0.48\pi$. The phase shift is related to an impurity potential U_0 via cot $\theta=1/\pi N_F U_0$. From Pan, Hudson, Lang, *et al.*, 2000.

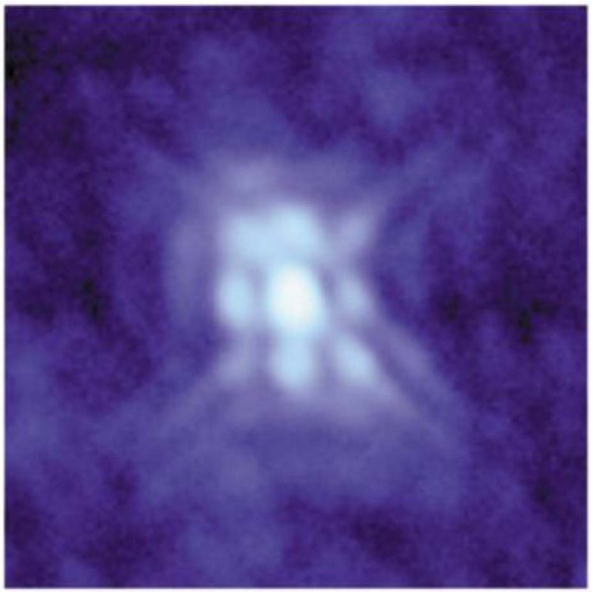

FIG. 16. (Color online) High-spatial-resolution image of the differential tunneling conductance at a negative tip voltage bias $eV=-1.5$ meV at a 60×60 Å^2 square. Also shown is d-wave gap nodes orientation and lattice sites to indicate that the impurity state is registered to the lattice. From Pan, Hudson, Lang, *et al.*, 2000.

Pan, Hudson, Lang, *et al.* mapped the differential tunneling conductance at zero bias over a large area and found randomly distributed sites corresponding to high LDOS, which they associated with Zn dopants. A typical tunneling spectrum at the center of such a site is shown in Fig. 15: it exhibits a very strong peak (up to six times greater than the normal-state conductance) at the energy $\Omega=-1.5\pm0.5$ meV. At the same location, the intensity of the superconducting coherence peak is strongly suppressed, indicating almost complete local destruction of superconductivity. Both features are in agreement with the predictions for quasiparticle scattering off of a strong nonmagnetic impurity in a d-wave superconductor.

The high intensity of the intragap peak allowed close inspection of the electronic structure around the Zn impurity. As shown in Fig. 16, the differential conductance map at $\Omega=-1.5$ meV exhibits two novel features. First, the intensity is the strongest directly at the impurity site, and local maxima and minima occur at the sites belonging to the different sublattices with respect to the impurity. Second, the intensity decays much faster along the nodal direction than along the bond direction. These features are at variance with the theory based on a purely potential scattering, which predicts vanishingly small intensity at the impurity near the unitarity limit. The discrepancy motivated additional studies. One approach focused on the Kondo resonance as a contribution to the zero-bias peak (Polkovnikov *et al.*, 2001; Zhang *et al.*, 2001; Zhu and Ting, 2001a); as discussed in Sec. XI. An alternative explanation considers the tunneling path via the BiO layer which is exposed when the sample is cleaved (Zhu *et al.*, 2000; Zhu and Ting, 2001b; Martin *et al.*, 2002); this is outlined later.

When the Ni atom is substituted for the plane Cu in BSCCO it is in the $3d^8$ state and therefore has spin $S=1$. The potential part of scattering is also present, but is much weaker than for Zn. The experimental study of Ni-doped samples in which two resonance states were found was reported by Hudson *et al.* (2001) as shown in Fig. 17 and 18. Observation of two distinct resonance

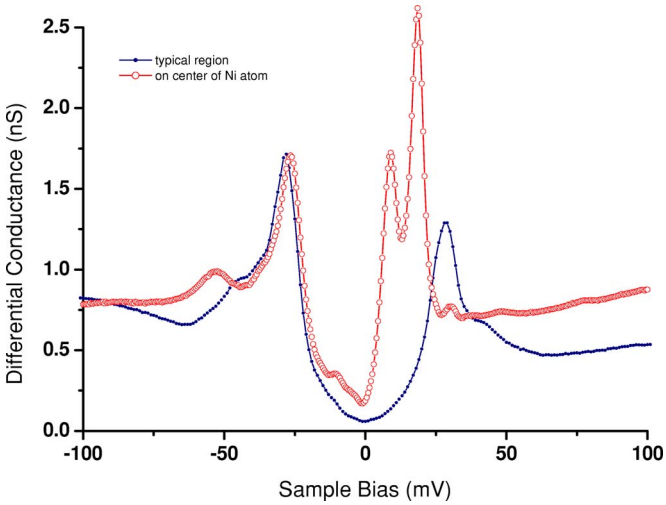

FIG. 17. (Color online) Tunneling DOS for tunneling on a Ni impurity site. Note that there are always states at opposite bias as well. The peak intensity is largest on either positive or negative bias depending on the position. To fit the data one needs to use both U_0 and J. From Hudson *et al.*, 2001.

energies is in agreement with theoretical models that include both nonmagnetic and magnetic scattering (Salkola *et al.*, 1997; Tsuchiura *et al.*, 2000) and predict spin-resolved states at the energies $\pm\Omega_{1,2}$ given by Eq. (7.13) (Salkola *et al.*, 1997). In experiment, $\Omega_1 = 9.2 \pm 1.1$ meV and $\Omega_2 = 18.6 \pm 0.7$ meV. Using the value for the superconducting energy gap $\Delta_0 = 28$ meV, one finds $N_F U = -0.67$ and $N_F J = 0.14$. This implies that the scattering on Ni atoms is dominated by potential interactions, even though the impurity has a magnetic moment. The experiment also showed that the intensity at the gap edge in the tunneling conductance directly at the Ni impurity site is almost unaffected.

B. Filter

As mentioned above, for strong potential scattering it is difficult, if not impossible, to produce a large intensity on the impurity site. Indeed, independent of the model, scattering in the near-unitarity limit produces a node in the wave function. Yet experimentally in the STM images the Zn-impurity site is bright (Pan, Hudson, Lang, *et al.*, 2000) indicating an enhanced low-energy DOS. One possible explanation for this discrepancy is that the image seen by STM is not simply the local intensity of the impurity state directly underneath the tip. The sample is cleaved, and the conduction plane where resonance resides is buried below the exposed layer so that tunneling occurs predominantly via a particular combination of atomic orbitals that allow electron transfer from the STM tip to the conduction plane. This provides a "filter" that emphasizes or hides certain features of the bare LDOS. Martin *et al.* (2002) proposed that the intensity seen by STM is a convolution of initial intensity due to impurity scattering and the filter function that accounts for the matrix element of hopping between CuO planes, $t_k \propto |\cos k_x - \cos k_y|^2$.

In a simplified form this idea is based on the essential role of copper s orbitals for interplane tunneling (Andersen *et al.*, 1995; Xiang and Wheatley, 1995). The DOS near the Fermi surface is dominated by the $d_{x^2-y^2}$ orbitals of Cu (for simplicity we treat hybridization with oxygen p orbitals perturbatively), while s orbitals are far from the chemical potential. However, interplane tunneling between $d_{x^2-y^2}$ orbitals in different planes via the apical oxygen p_z shell is prohibited by symmetry and therefore must occur via virtual hopping on s orbitals. Locally, $d_{x^2-y^2}$ and s orbitals are orthogonal on a given site, and the next available s orbitals are on the four nearest copper atoms. Therefore the electron hops virtually onto p_x or p_y orbitals of nearest O and then onto the Cu s orbital, as shown in Fig. 19.

It is clear from Fig. 19 that the sign of the hopping amplitude $\mathrm{Cu}d_{x^2-y^2} \rightarrow \mathrm{O}p_{x,y} \rightarrow \mathrm{Cu}\ s$ is different for motion along horizontal and vertical directions. Compare the amplitudes $A_{i,i+x(y)}$ for the hopping to the Cu site on the right and on the top,

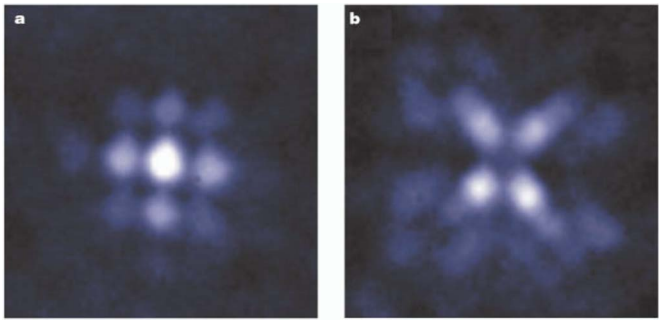

FIG. 18. (Color online) Differential conductance spectra above the Ni atom and at several nearby locations. Differential conductance spectra obtained at four positions near the Ni atom showing the maxima at $eV = \pm\Omega_1$. Intensity as a function of position relative to the impurity site reverses upon change of the bias sign. This effect is explained as a result of particle and hole components of the impurity state. From Hudson *et al.*, 2001.

$$A_{i,i+x} \propto \frac{\langle d_i|p_x\rangle\langle p_x|s_{i+x}\rangle}{[E_p - E_d][E_s - E_p]} \sim \frac{(-1)\exp(ik_x a)}{[E_p - E_d][E_s - E_p]},$$

$$A_{i,i+y} \propto \frac{\langle d_i|p_y\rangle\langle p_y|s_{i+y}\rangle}{[E_p - E_d][E_s - E_p]} \sim \frac{(+1)\exp(ik_x a)}{[E_p - E_d][E_s - E_p]}. \tag{9.1}$$

So far we consider plane waves that describe states without impurity scattering. It was argued (Martin *et al.*, 2002) that the same holds for states produced by impurity scattering. Quantum-mechanical hopping from one site to its nearest-neighbor s orbital has contributions from four processes,

$$A_{\mathrm{tot}} = A_{i,i+x} + A_{i,i-x} + A_{i,i+y} + A_{i,i-y} \sim \cos(k_x a) - \cos(k_y a). \tag{9.2}$$

Here the second line refers to the pure plane wave in connection with band structure calculations (Andersen *et al.*, 1995). Upon hopping onto the s orbitals, the elec-

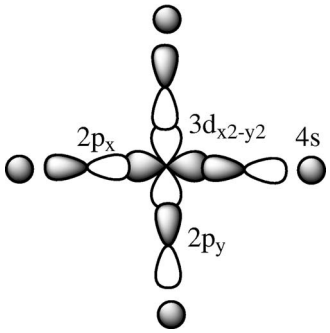

FIG. 19. The real-space image of different orbitals on Cu; nearest O and nearest Cu sites are shown. Dark orbitals and lobes represent the positive phase of the orbital wave function, white represents the negative phase. Quantum-mechanical interference produces the filter effect that changes the distribution of the impurity state intensity. From Martin *et al.*, 2002.

tron moves to the next layer and retraces its path. Therefore the net amplitude for the hopping will be proportional to $|A_{\rm tot}|^2$ and has $|d_{x^2-y^2}|$ modulations,

$$|A_{\rm tot}|^2 \propto |\cos(k_x a) - \cos(k_y a)|^2. \tag{9.3}$$

This particular filter appears in the interplane hopping matrix element obtained using the band-structure calculation (Andersen *et al.*, 1995; Xiang and Wheatley, 1995). However, the Cu *s* orbitals are also relevant for probing an exposed Cu-O layer since electrons tunnel from the STM tip predominantly into these states (Misra *et al.*, 2002). The 4*s*-orbital-assisted hopping was also argued to have profound consequences for the experimental measurement of vortex core states in cuprates (Wu *et al.*, 2000).

Filters of another type, due to blocking of certain hopping, were considered by Zhu, Ting, and Hu (2000), who analyzed the local tunneling matrix elements that connect impurity orbitals to *s* orbitals on neighboring Cu atoms. The net effect is to add probabilities $\Sigma_{nn\delta}|A_{i,i+\delta}|^2$ rather than interfering amplitudes. This filter was argued to produce a large spectral intensity on an impurity site and to suppress it on nearest-neighbor sites. More recently, STM data have been converted to a set of LDOS defined on a two-dimensional lattice (Wang and Hu, 2004), which has allowed for a rigorous comparison between tight-binding model studies and STM experimental data.

An important observation arises from comparing STM and NMR results on a Li-doped YBCO superconductor (Bobroff *et al.*, 2001). Li appears to be a strong scatterer, and the maximum intensity of the NMR signal comes from four nearest-neighbor Cu sites, hence it is localized near the impurity. This is consistent with the notion that a strongly scattering impurity produces large density of states on nearest sites. The crucial difference between NMR and STM is that no electron tunneling is associated with NMR observations, and therefore it measures real-space distribution of spin. Consequently, NMR results provide another confirmation, albeit indirect, of scattering resonance theory.

C. Spatial distribution of particle and hole components

It is clear by comparing the left and right panels of Fig. 18 that the tunneling intensity is not symmetric with the bias voltage. On the contrary, the maxima and minima in the LDOS map are interchanged: bright spots in the STS map at a positive bias V corresponding to dark spots at $-V$, and vice versa. This effect is a general property of superconductors and is seen in both *s*- and *d*-wave systems (Yazdani *et al.*, 1997; Pan, Hudson, Gupta, *et al.*, 2000; Hudson *et al.*, 2001); see also Sec. X. It results from the interplay between particle and hole components of Bogoliubov quasiparticles, which are "native" elementary excitations of a superconductor. In the spatial LDOS pattern created by the quasiparticle resonance, sites with large particle components have a large intensity on the positive bias site, while sites with large hole components are bright at negative bias; see Fig. 20.

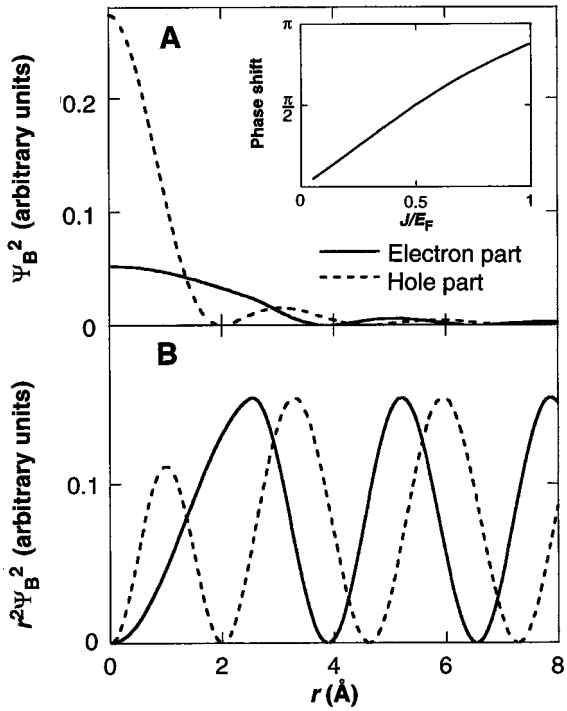

FIG. 20. Particle and hole components of the impurity wave function for a magnetic impurity in an *s*-wave superconductor. (a) Impurity wave function $\Psi_B(r)$ and (b) $r^2\Psi_B(r)$. The maxima of particle and hole components occur at different positions. This results in the different image of the impurity state, seen on the positive and negative bias. This effect is a general property of a superconductor regardless of the symmetry of the pairing state. From Yasdani *et al.*, 1997.

Formally, we define the particle and hole amplitudes of the Bogoliubov quasiparticle, $u_n(i)$ and $v_n(i)$, at site i and for a particular eigenstate n; see also Eq. (7.12). They obey the normalization condition $\Sigma_n|u_n(i)|^2 + |v_n(i)|^2 = 1$ at each site. Therefore at a site where $u_n(i)$ is large, $v_n(i)$ is small, and vice versa. A large $u_n(i)$ component means that the quasiparticle state is predominantly electronlike at that site, and the probability for electron tunneling into a superconductor is locally enhanced. Hence the tunneling intensity at the positive sample bias is large. At the same site the hole amplitude $|v_n(i)| \ll |u_n(i)|$ and the intensity at negative sample bias is small. Similarly, sites with large hole amplitudes $|v_n(i)|$ are bright at negative bias. It follows that if a particular intensity pattern is observed at positive bias (electron tunneling), quite generally, the complementary pattern is found at negative bias (hole tunneling). This is simply a consequence of particle-hole mixing in superconductors and lies at the heart of the intensity pattern change upon switching bias, seen in experiments (Pan. Hudson, Gupta, *et al.*, 2000; Hudson *et al.*, 2001); see Fig. 19.

D. Fourier-transformed STM maps

The spatial dependence of the impurity-induced state has additional information on the underlying system.

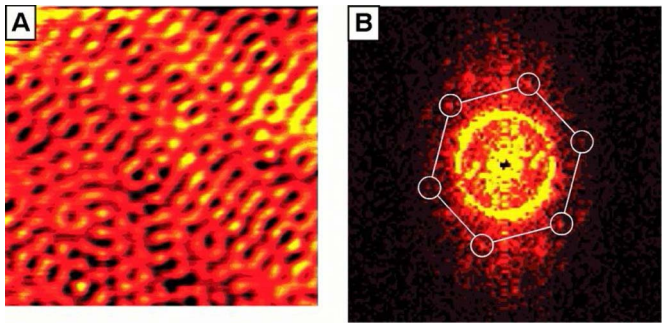

FIG. 21. (Color online) Example of Fourier-transformed scanning-tunneling microscopy (FT-STM). (a) Be (001) surface, as seen by STM, with standing waves (Friedel oscillations) produced by defects. (b) A Fourier transform of (a) reveals a cut through the Fermi surface corresponding to the surface states. From Sprunger *et al.*, 1997; Petersen *et al.*, 1998.

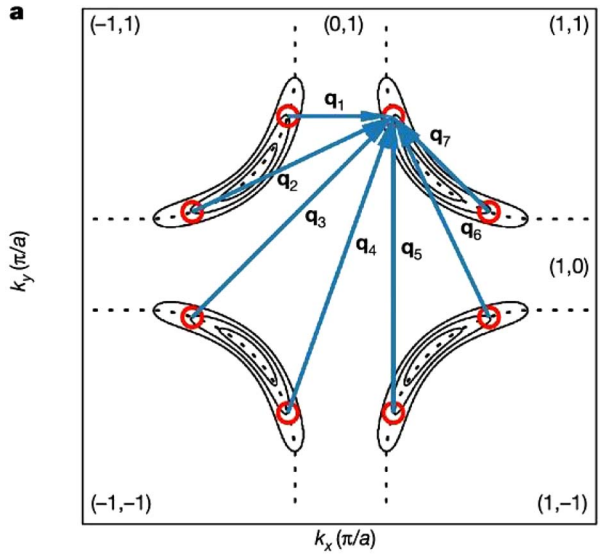

FIG. 22. (Color online) A representative set of seven scattering vectors $\mathbf{q}_i(E)$ of the "octet" model. Reproduced with permission from McElroy *et al.*, 2003.

Consider the simple case of a metal surface with an impurity atom; see Sec. V. Modifications of the DOS induced by the impurity, such as Friedel oscillations, vary at the wave vector k_F and decay a distance from the scattering center; see, for example, Eq. (5.12). Therefore, if an area of the surface contains a number of dilute randomly distributed impurities, the LDOS exhibits a pattern of standing waves. A Fourier transform of the intensity map at a given bias therefore shows a pronounced maximum at the Fermi wave vector (or its 2D slice) and can be used to map out the Fermi surface of the underlying compound. This technique was pioneered by Sprunger *et al.* (Sprunger *et al.*, 1997; Petersen *et al.*, 1998) for Be, Cu, and other metallic surfaces and became known as the Fourier-transform STM (FT-STM) method. In simple cases, this method directly reveals the Fermi surface of a metallic band; see Fig. 21.

The above discussed technique was recently extended to the superconducting state of the cuprates (Hoffman, Hudson, *et al.*, 2002; Hoffman, McElroy, *et al.*, 2002; Howald *et al.*, 2003; McElroy *et al.*, 2003). In unconventional superconductors, the information contained in FT-STM maps is more extensive than in metals. In cuprates not all experimental features are understood, and theory generally followed experiment, so that here we review several aspects of the data.

The enhanced signal in the FT-STM image at a wave vector $\mathbf{q}$ and bias $eV=\omega$ corresponds to a large amplitude for scattering off of an impurity. Qualitatively, this amplitude depends on the number of available initial and final states at a given energy in regions of the Brillouin zone separated by $\mathbf{q}$, i.e., the amplitude is proportional to $\int N_{\mathbf{k}}(\omega)N_{\mathbf{k}+\mathbf{q}}(\omega)d\mathbf{k}$, where $N_{\mathbf{k}}(\omega)$ is the momentum-dependent DOS. The greater the number of "matching" pairs of initial and final states, the more a quasiparticle scatters from one into another, producing a feature in the FT-STM image (we consider low temperatures and therefore ignore Fermi factors). In most metals the density of states is constant around the Fermi surface. In nodal superconductors the loci of low-energy excitations depend on the location of the nodes and shape of the Fermi surface. Experiment and analysis for BSCCO have first been carried out by McElroy *et al.* (2003). At energies below the gap maximum $\omega \ll \Delta_0$ the energy contours $E(\mathbf{k}=\omega)$ are banana shaped, as shown in Fig. 22. The dominant contribution to the density of states, $N(E=\omega) \propto \int \delta(E(\mathbf{k})-\omega)|\nabla_k E_k|^{-1}dk$, arises from regions of the greatest curvature of $E(\mathbf{k})$, i.e., from the tips of each banana. Therefore the primary contribution to $N(\omega)$ is from small regions around eight wave vectors (octet) $\mathbf{k}_j(E), j=1,2,\ldots,8$, at the banana tips [(red) circles in Fig. 22].

Consequently, the maximal scattering intensity at a given ω is from one element of the octet to another, simply due to the large DOS of the initial and final states. For each $\mathbf{k}_j$, there are seven counterparts for enhanced scattering, producing a total of 56 scattering wave vectors. Of these, 32 are inequivalent, and therefore 16 distinct $\pm\mathbf{q}$ pairs can be detected by Fourier-transformed scanning-tunneling spectroscopy. The experimental data (McElroy *et al.*, 2003) were found to be in good agreement with this model. The samples were not intentionally doped, so that scattering was on intrinsic disorder. It is important to note that the model predicts the dispersion of each resonance wave vector with energy (bias voltage) determined by the underlying Fermi surface and shape of the gap, i.e., by the growth of bananas with energy. The peaks associated with these Friedel oscillations of quasiparticles scattering on impurities have been extensively investigated (Byers *et al.*, 1993; Wang and Lee, 2003; Zhang and Ting, 2003, 2004), and interference effects from many impurities have been analyzed by Capriotti *et al.* (2003) and Zhu, Atkinson, and Hirschfeld (2004).

However, results on cuprates show features beyond the simple Fermi-surface resonances. First, it has been argued that some of the Fourier-transform features do not disperse (Howald *et al.*, 2003), and LDOS modula-

tions should be interpreted by invoking a static (or fluctuating) competing charge- or spin-ordered state (Kivelson *et al.*, 2003; Podolsky *et al.*, 2003; Polkovnikov *et al.*, 2003). Experimentally observed nanoscale inhomogeneities (Howald *et al.*, 2001; Pan *et al.*, 2001; Lang *et al.*, 2002) also indicate the proximity to such a state. Furthermore, electronic states at low energies in the pseudogap state in BSCCO exhibit spatial modulations with an energy-independent incommensurate periodicity (Vershinin *et al.*, 2004).

Second, a static Cu-O bond-oriented "checkerboard" pattern with $4a_0$ periodicity was found near the vortex core in the mixed state (Hoffman, Hudson, *et al.*, 2002). This charge modulation is consistent with the field-induced spin modulation with period $8a_0$ observed in neutron scattering (Lake *et al.*, 2001, 2002; Khaykovich *et al.*, 2002) with other cuprate materials. The checkerboard pattern was interpreted as the onset of the competing spin-density wave order around the vortex core where the superconductivity is suppressed (Zhu and Ting, 2001c; Zhu *et al.*, 2002; Andersen and Hedegård, 2003; Takigawa *et al.*, 2003), nucleation of the antiferromagnetic order brought about by local quantum fluctuations of a vortex (Franz *et al.*, 2002), and crystallization of *d*-wave hole pairs by the magnetic field (Chen *et al.*, 2002). A similar pattern has also been predicted around a single strong impurity with an induced local moment in optimally doped cuprates (Liang and Lee, 2002; Zhu *et al.*, 2002; Chen and Ting, 2003, 2004). These predictions depend on the details of a complete microscopic model that has not yet been developed.

X. QUANTUM PHASE TRANSITION IN *s*-WAVE SUPERCONDUCTORS WITH MAGNETIC IMPURITY

A. Introduction

Here we revisit the well-studied problem of a localized classical magnetic moment in a superconductor. We focus on one aspect of this model: the first-order zero-temperature transition that takes place in an *s*-wave superconductor as a function of the effective magnetic moment J_0S, where S is the local impurity spin and J_0 is the exchange coupling between spin and the spins of conduction electrons. In this transition, the spin quantum number s of the electronic ground state $|\Psi_0\rangle$ changes from zero for a subcritical moment $J_0<J_{\rm crit}$ to $1/2$ for $J_0>J_{\rm crit}$. The total spin becomes $S\pm 1/2$ depending on the sign of J_0. Sakurai (1970) was the first to point out this transition, which corresponds to a level crossing between two ground states as a function of the exchange coupling. In a singlet superconductor the level crossing occurs between the state with the partially screened impurity spin and that with S unscreened. The two states have different spin quantum numbers, and hence level crossing is generally allowed. This quantum phase transition is of first order and thus is not associated with divergent time or length scales.

We address the above problem at zero temperature using the mean-field approximation within the T-matrix formulation and utilizing the self-consistent approach, which takes into account local gap-function relaxation. The local Coulomb interaction U breaks particle-hole symmetry and leads to an asymmetric spectral density for the impurity-induced quasiparticle states. Figure 23 illustrates the local effect of a magnetic moment on the low-energy spectral density in an *s*-wave superconductor. Since we limit our considerations to a classical spin $S\gg 1$, the impurity moment cannot be screened completely by quasiparticles. We show that the gross features of impurity-induced quasiparticle states in *s*- and *d*-wave superconductors can be qualitatively understood within the non-self-consistent T-matrix formalism. The transition itself is not restricted to the classical spin: a similar effect is found in a Kondo model; see Sec. XI.

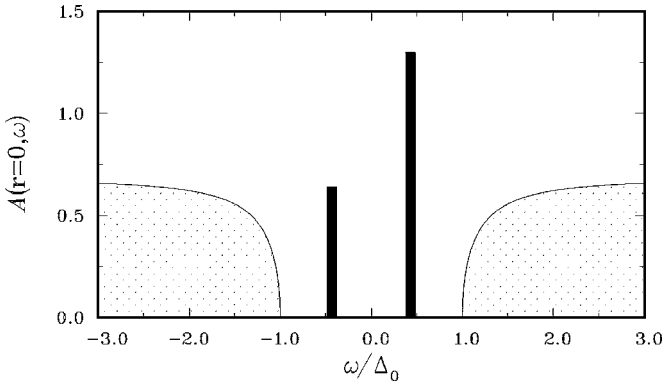

FIG. 23. The local effect of a magnetic moment on the low-energy spectral density in an *s*-wave superconductor.

B. Quantum phase transition as a level crossing

The physical picture of the quantum transition follows from the behavior of the impurity-induced bound state. The transition results from the instability of the spin-unpolarized ground state. For a large enough value of J_0, the energy of the impurity-induced quasiparticle state falls below the chemical potential.

In the Yu-Shiba-Rusinov solution for a classical spin, see Sec. VI, the energy of the impurity state is always below the gap threshold:

$$\Omega_0/\Delta_0=\frac{1-(\pi J_0SN_0)^2}{1+(\pi J_0SN_0)^2} \tag{10.1}$$

and the particle (u_{-1}) and hole (v_{-1}) amplitudes at positive and negative energies. The level crossing and change of the ground state follow from this result. Ignoring the self-consistent solution and using Eq. (10.1), we find that the transition occurs at

$$J_0=J_{\rm crit}=1/\pi N_0S. \tag{10.2}$$

For weak coupling $J_0<J_{\rm crit}$, the ground state of the superconductor is a paired state of time-reversed single-particle states in the presence of impurity scattering, with the BCS-like ground-state wave function,

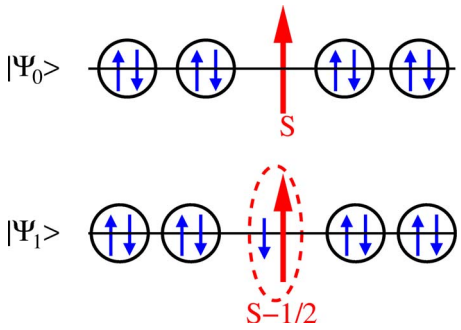

FIG. 24. (Color online) Two variational states are shown schematically. $|\Psi_0\rangle$ is a standard BCS wave function that contains only paired particles and has unscreened impurity spin S. $|\Psi_1\rangle$ is a variational wave function that describes the formation of the bound state between particles with the spin opposite to the local spin (for antiferromagnetic coupling); this state is inherently a non-BCS state and the electronic-spin quantum number differs by one unpaired spin compared to $|\Psi_0\rangle$.

$$|\Psi_0\rangle_{J_0<J_{\rm crit}} \sim \prod_n [u_n + v_n \psi_n^\dagger \psi_{-n}^\dagger]|0\rangle = |\Psi_0\rangle. \tag{10.3}$$

Here, since the translational symmetry is broken by the impurity, we consider eigenstates of the scattering problem in the presence of an impurity. These states are labeled by a discrete index $n=1,\ldots,\infty$ and form the basis for the Bogoliubov Hamiltonian with an impurity. The $n=1$ state corresponds to an impurity bound state, localized on an impurity site. The index $-n$ corresponds to a time-reversal state, i.e., the localized state with opposite spin. The first excited state above the condensate corresponds, at $J_0<J_{\rm crit}$, to a single-quasiparticle excitation, and its energy is that of the intragap Yu-Shiba-Rusinov state at energy Ω_0; see Fig. 24.

The wave function of this excited state is

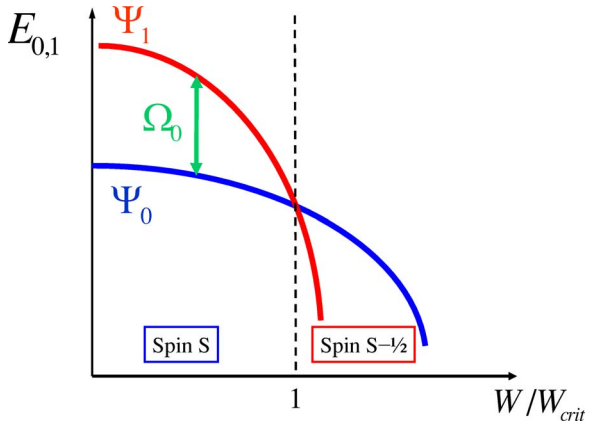

FIG. 25. (Color online) Energies of two variational states are shown. $|\Psi_0\rangle$ is a standard BCS state with energy E_0. $|\Psi_1\rangle$ is a variational state that describes the formation of the bound state between particles with the spin opposite to the local spin with energy E_1. Level crossing between states with different symmetry occurs at some critical value of the coupling $J_{\rm crit}$. This is an example of a first-order quantum phase transition with no divergent length or time scale associated with it.

$$|\Psi_{-1}\rangle_{J_0<J_{\rm crit}} \sim \gamma_{-1}^\dagger |\Psi_0\rangle = |\Phi_{-1}\rangle,$$

$$|\Phi_{-1}\rangle = \psi_{-1}^\dagger \prod_{n>1} [u_n + v_n \psi_n^\dagger \psi_{-n}^\dagger]|0\rangle, \tag{10.4}$$

with the standard quasiparticle definitions $\gamma_1 = u_1\psi_1 - v_1\psi_{-1}^\dagger$, $\gamma_1^\dagger = u_1\psi_1^\dagger - v_1\psi_{-1}$, $\gamma_{-1}^\dagger = u_1\psi_{-1}^\dagger + v_1\psi_1$, etc., where $u_n^2 + v_n^2 = 1$. We introduce the notation

$$|\tilde{\Psi}_0\rangle = \prod_{n>1} [u_n + v_n \psi_n^\dagger \psi_{-n}^\dagger]|0\rangle, \tag{10.5}$$

so that $|\Phi_{-1}\rangle = \psi_{-1}^\dagger |\tilde{\Psi}_0\rangle$. The state $\gamma_1^\dagger|\Psi_0\rangle$ is far above the superconducting gap and hence is not relevant for this discussion. Note that $|\Psi_0\rangle$ is a true vacuum for all quasiparticles: e.g., $\gamma_{\pm 1}\Pi_{n>0}[u_n + v_n\psi_n^\dagger\psi_{-n}^\dagger]|0\rangle = 0$.[8] This is a true spin-singlet state, $\langle\Psi_0|\mathbf{S}_{\rm electron}|\Psi_0\rangle = 0$. To avoid confusion with impurity spin S, we explicitly indicate that $\mathbf{S}_{\rm electron}$ is the net spin of conduction electrons. Hence if $|\Psi_0\rangle_{J_0<J_{\rm crit}} = |\Psi_0\rangle$ is a ground state, the total spin of electrons is zero, and only the spin of impurity counts. The first excited state at energy Ω_0 has a spin $1/2$ quasiparticle in it: $\langle\Phi_{-1}|S^z_{\rm electron}|\Phi_{-1}\rangle = -1/2$.

Upon increasing the coupling constant J_0 one reaches the critical value where energies of the two states cross, Fig. 25. Beyond that point, the excited and ground states change roles,

$$|\Psi_0\rangle_{J_0>J_{\rm crit}} = |\Psi_{-1}\rangle = |\Phi_{-1}\rangle,$$

$$|\Psi_{-1}\rangle_{J_0>J_{\rm crit}} = |\Psi_0\rangle. \tag{10.6}$$

A clear way to see this quantum phase transition is by examining the energy levels as a function of $J_0/J_{\rm crit}$. For variational wave functions $|\Psi_{0,-1}\rangle$, we define the respective energies as expectation values of the Hamiltonian,

$$E_{0,-1}(J_0/J_{\rm crit}) = \langle\Psi_{0,-1}|H|\Psi_{0,-1}\rangle. \tag{10.7}$$

The energy of the first excitation is then

$$\Omega_0(J_0/J_{\rm crit}) = E_{-1} - E_0, \quad J_0 < J_{\rm crit},$$

$$\Omega_0(J_0/J_{\rm crit}) = E_0 - E_{-1}, \quad J_0 > J_{\rm crit}. \tag{10.8}$$

There are several implications of this result. First, the ground state of a superconductor with a magnetic impurity in the strong-coupling limit is a non-BCS state: there is one unpaired occupied single-particle state in the ground state. In contrast, all states are paired in the BCS theory. A similar result was observed for Kondo screening in a superconductor (Sakai *et al.*, 1993). One can understand the result by considering the strong-coupling limit $J_0 N_0 \gg 1$, when, well before any superconducting

[8]Here the spin of state $n=1$ is determined by the sign of the exchange coupling J_0. We assume it to be antiferromagnetic. The electronic spin of the state $n=-1$ in Eq. (10.4) is opposite to the local spin S, assumed to be up, without loss of generality. The case of ferromagnetic coupling is similar. Indeed, the classical spin solution Eq. (10.1) is symmetric between $J_0 \to -J_0$ as it contains only even powers of exchange.

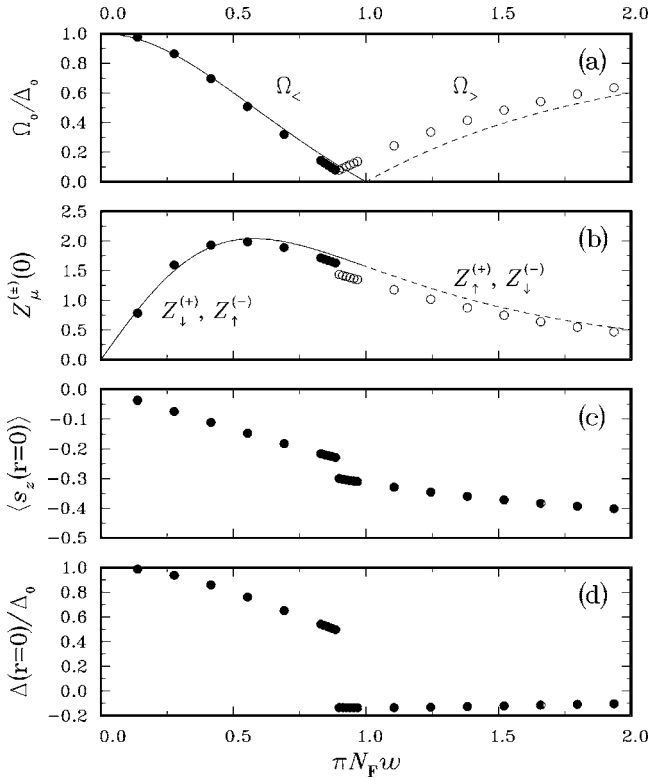

FIG. 26. Magnetic-impurity-induced bound state in *s*—wave superconductor. (a) The bound-state energy Ω_0, (b) the spectral weight of the pole $Z^\pm$ for positive and negative energies in units of $N_0 J_0, N_0 = N_F$, (c) the spin polarization $\langle \mathbf{s}(\mathbf{r}=\mathbf{0})\rangle$, and (d) the gap function $\Delta(\mathbf{r}=0)/\Delta_0$ at the impurity site $\mathbf{r}=\mathbf{0}$ as a function of J_0 in the *s*-wave superconductor. Lines denote the *T*-matrix results for the uniform order parameter and symbols denote the self-consistent mean-field results on a square lattice at half-filling. The quantities of the impurity-induced intragap quasiparticle state belonging to the branch $J_0 < J_{\rm crit}$ are denoted by solid lines and solid symbols, whereas those belonging to the branch $J_0 > J_{\rm crit}$ are marked by dashed lines and open symbols. Taken from Salkola *et al.*, 1997.

correlations are established, a single electron state is bound to the impurity site. This is equivalent to the strong-coupling limit for Kondo screening. In our case the bound electron partially screens the large impurity spin. For spin $S=1/2$, the screening is complete and the state is a singlet (Sakai *et al.*, 1993). Thereafter, a superconducting state emerges with one unpaired electron bound to the impurity; it is stabilized by the energy balance between superconducting and magnetic energies. A single electron state bound to a local spin yields an energy gain $\sim J_0$, which is large compared to the pairing energy Δ_0. The crossing point and related quantities are shown in Fig. 26. This level crossing point corresponds to a quantum phase transition.

The crossing point occurs exactly at the critical point of Eq. (10.1) only in a non-self-consistent treatment in which single-particle levels provide the only contribution to the total energy. The true phase transition occurs slightly earlier. The gap suppression and quasiparticle interaction also contribute to the free energy and, in the self-consistent mean-field approximation, the order-parameter relaxation shifts $J_{\rm crit}$ downwards and the energy of the impurity-induced bound state does not reach zero when a first-order transition between two ground states occurs. In practice the analytical results are within 10% of numerical results obtained in a self-consistent treatment (Salkola *et al.*, 1997). In contrast, a *d*-wave superconductor has no quantum transition for any magnetic moment value when its quasiparticle spectrum in the normal state has particle-hole symmetry. The absence of the transition follows from the behavior of impurity-induced quasiparticle states, which are pinned at the chemical potential for an arbitrarily large magnetic moment; see Sec. VII. However, if particle-hole symmetry is broken or if the pairing state acquires a small *s*-wave component, the transition is possible for a large enough moment. The impurity moment induces two virtual bound states which have fourfold symmetry and extend along the nodal directions of the energy gap.

C. Particle and hole component of impurity bound state

In this section we show that excited states inside the gap in a superconducting state appear in pairs at positive and negative energies. This is a direct consequence of the fact that natural excitations are Bogoliubov excitations. Particle and hole coefficients of the excited state $|\Psi_{-1}\rangle_{J_0<J_{\rm crit}}$ are given by the u and v components of the quasiparticle operators γ_n; see Sec. II. To be specific we confine subsequent discussion to the *s*-wave case, however, the results are applicable to a superconducting state of any symmetry.

Consider two independent processes: (a) an electron at energy Ω_0 and spin down, $n=-1$, and (b) a hole with spin up, $n=1$, injected in a superconductor with the same energy Ω_0. Hole creation means that an electron with spin up is extracted from a superconductor. In experiment, this is achieved by reversing the bias of the STM tip, corresponding to the negative-energy axis. Variational wave functions that describe these processes are

$$\psi_{-1}^\dagger |\Psi_0\rangle_{J_0<J_{\rm crit}} = -u_1 |\Phi_{-1}\rangle,$$

$$\psi_1 |\Psi_0\rangle = v_1 |\Phi_{-1}\rangle. \tag{10.9}$$

Here, to be specific, we consider the case $J_0 < J_{\rm crit}$. This illustrates the point that in a BCS-like ground state the particle excitation with energy Ω_0 and hole excitation with negative energy $-\Omega_0$, aside from irrelevant normalization factors, is the same excited state, namely, $|\Phi_{-1}\rangle$. Therefore, the poles in the density of states (and contributions to the electronic LDOS) come in pairs at positive and negative energies. True quasiparticles in a superconducting state are Bogoliubov excitations γ_n that have finite particles and holes with amplitudes u_n and v_n. The strength of the electron absorption and emission process is controlled by coherence factors. This is true for a BCS superconductor even without impurities. For the case at hand, impurity states are distinct from the

continuum. The two poles at $\pm\Omega_0$ are part of the same physical excitation. The local spectral function $A_1(\mathbf{r},\omega) = -\mathrm{Im}\, G_{11}(\mathbf{r},\omega)/\pi$ at the impurity site is

$$A_1(\omega) = Z^+\delta(\omega-\Omega_0) + Z^-\delta(\omega+\Omega_0), \tag{10.10}$$

and the relative strength of the particle and hole components is $Z^+ \sim u_{-1}^2$ and $Z^- \sim v_{-1}^2$, so the net strength of poles $Z^+ + Z^- \geqslant 1$ as it should be for a physical excitation. For more details and references, the reader is referred to Salkola *et al.* (1997).

The analysis for $J_0 > J_{\mathrm{crit}}$ is more involved. The ground-state wave function is now $|\Phi_{-1}\rangle$. Injection of an electron with spin opposite to the bound state and extraction of an electron with the same spin produces

$$\psi_1^\dagger|\Phi_{-1}\rangle = \psi_1^\dagger\psi_{-1}^\dagger|\tilde{\Psi}_0\rangle, \quad \psi_{-1}|\Phi_{-1}\rangle = |\tilde{\Psi}_0\rangle, \tag{10.11}$$

respectively, with the complementary annihilated states $\psi_1^\dagger|\Phi_{-1}\rangle = 0$ and $\psi_{-1}^\dagger|\Phi_{-1}\rangle = 0$. Although the two states written in Eq. (10.11) are different, the sole difference is that one of them has an extra Cooper pair. For a macroscopically large system with the number of Cooper pairs $N \gg 1$ this produces a negligible difference in the energies and matrix elements. Therefore the injection of an electron with spin up (in our convention) and extraction of an electron with spin down produce the same physical state. This state has a particle and hole projection as discussed in the case of $J_0 < J_{\mathrm{crit}}$.

A similar quantum phase transition occurs in a *d*-wave superconductor for a nonmagnetic impurity. In the case of a particle-hole symmetric band unitary scattering produces a zero energy state; see Sec. VII, Eq. (7.1). However, for the particle-hole asymmetric band the impurity state reaches zero energy and eventually changes sign as a function of impurity strength. This transition occurs at $U_0 > U_{\mathrm{crit}} \sim \mu$, where μ is the chemical potential which leads to a particle-hole asymmetric band. It is known that a single-quasiparticle bound state forms at $U_0 > U_{\mathrm{crit}}$, and the ground-state wave function has a single unpaired quasiparticle in addition to the BCS pairs; see Salkola *et al.* (1996, 1997).

D. Intrinsic π phase shift for $J_0 > J_{\mathrm{crit}}$ coupling

Here we point out a little known but important fact that near an impurity site the phase of the superconducting order parameter changes by π. As shown Fig. 26(d), the self-consistent solution indicates that at $J_0 > J_{\mathrm{crit}}$ the phase of the order parameter on the impurity site is shifted by π with respect to the phase in the bulk. This is illustrated in Fig. 27.

In numerical calculations the spatial extent of the π-shifted region was found to be a few atomic sites. Such a sharp change in the phase of the order parameter costs significant superconducting condensate energy and is not preferred under normal circumstances. In the case at hand, however, in the strong-coupling limit near the impurity site, the condensate energy is secondary to the magnetic exchange energy, and the physics is driven by magnetic interactions. Even though the phase shift is π, it does not lead to any time-reversal-violating observable effects as there are no superconducting currents near the impurity: $I = I_c \sin\phi = 0$. These results were obtained with the self-consistent treatment using a negative U model that allows for on-site pairing (Salkola *et al.*, 1997).

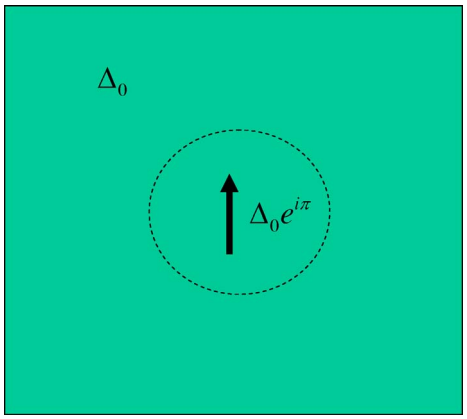

FIG. 27. (Color online) Cartoon of the intrinsic π junction near the magnetic impurity in an *s*-wave superconductor.

We are not aware of a simple explanation of this effect. It appears to be general and not restricted to a particular model. It is related to the π-shift superconducting junctions with tunneling barriers containing a magnetic impurity or a ferromagnetic layer. This subject is covered extensively; see, e.g., a recent review and other papers (Bulaevskii *et al.*, 1977; Buzdin *et al.*, 1982; Glazman and Matveev, 1989; Spivak and Kivelson, 1991; Buzdin, 2005).

XI. KONDO EFFECT AND QQUANTUM IMPURITIES

Above we have concentrated on static impurities. In the next two sections, we consider examples when impurity atoms have their own internal degrees of freedom and impurities are dynamically coupled to conduction electrons. The fact that dynamical behavior often leads to qualitatively new results is well known from Kondo effect studies (Kondo, 1964): scattering of conduction electrons off of a single magnetic impurity.

At low T, dilute magnetic impurities doped into an otherwise nonmagnetic metallic host have dramatic effects on the resistivity and susceptibility. The anomalies are due to screening of the impurity spin by conduction electrons. For a local spin $S = \frac{1}{2}$ and antiferromagnetic exchange, a global singlet is formed by coupling an electron state to the impurity site; quantum dynamics of spin flips is crucial for its formation. The process is manifested in the crossover of the susceptibility from Curie-like at high temperatures, $\chi = C/T$ with $C = 4\mu_B^2 S(S+1)/3k_B$, to Pauli-like below a characteristic Kondo temperature, $T_K \simeq W \exp(-1/2JN_0)$. Here W is the electron half bandwidth and J is the exchange constant. Importantly, (a) Kondo screening occurs only for the antiferromagnetic exchange constant $J > 0$, and (b) the process is nonperturbative, as is clear from the nonana-

lytic dependence of T_K on the exchange constant. A full understanding of the single-impurity Kondo problem in a metal required concerted use of the renormalization group (Anderson, 1970; Anderson *et al.*, 1970), numerical renormalization group (Wilson, 1975), exact solutions via the Bethe ansatz (Andrei, 1980; Wiegmann, 1980), and large-N expansions (Read and Newns, 1983a, 1983b; Coleman, 1984, 1985; Read, 1985). Many results were summarized in reviews (Hewson, 1993; Cox and Zawadowski, 1998).

Kondo screening involves quasiparticles near the Fermi energy E_F. In metals, the density of states near E_F varies weakly, $N(\epsilon) \approx N_0$, which simplifies the analysis. In contrast, if $N(\epsilon)$ varies strongly with $\epsilon \approx E_F$ the Kondo effect is realized differently. In a band-gap insulator this was investigated by Ogura and Saso (1993), who found that the ground state of the magnetic impurity changes from a singlet to multiplet when the band gap increases, as in the case of the magnetic impurity in a conventional BCS superconductor. In superconductors, however, the Cooper instability that gaps the Fermi surface and depletes the density of states is itself driven by the finite DOS in the normal state. Consequently, the two effects compete.

For simplicity, and following the historical development, we have so far considered properties of classical spin for which no reduction in magnitude due to Kondo screening is possible; see Sec. VI. We now overview the current understanding of the Kondo screening in superconductors, focusing especially on the similarities and differences between the cases of quantum and classically impurity spins.

A. Kondo effect in fully gapped superconductors

In normal metals antiferromagnetic exchange leads to Kondo screening below T_K, while ferromagnetic exchange does not. In superconductors, within the Shiba-Rusinov analysis the sign of the exchange interaction between conduction electrons and impurity spins is irrelevant. Consequently, treatment of quantum impurity spins must bring out the differences between the two signs of J.

For $J>0$ the opening of the superconducting gap competes with Kondo screening as both instabilities are driven by the finite DOS at zero energy. Clearly, if $T_K \gg T_c$, the impurity is completely screened at the onset of superconductivity. In contrast, for $T_K \ll T_c$ Kondo screening is suppressed by the depletion of states upon the opening of the superconducting gap.

In the renormalization-group picture, Kondo screening is viewed as growth (and divergence) of the effective exchange coupling J_{eff} as we focus on the properties of the system at lower energies. Therefore J_{eff} and, with it, the phase shift of scattering on the impurity, depends on the energy of the incoming electron. Consequently, the effect of scattering varies with temperature.

1. Ferromagnetic exchange

Early analytical attempts were carried out (Zittartz and Müller-Hartmann, 1970, Müller-Hartmann, 1973) in the framework of the Nagaoka decoupling scheme (Nagaoka, 1965, 1967; Hamann, 1967). For $J<0$ the bound state splits off the band edge and was found to move towards an asymptotic value,

$$\epsilon \equiv \frac{E_0}{\Delta} = [1 + g^2\pi^2 S(S+1)]^{-1/2}, \tag{11.1}$$

where $g=\lambda N_0$ and λ is the superconducting coupling constant. For weak coupling $g \ll 1$ the bound state remains close to the gap edge for values of $J<0$. This qualitative result was later confirmed by numerical-renormalization-group calculations (Satori *et al.*, 1992; Sakai *et al.*, 1993), which showed the binding energy approximated by $\epsilon \approx 1 - \pi^2 J_{\text{eff}}^2/8$, where

$$J_{\text{eff}} = \frac{2|J|/W}{1 + (2|J|/W)\ln(W/\Delta)}. \tag{11.2}$$

where W is the bandwidth. Therefore, the ferromagnetic case corresponds to weak coupling and small phase shift of scattering at low temperatures.

The ground state of this system was argued to be a doublet (Soda *et al.*, 1967; Satori *et al.*, 1992; Sakai *et al.*, 1993) since the ferromagnetic interaction renormalizes to weak coupling and the impurity spin remains essentially free. Recently it was suggested that the superconducting interaction is relevant (in the renormalization-group sense) in this model, and therefore above a critical Δ-dependent coupling J_C (J_C is larger for smaller Δ) the ground state of the coupled superconductor-impurity system is a triplet ($m_z=0,\pm 1$) (Yoshioka and Ohashi 1998). This suggestion needs to be explored further.

2. Antiferromagnetic coupling

In a normal metal Kondo screening corresponds to $J_{\text{eff}} \to \infty$ and hence to the scattering in the unitarity limit, with the scattering phase shift $\delta \to \pi/2$. The Hartree-Fock analysis (Shiba, 1973) is insufficient to describe this effect.

Several authors considered the limit $T_K \ll \Delta$ (Soda *et al.*, 1967; Zittartz and Müller-Hartmann, 1970; Müller-Hartmann, 1973) and found the position of the localized excited state with various degrees of accuracy. In this regime the localized state lies close to the gap edge, as it does for ferromagnetic coupling. In the opposite limit $T_K \gg \Delta$ the approximate solution for the position and residue of the bound state was obtained by Zittartz and Müller-Hartmann (1970) and Müller-Hartmann (1973), however, the results were inexact due to the nature of their approximation. Later, within the local Fermi-liquid approach, the energy of the bound state in this limit was found to be (Matsuura, 1977)

$$\epsilon = \frac{1-\alpha^2}{1+\alpha^2}, \tag{11.3}$$

where

$$\alpha \approx \frac{\pi\Delta}{4T_K} \ln \frac{4eT_K}{\pi\Delta}. \tag{11.4}$$

This result clearly shows that the phase shift of scattering depends on the ratio T_c/T_K.

The properties of the bound state, including its position and spectral weight, for arbitrary values of T_K/T_c were obtained with the help of numerical-renormalization-group calculations (Satori *et al.*, 1992; Sakai *et al.*, 1993). They found level crossing similar to the quantum phase transition (discussed above) at $T_K/\Delta \sim 0.3$. For $T_K/\Delta > 0.3$, the impurity moment is mostly quenched when the depletion of states caused by superconductivity begins to affect screening. In that case the ground state is a Kondo-screened singlet, while the excited intragap state is a doublet with spectral weight $\nu \approx 2$ for $T_K\Delta \gg 1$, corresponding to a single-particle state. Here ν is defined from

$$-\frac{1}{\pi} \mathrm{Im}\, G(\omega + i\delta)/\pi = \frac{\nu}{2}[\delta(\omega - E_0) + \delta(\omega + E_0)]. \tag{11.5}$$

On the other hand, for $T_K/\Delta < 0.3$ the Kondo effect is suppressed by the opening of the superconducting gap, the ground state is a doublet corresponding to a free-spin state, while the bound excited state is a Kondo singlet. The spectral weight $\nu \approx 0.5$ for $T_K \ll \Delta$, and changes discontinuously at the phase transition point.

Level crossing means that the bound state is at zero energy for $T_K/\Delta \approx 0.3$, while it is close to the gap edge for both $T_K \gg \Delta$ and $T_K \ll \Delta$. Numerical results show that the energy of the bound state is not symmetric with respect to the crossing point: $E_0/\Delta < 0.5$ for $0.03 \lesssim T_K/\Delta \lesssim 1$ (Satori *et al.*, 1992).

3. Anisotropic exchange and orbital effects

Several more complicated aspects of Kondo screening in superconductors have attracted attention in recent years, and we review them briefly, referring the reader to the original papers for further information. An anisotropic exchange interaction, $J_z \neq J_\pm$, allows the investigation of the crossover between the Ising regime, $J_\pm = 0$, when the spin flip is disallowed and there is no Kondo screening, and the isotropic exchange considered so far. The main features of the phase diagram are discussed by Yoshioka and Ohashi (1998), and new phases occur on the ferromagnetic side. In particular, these authors found an extended regime of the Ising-dominated ground state for $J_\pm \neq 0$. In addition, they found small regions of the phase diagram around isotropic ferromagnetic and Ising antiferromagnetic lines, where two localized intragap states exist. They also obtained a perturbative analytic expression for the shift of the bound-state energy due to anisotropy of the interaction.

Using the numerical-renormalization-group approach to analyze Anderson's model allows us to interpolate between asymmetric magnetic scattering, the Kondo problem, and nonmagnetic scattering, including the resonance $U=0$ limit (Yoshioka and Ohashi, 2000). In particular, the crossover from the magnetically induced bound state to the resonance nonmagnetic scattering regime (Machida and Shibata, 1972) was studied.

Finally, so far we have only discussed purely *s*-wave superconductors. Fully gapped systems also include materials with a complex order parameter combining two (or more) out-of-phase unconventional gaps, such as $d_{x^2-y^2}+id_{xy}$ or p_x+ip_y. In both of these cases, Cooper pairs have orbital degrees of freedom that also couple to impurity spins, leading to the multichannel Kondo effect. In addition, for *p*-wave pairing the total spin of Cooper pairs is $s=1$, so that nontrivial changes in screening occur depending on whether the impurity spin $S=1/2$ or 1. The numerical-renormalization-group analysis of the Kondo problem in this system was carried out very recently (Koga and Matsumoto, 2002a, 2002b; Matsumoto and Koga, 2002). It was found that two order parameters are indistinguishable when only the $l=0$ impurity scattering partial wave is taken into account, i.e., only the depletion of the density of states due to the gap rather than the spin structure of the Cooper pair dictated the Kondo screening. In that case the ground state moment is determined by the orbital structure of the Cooper pair. However, inclusion of higher harmonics with $l \neq 0$ for scattering (extended impurity potential) leads to dependencies of the screening and ground states on exchange couplings.

B. Kondo effect in gapless superconductors

The systems analyzed above are either metals with a constant DOS at the Fermi surface or superconductors with a hard gap. Gapless superconductors, such as *d*-wave superconductors, with the power law DOS $N(E) \propto |E|^r$ with $r>0$, present new situations that have attracted much attention in recent years. The Kondo effect in systems in which the host single-particle density of states follows a power law has been studied intensively.[9] Notice that considering the Kondo effect in a system with the power-law dependence of the DOS is not the same as analyzing the competition between superconducting and Kondo correlations for *d*-wave systems.

Fradkin and co-workers (Withoff and Fradkin, 1990; Cassanello and Fradkin, 1996, 1997) first employed a combination of the poor man's scaling argument and large-N approach to spin-$\frac{1}{2}$ impurity for $0 < r \leq 1$ and showed that for $r>0$ there is a critical coupling value J_c such that (i) at $J<J_c$ the system is in the weak-coupling

[9] See, for example, Withoff and Fradkin, 1990; Borkowski and Hirschfeld, 1992, 1994; Itoh, 1993; Chen and Jayaprakash, 1995; Cassanello and Fradkin, 1996, 1997; Ingersent, 1996; Bulla *et al.*, 1997, 2000; Conzalez-Buxton and Ingersent, 1998; Ingersent and Si, 1998; Logan and Glossop, 2000; Polkovnikov *et al.*, 2001; Vojta, 2001; Vojta and Bulla, 2001; Zhang *et al.*, 2001, 2002; Zhu and Ting, 2001a, 2001b; Han *et al.*, 2002, 2004; Polkovnikov, 2002.

regime when the Kondo interaction is irrelevant ($J=0$ is a stable fixed point), and the impurity decouples from the band; and (ii) for $J>J_c$ Kondo screening takes place. Further studies based on the numerical-renormalization-group approach (Chen and Jayaprakash, 1995; Ingersent, 1996) identified particle-hole asymmetry as a key factor in determining the low-temperature physics. Their analysis indicated that at $J=\infty$ the impurity spin is only partially screened. In the particle-hole symmetric case, for $0<r\leqslant\frac{1}{2}$, there exists a critical coupling J_c above which the $J=\infty$ fixed point becomes stable. In contrast, for $r>\frac{1}{2}$ the moment remains unscreened as the exchange $0<J<\infty$ renormalizes to zero. When the particle-hole symmetry is broken by introducing a static potential scattering at the impurity, a critical J_c exists for an arbitrary r. For a fixed value of r $(\geqslant\frac{1}{2})$, the critical coupling depends on the potential scattering. A detailed dependence of J_c on the potential scattering is complicated and readers are referred to the article by Ingersent (1996).

In real systems the power-law variation of $N(\epsilon)$ is restricted to an energy range $|\epsilon|\leqslant\Delta_0$, with $N(\epsilon)\approx N(\Delta)$ for $\Delta_0<|\epsilon|\leqslant W$. The numerical-renormalization-group approach gave results entirely consistent with those known for gapped systems (the full gap $2\Delta_0$ in the spectrum corresponds to the $r=\infty$ limit). For the particle-hole symmetric case an impurity in an insulator retains its moment, no matter how large J is. Away from particle-hole symmetry, the spin is screened provided that $J>J_c\approx 2W/\ln(W/\Delta_0)$ (Takegahara *et al.*, 1992). Formation and screening of the local moments in d-wave superconductors was investigated using the variational wave-function approach (Simon and Varma, 1999).

The Hamiltonian of a magnetic impurity in a metal with a nontrivial DOS is

$$H=\sum_{\sigma}\int_{-\infty}^{\infty}d\epsilon N(\epsilon)\epsilon c_{\epsilon\sigma}^{\dagger}c_{\epsilon\sigma}+\frac{1}{N_L}\sum_{k,k'}\left[\left(U_0+\frac{J}{2}\right)c_{k\uparrow}^{\dagger}c_{k'\uparrow}+\left(U_0-\frac{J}{2}\right)c_{k\downarrow}^{\dagger}c_{k'\downarrow}\right]+\frac{J}{2}\sum_{k,k'}[c_{k\uparrow}^{\dagger}c_{k'\downarrow}S_{-}+c_{k\downarrow}^{\dagger}c_{k'\uparrow}S_{+}],\tag{11.6}$$

where $N(\epsilon)$ is the electron density of states, N_L is the lattice size, and we included both potential scattering and exchange.

Interest in the Kondo impurities in d-wave systems is motivated by the recent STM and NMR experiments around single impurities in high-T_c cuprates. Zn and Ni are believed to replace Cu in the copper-oxide plane and change the local electronic structure without changing the net carrier concentration. Simple valence counting suggests that if Zn and Ni impurities maintain a nominal Cu^{2+} charge, Zn^{2+} has a $(3d)^{10}$, $S=0$ configuration and acts as a nonmagnetic impurity. In contrast Ni^{2+} is in a $(3d)^8$, $S=1$ state and is magnetic. Direct comparison between the two cases is difficult.

Nuclear magnetic resonance (NMR) experiments performed with nonmagnetic spin 0 (Zn,Li,Al) in doped cuprates (Alloul *et al.*, 1991; Ishhida *et al.*, 1993, 1996; Mahajan *et al.*, 1994, 2000; Mendels *et al.*, 1999) clearly showed these impurities induce a local $S=\frac{1}{2}$ moment on the nearest-neighbor Cu. It was also demonstrated that the magnetic properties associated with the substitution of these impurities depend on hole doping. In the underdoped regime the susceptibility obeys Curie's law below the superconducting transition temperature T_c. Near optimal doping the Kondo screening (albeit strongly reduced) may persist to the lowest T.

NMR shows that the induced moment is spatially distributed around the impurity. It is important to emphasize that this moment is merely a particular bound state of conduction electrons near the impurity and the precise form of the interaction of the induced moment with other conduction electrons is *a priori* unknown. The Kondo effect in cuprates does not stem simply from the screening of the preformed local moment: Moment formation and screening (as well as pairing) result from the same bare interactions.

Nonetheless, in the absence of a microscopic theory for high-T_c superconductivity, many authors use Kondo screening as a starting point for the analysis of experiments. Moreover, in most unconventional superconductors other than cuprates, the properties of a magnetic impurity embedded in a superconductor are a well-defined theoretical problem. The Hamiltonian consists of an unconventional (d-wave in our case) BCS state $\mathcal{H}_{\mathrm{BCS}}$, a potential scattering term $\mathcal{H}_{\mathrm{pot}}$, and a magnetic term $\mathcal{H}_{\mathrm{mag}}$. The magnetic term can be described by either the Anderson impurity model or the Kondo exchange model, and the impurity spin can be either localized at a single site or spatially distributed in its vicinity. For the Anderson model with single-site coupling, the magnetic term is given by

$$\mathcal{H}_{\mathrm{mag}}=\sum_{k\sigma}[V_{kd}c_{k\sigma}^{\dagger}d_{\sigma}+\mathrm{H.c.}]+\epsilon_d\sum d_{\sigma}^{\dagger}d_{\sigma}+U_d n_{d\uparrow}n_{d\downarrow}.\tag{11.7}$$

In the strong U_d limit, the Anderson model can be mapped onto a Kondo s-d exchange model through the Schrieffer-Wolff transformation (Hewson, 1993) leading to

$$\mathcal{H}_{\mathrm{mag}}=J\mathbf{s}_0\cdot\mathbf{S},\tag{11.8}$$

where $\mathbf{s}_0=\frac{1}{2}\Sigma_{\sigma\sigma'}c_{0\sigma}^{\dagger}\boldsymbol{\sigma}_{\sigma\sigma'}c_{0\sigma'}$ is the spin operator for the conduction electron at the impurity site. For multisite coupling

$$\mathcal{H}_{\mathrm{mag}}=\sum_{I\sigma}[V_{Id}c_{I\sigma}^{\dagger}d_{\sigma}+\mathrm{H.c.}]+\epsilon_d\sum_{\sigma}d_{\sigma}^{\dagger}d_{\sigma}+U_d n_{d\uparrow}n_{d\downarrow},\tag{11.9}$$

where I is the set of nearest-neighbor sites

$$\mathcal{H}_{\mathrm{mag}}=\sum_{I}J_I\mathbf{s}_I\cdot\mathbf{S}.\tag{11.10}$$

The Anderson impurity model for a single-site coupling in d-wave superconductors, Eq. (11.7), was studied by Zhang, Hu, and Yu (2001). A sharp localized resonance above the Fermi energy was predicted for the impurity state. The marginal Fermi-liquid behavior, i.e., a logarithmic (in frequency) real part of the self-energy, along with a linear relaxation rate, was also obtained, indicating a new universality class for the strong-coupling fixed point. Almost at the same time, the multisite-coupling Anderson impurity model, Eq. (11.9), was considered by Zhu and Ting (2001a, 2001b), while the multisite-coupling Kondo impurity was studied by Polkovnikov, Sachdev, and Vojta (Polkovnikov *et al.*, 2001; Polkovnikov, 2002). These works show the existence of Kondo resonance. The low-energy structure of spectral weight of conduction electrons was found to be sensitive to the local environment surrounding the dynamic impurity. The on-site potential scattering was taken to be either zero (Zhang *et al.*, 2001) or very weak (Polkovnikov *et al.*, 2001; Polkovnikov, 2002) and the resonance peak was close to the Fermi energy. Zhu and Ting (2001a) took into account quasiparticle scattering from a geometrical hole, where electrons are allowed to hop onto four neighbors of the impurity site and obtained a double-peak structure around the Fermi energy. Furthermore, Zhu and Ting (2001b) considered the potential scattering term to be in the unitary limit ($U \to \infty$) and found that the Kondo screening and strong potential scattering determine the low-energy quasiparticle states. The influence of the potential scattering on the Kondo physics as well as the local electronic structure in d-wave superconductors has been reemphasized by Vojta and Bulla (2001).

Here we present a discussion based on the multisite-coupling Kondo impurity model, as given by Eq. (11.10). As demonstrated previously, the problem of a single-site potential scattering can be exactly solved. In Nambu space, the full-matrix Green's function is

$$G(i,j;i\omega_n) = G^0(i,j;i\omega_n) + G^0(i,0;i\omega_n)T(i\omega_n)G^0(0,j;i\omega_n), \quad (11.11)$$

where the T matrix due to the potential scatterer is

$$T^{-1}(i\omega_n) = \tau_3/U - G^0(0,0;i\omega_n), \quad (11.12)$$

and G^0 is the Green's function for the clean system. In the presence of both potential and magnetic scattering, the Green's function is

$$\tilde{G}(i,j;i\omega_n) = G(i,j;i\omega_n) + \sum_{l,l'} \varphi_l \varphi_{l'} G(i,l;i\omega_n)\mathcal{T}_K(i\omega_n) \times G(l',j;i\omega_n). \quad (11.13)$$

Here l and l' label the nearest neighbors to the impurity site at (0,0) and $\mathcal{T}_K$ is the T matrix for the Kondo impurity. The variables φ_l have a different meaning depending on the approach to $\mathcal{T}_K$. In the large-N approximation (equivalent to the slave-boson mean-field theory),

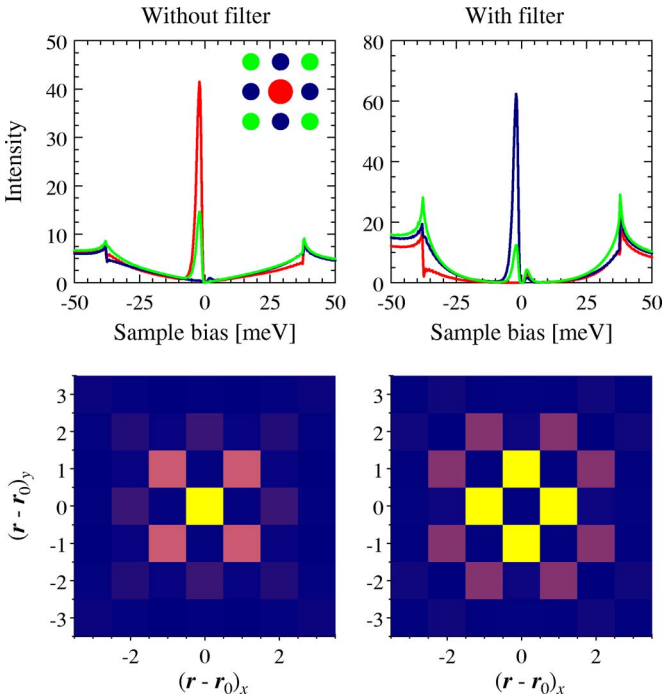

FIG. 28. (Color online) Calculated tunneling density of states for the four-site Kondo impurity model at 15% hole doping with a realistic band structure (t=0.15 eV, $t'=-t/4$, $t''=t/12$), Δ_0=0.04 eV, and $\mu=-0.14$ eV. The Kondo coupling is J =0.09 eV and the potential scattering is U=0. Top: Local DOS vs energy for the impurity site [with largest peak intensity without filter while smallest peak intensity with filter (red)] and the nearests- [with smallest peak intensity without filter while largest peak intensity with filter (blue)] and second- [with intermediate peak intensity with/without filter (green)] neighbor sites. Bottom: Spatial dependence of the local DOS at $\omega=-2$ meV. Left: Local DOS in the CuO_2 plane. Right: Local DOS after applying the filter effect proposed by Martin, Balatsky, and Zaanen (2002). From Vojta and Bulla, 2001.

$$\mathcal{T}_K^{-1} = i\omega_n - \lambda\tau_3 - \sum_{l,l'} \varphi_l \varphi_{l'} \tau_3 G(l,l';i\omega_n)\tau_3, \quad (11.14)$$

and φ_l are the complex Hubbard-Stratonovich fields, which are determined, together with the Lagrange multiplier λ, by the saddle-point solution. Within the numerical-renormalization-group approach, only the strongest d-wave scattering channel is considered, and the variables are taken to be $\varphi_l = +(-)1$ depending on the bond orientation. Note that this d-wave pattern is simply a band-structure effect and is not related to the d-wave symmetry of the superconducting order parameter of the host. The LDOS is

$$\rho_i(\omega) = -\frac{1}{\pi}\,\mathrm{Im}\left\{\mathrm{Tr}\left[\tilde{G}(i,i;\omega + i0^+)\frac{1+\tau_3}{2}\right]\right\}. \quad (11.15)$$

Figures 28–30 show the LDOS for a four-site Kondo impurity model and different strengths of the potential scattering, calculated using the numerical-renormalization-group technique (Vojta and Bulla,

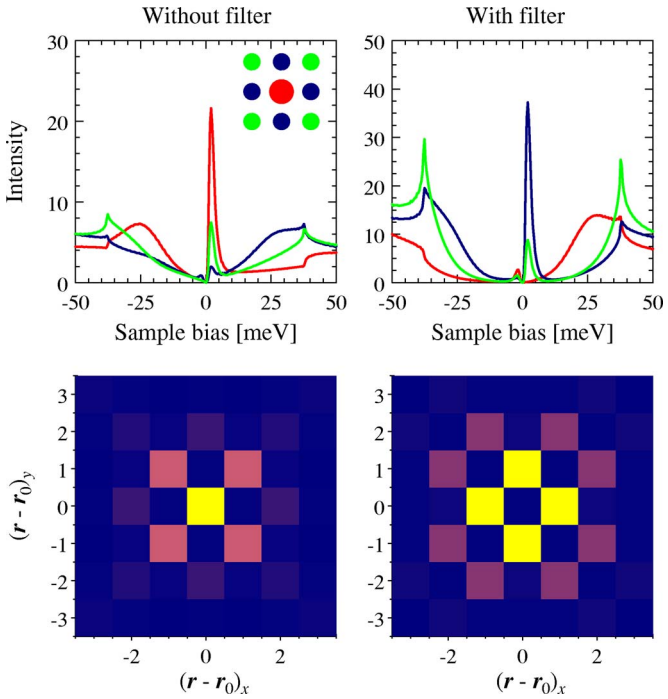

FIG. 29. (Color online) Same as Fig. 28, but with potential scattering $U=t=0.15$ eV. Here, $J=0.065$ eV. The lower panel shows the local DOS at $\omega=+2$ meV. From Vojta and Bulla, 2001.

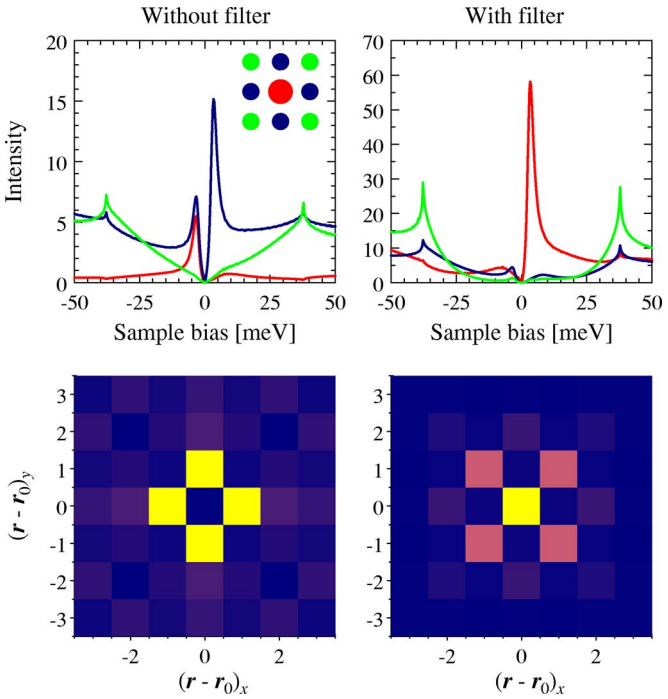

FIG. 30. (Color online) Same as Fig. 28, but with potential scattering $U=4t=0.6$ eV. Here, $J=0.04$ eV. The lower panel shows the local DOS at $\omega=+3$ meV. From Vojta and Bull, 2001.

2001). It is clear that the spatial structure of the resonance state is sensitive to the strength of the potential scattering: if it is absent, a sharp resonance peak appears directly on the impurity site, as well as on its next-nearest neighbors, with reduced intensity. This is consistent with experimental observations (Pan, Hudson, Lang, *et al.*, 2000). For a moderate potential scattering value, as shown in Fig. 29, the global particle-hole asymmetry changes sign and the Kondo peak appears at the opposite side of the Fermi level as compared to Fig. 28. For strong (but finite) potential scattering, the resonance peak due to impurity scattering becomes dominant, and the Kondo effect is weaved into the overall structure of the LDOS. In this case, the intensity of the on-site peak is strongly suppressed and a double-peak structure with enhanced intensity is seen in the LDOS at the nearest-neighbor sites. The same results were also obtained by Zhu and Ting (2001a) based on the Anderson impurity model. In this simple model the large LDOS from the resonance state induced by the strong potential scatterer dramatically reduces the critical Kondo coupling, indicating that the fate of the Kondo effect is determined by a local rather than a global environment in which the magnetic impurity is embedded. In the unitary limit (infinite impurity potential) LDOS has a zero intensity at the impurity site and a sharp single peak at its nearest neighbors. Consequently, to achieve agreement with the pattern observed in experiment, one needs to invoke the filter effect (Zhu, Ting, and Hu, 2000; Martin *et al.*, 2002), which is detailed in Sec. IX.

XII. INELASTIC SCATTERING IN *d*-WAVE SUPERCONDUCTORS

A. Inelastic scattering: General remarks

The previous section provided the simplest example of an impurity with an internal degree of freedom—spin for the Kondo effect. As a result, we extended the previous treatment of static impurities to account for scattering processes that involve spin flips, which resulted in a qualitatively new behavior. We now take this idea further and explore inelastic-scattering processes.

By definition, impurity scattering changes the direction of the quasiparticle momentum. However, purely potential scattering is elastic, i.e., the quasiparticle energy does not change. The Kondo impurity affects electron spin, however, scattering remains elastic: energies of spin-up and spin-down impurity states are identical; this degeneracy is at the origin of the Kondo singlet formation. In this section we consider inelastic-scattering processes that involve not only momentum but also energy transfer. There are two distinct scenarios for inelastic scattering. One possibility is that impurities themselves are dynamic, and energy is transferred to/from electrons during scattering only when they are in the immediate vicinity of the impurity. This is an extension of the previous treatment. Another possibility is that electrons scatter off of a delocalized (extended) collective mode, such as a spin wave or a phonon, while scattering on impurities remains elastic.

We consider the two situations separately. In the former case the impurity-induced electron self-energy

contains information about both the spatial and temporal, or dynamical, structure of the impurity. The latter case is even more interesting, as information about the extended collective mode is encoded in real-space Friedel oscillations around the impurity site, and its determination is only possible due to the presence of impurities. Below we discuss a proposal to combine Fourier transform and inelastic electron-tunneling spectroscopy (IETS). Fourier-transformed IETS, which is an extension of the FT-STM discussed above, allows, in principle, the investigation of both characteristic momentum and energy for inelastic scattering. The central object we deal with in this technique is $d^2I(\mathbf{q},eV)/dV^2$, similar to real-space IETS STM (Stipe *et al.*, 1998; Hahn and Ho, 2001): Extension of the IETS analysis to reciprocal space reveals nontrivial features in the spectra with simultaneous momentum and energy resolution.

The rest of the section is devoted to IETS in *d*-wave superconductors. A similar analysis can be done for the *s*-wave case (Brandt, 1970). We expect IETS features at energies above the gap to be similar for *s*- and *d*-wave superconductors, while below the gap a detailed analysis is required.

B. Localized modes in *d*-wave superconductors

Two examples reviewed explicitly are the local vibrational mode (arising, for example, from a substitution atom in the lattice) and scattering on an impurity spin in an applied magnetic field. Essentially the same techniques are used to analyze both situations, and here we follow the work of Balatsky *et al.* (2003) and Morr and Nyberg (2003).

The Hamiltonian for a local distortion coupled to electrons is known from the standard electron-phonon coupling theory. Here, however, the interaction occurs only at the impurity site, so that

$$H=\sum_{k\sigma}\xi_k c^\dagger_{k\sigma}c_{k\sigma}+\sum_k[\Delta_k c^\dagger_{k\uparrow}c^\dagger_{-k\downarrow}+\text{H.c.}] + g\sum_\sigma (b^\dagger+b)c^\dagger_{0\sigma}c_{0\sigma}. \tag{12.1}$$

The Hamiltonian for a spin S interacting with electrons via a contact exchange $J\mathbf{S}\cdot\boldsymbol{\sigma}$ is quite different,

$$H=\sum_{\mathbf{k}}\xi(\mathbf{k})c^\dagger_{\mathbf{k}\sigma}c_{\mathbf{k}\sigma}+\sum_{\mathbf{k}}[\Delta(\mathbf{k})c^\dagger_{\mathbf{k}\uparrow}c^\dagger_{-\mathbf{k}\downarrow}+\text{H.c.}] + \sum_{\mathbf{k},\mathbf{k}',\sigma,\sigma'} J\mathbf{S}\cdot c^\dagger_{\mathbf{k}\sigma}\sigma_{\sigma\sigma'}c_{\mathbf{k}'\sigma'}+g\mu_B\mathbf{S}\cdot\mathbf{B}. \tag{12.2}$$

The external magnetic field $\mathbf{B}\|\hat{\mathbf{z}}$ leads to Zeeman splitting of spin states by the Larmor frequency $\omega_0=g\mu_B B$. If the spin is in an equilibrium with a thermal bath, Zeeman splitting of spin levels is analogous to the frequency of a local mode, and electrons can scatter off the spin inelastically. We focus on the latter case.

In Eq. (12.2) we used a mean-field description of a superconducting state and ignored both the orbital and Zeeman effect of the field with conduction electrons. This is justified for $B\ll H_{c2}$.[10] In the following we choose $|S|=1/2$ and consider a *d*-wave superconductor, $\Delta(\mathbf{k})=(\Delta/2)(\cos k_x-\cos k_y)$, at low temperatures $T\ll T_c$. Clearly, this treatment is only justified when the spin is not screened via the Kondo interaction at low T.

Since spin splitting (and hence inelastic scattering) involves only components transverse to the field, information about scattering, to second order, is contained in the self-energy with the normal Green's function,

$$\Sigma(\omega_l)=J^2T\sum_{\mathbf{k},\Omega_n}G(\mathbf{k},\omega_l-\Omega_n)\chi^{+-}(\Omega_n). \tag{12.3}$$

Here the spin propagator $\chi(\tau)=\langle T_\tau S^+(\tau)S^-(0)\rangle$ in the frequency space is given by $\chi_0(\omega)=\langle S^z\rangle/[\omega_0^2-(\omega+i\delta)^2]$. For a local mode that is present on a single site there is no contribution to Σ from the anomalous Green's function, $\Sigma_{\mathbf{k}}F(\mathbf{k},\omega)=0$. For a free spin in a field $\langle S_z\rangle=\tanh(\omega_0/2T)/2$, but we keep the notation $\langle S_z\rangle$ to account for magnetic anisotropy. The functional form of the propagator is identical to that of a phonon mode, and therefore subsequent analysis is applicable to both situations.

In Eq. (12.3) the Green's function is determined self-consistently, $G^{-1}=G^{0-1}-\Sigma$, where G^0 is the Green's function of the pure *d*-wave superconductor and Ω_l (ω_l) are bosonic (fermionic) Matsubara frequencies. After analytic continuation to the real axis, $i\omega_n\to\omega+i\delta$, we find for the imaginary part of the self-energy

$$\text{Im}\,\Sigma(\omega)=-J^2\langle S_z\rangle\text{Im}\,G(\omega-\omega_0)[n_F(\omega-\omega_0)-n_B(\omega_0)-1], \tag{12.4}$$

where $n_{F(B)}(\omega)=1/[\exp(\beta\omega)+(-)1]$ are Fermi (Bose) distribution functions. Information on the tunneling DOS is contained solely in the self-energy. Modifications of the superconducting order parameter and bosonic propagator are ignored here.

Figure 31 shows the results for the local density of states at the impurity site, solved numerically by finding Σ and G. To proceed with an analytical treatment, below we limit ourselves to second-order scattering in Σ. We find that the differences between the self-consistent solution and the second-order calculation are only quantitative. To that accuracy, the corrections to the Green's function are $G(\mathbf{r},\mathbf{r}',\omega)=G^0(\mathbf{r},\mathbf{r}',\omega)+G^0(\mathbf{r},0,\omega)\Sigma(\omega)G^0(0,\mathbf{r}',\omega)+F^0(\mathbf{r},0,\omega)\Sigma(\omega)F^{*0}(0,\mathbf{r},\omega)$. We define $K(T,\omega,\omega_0)=-[n_F(\omega-\omega_0)-n_B(\omega_0)-1]$ and focus on $T\ll\omega_0$, when $K(T,\omega,\omega_0)\simeq\Theta(\omega-\omega_0)$. From this expression, the correction to the LDOS at point $\mathbf{r}$ is

$$\delta N(\mathbf{r},\omega)=(1/\pi)\text{Im}[G^0(\mathbf{r},0,\omega)\Sigma(\omega)G^0(0,\mathbf{r},\omega) \pm F^0(\mathbf{r},0,\omega)\Sigma(\omega)F^{*0}(0,\mathbf{r},\omega)].$$

Here a plus (minus) sign corresponds to the coupling to

[10] To minimize the orbital effect of the magnetic field one can apply it parallel to the surface of a superconductor. The magnetic field is screened on the penetration depth scale so that its effect on superconducting electrons is small.

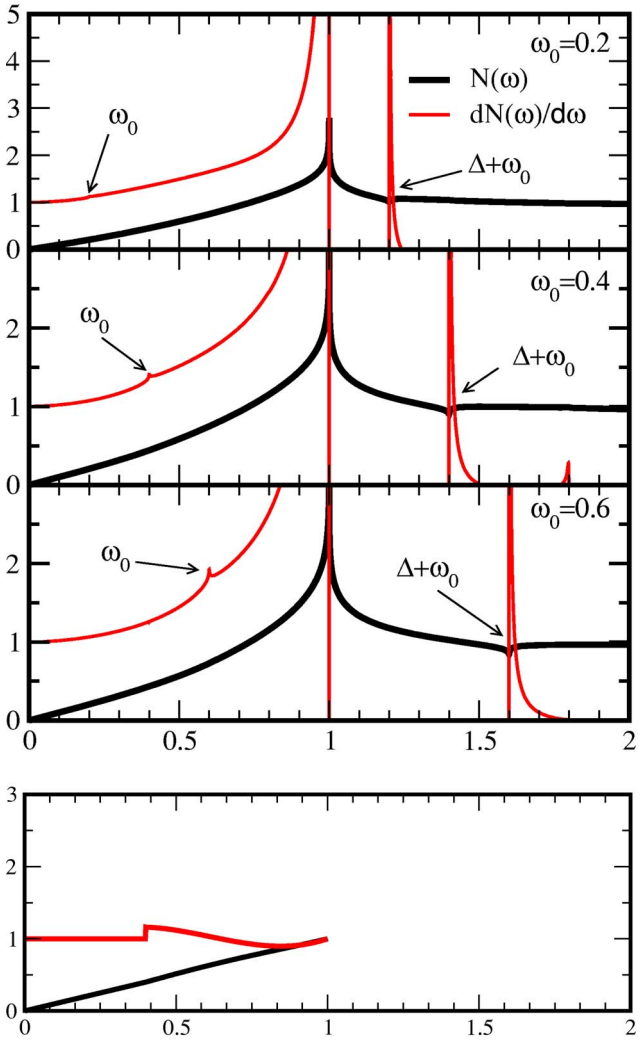

FIG. 31. (Color online) The DOS thick (black) line and its energy derivative thin (red) line for a local boson-mode scattering in a d-wave superconductor. The normal self-energy was treated self-consistently in Eq. (12.4). We ignored vertex corrections and gap modification. In addition to the feature at $\omega=\omega_0$ we find strong satellite peaks at $\Delta+\omega_0$ resulting from the coherence peak in the DOS of a d-wave superconductor. Satellites are not present in the pseudogap state with no off-diogonal long-range order (ODLRO). These features are best seen in $dN/d\omega$. Energy is in units of Δ; the dimensionless coupling constant is 1. The top three panels are for local mode frequencies $\omega_0/\Delta=0.2,0.4,0.6$. The lower panel shows the asymptotic analytic solution, which assumes $\omega_0 \ll \Delta$ and uses Eq. (12.2), for $\omega_0=0.4$. The overall features are similar for both cases, however, the analytic solution shows a somewhat larger feature. From Balatsky *et al.*, 2003.

the local vibrational (spin) mode, i.e., to the cases of preserved (broken) time-reversal symmetry. The modification of the LDOS is most pronounced at the impurity site, where we find

$$\frac{\delta N(\mathbf{r}=0,\omega)}{N_0}=\frac{\pi^2}{2}(JSN_0)^2\frac{\omega-\omega_0}{\Delta}K(T,\omega,\omega_0)\times\left[\frac{2\omega}{\Delta}\ln\left(\frac{\Delta}{\omega}\right)\right]^2,\quad \omega\ll\Delta, \tag{12.5}$$

$$\frac{\delta N(\mathbf{r}=0,\omega)}{N_0}=2\pi^2(JSN_0)^2K(T,\omega,\omega_0)\ln^2\left(\frac{|\omega-\Delta|}{4\Delta}\right)\times\ln\left(\frac{4\Delta}{|\omega+\omega_0-\Delta|}\right)+(\omega_0\to-\omega_0),\quad \omega\simeq|\Delta|. \tag{12.6}$$

To obtain this result we retained only the dominant real part of $G^0(0,0,\omega)=N_0(2\omega/\Delta)\ln(4\Delta/\omega)$ for $\omega\ll\Delta$ and the dominant imaginary part of $G^0(0,0,\omega)=i\pi N(\omega)=-2iN_0\ln(|\omega-\Delta|/4\Delta)$, in the opposite limit $\omega\simeq\Delta$. The results for the LDOS $N(\omega)$ and its derivative $dN(\omega)/d\omega$ are shown in the lower panel of Fig. 31.

Away from the impurity site $N(\mathbf{r},\omega)$ exhibits Friedel oscillations. A standing wave produced by inelastic scattering has fingerprints of the energy transfer: there is a peak (or a cusp) in the derivative of the DOS with respect to energy. These oscillations can be called *inelastic* Friedel oscillations, stressing the oscillating nature of the inelastic signal d^2I/dV^2 in real space. These oscillations can also be analyzed in reciprocal space, similar to the elastic case in Sec. IX.D. The real-space pattern at $\omega\ll\Delta$ is given by $\Lambda(\mathbf{r})=[|G^0(\mathbf{r},\omega)|^2\pm|F^0(\mathbf{r},\omega)|^2]\sim\sin(k_Fr)/[(k_Fr_\parallel)^2+(r_\perp/\xi)^2]$. Here we have separated $\mathbf{r}=(\mathbf{r}_\perp,\mathbf{r}_\parallel)$ into components along $(\mathbf{r}_\perp)$ and normal to $(\mathbf{r}_\parallel)$ the Fermi surface near the nodal point. The existence of nodes in the superconducting gap leads to the power-law decay of $\Lambda(\mathbf{r})$ in all directions and to its fourfold modulation due to gap anisotropy; see Salkola *et al.* (1997) and Sec. VII.

It is important to emphasize the differences between the resulting LDOS behavior for a nodal superconductor and a normal metal. For a d-wave superconductor, using the connection between the differential conductance in STM experiments and DOS, we find

$$\delta\frac{dI}{dV}\Big/\frac{dI}{dV}\sim\delta N(\mathbf{r}=\mathbf{0},V)/N_0\sim(JSN_0)^2\frac{V-\omega_0}{\Delta}\Theta(V-\omega_0),$$

$$\delta\frac{d^2I}{dV^2}\sim(JSN_0)^2\Theta(V-\omega_0). \tag{12.7}$$

In contrast, for a metal with the energy-independent normal-state DOS, from Eq. (12.5) for $T\ll\omega_0$,

$$\frac{dI}{dV}\sim\delta N(\mathbf{r}=\mathbf{0},V)\sim J^2N_0^3\Theta(V-\omega_0), \tag{12.8}$$

and the second derivative reveals a delta function $d^2I/dV^2\sim J^2N_0^3\delta(\omega-\omega_0)$. We emphasize that the dominant effect is due purely to the energy dependence of the DOS, and therefore both in a d-wave superconductor and in a metal with vanishing DOS $N(\omega)=N_0(\omega/\Delta)$ (such as in some of the models of the pseudogap) there is a step discontinuity in d^2I/dV^2 at the energy of a local mode with the strength $J^2N_0^2$ (see Fig. 31).

The result can be generalized to a metal with a power-law DOS, $N(\omega)=(1/\pi)\mathrm{Im}\, G^0(0,0,\omega)=(\omega/\Delta)^\gamma N_0$, with $\gamma>0$. From Eqs. (12.4) and (12.5) we have for $\omega\ll\Delta$,

$$\delta\frac{dI}{dV}\Big/\frac{dI}{dV}\sim \delta N(\mathbf{r}=0,V)/N_0\sim (V-\omega_0)^\gamma\Theta(V-\omega_0),$$

$$\delta\frac{d^2I}{dV^2}\sim (V-\omega_0)^{\gamma-1}\Theta(V-\omega_0). \tag{12.9}$$

Thus we find a singularity at ω_0 for $\gamma<1$ and a power law for $\gamma\geqslant 1$. For $\gamma=1$ we recover the result for a d-wave superconductor.

These results can be expressed more generally via the energy spectrum of the superconductor. Using a spectral representation for $G(\mathbf{r},\omega)$ with Bogoliubov's functions $u_\alpha(\mathbf{r}), v_\alpha(\mathbf{r})$ for the eigenstate α,

$$G(\mathbf{r},\omega)=\sum_\alpha\left[\frac{|u_\alpha(\mathbf{r})|^2}{\omega-E_\alpha+i\delta}+\frac{|v_\alpha(\mathbf{r})|^2}{\omega+E_\alpha+i\delta}\right]. \tag{12.10}$$

For $T\ll\omega_0$, we find

$$\mathrm{Im}\,\Sigma(\omega)=\frac{\pi J^2}{2\omega_0}\langle S_z\rangle[|u_\alpha(\mathbf{r}=0)|^2\delta(\omega-\omega_0-E_\alpha)+|v_\alpha(\mathbf{r}=0)|^2\delta(\omega-\omega_0+E_\alpha)],\quad \omega>0. \tag{12.11}$$

In the preceding equation for $\omega<0$ we need to symmetrize, $\omega_0\to-\omega_0$. Consider a magnetic impurity resonance in a d-wave superconductor at energy ω_{imp} (such as a Ni resonance in cuprates) (Salkola *et al.*, 1997; Hudson *et al.*, 2001). Then the sum is dominated by the term with resonance level $E_\alpha=\omega_{\mathrm{imp}}$ in the vicinity of the impurity site. Inelastic scattering produces satellites of the main level split from it by energy ω_0; see Fig. 32. Similar splitting occurs for a phonon mode with energy ω_0.

For cuprates, taking the experimentally measured DOS $N_0\simeq 1/eV$ with $JN_0\simeq 0.14$, $\Delta=30$ meV (Hudson *et al.*, 2001) and assuming a field of ~ 10 T we find $\omega_0=1$ meV. Then from Eqs. (12.5)–(12.7)

$$\delta N(\mathbf{r}=0,\omega)/N_0\simeq 10^{-2}\frac{\omega-\omega_0}{\Delta}\Theta(\omega-\omega_0). \tag{12.12}$$

To observe this effect one has to sample DOS in the vicinity of $eV=\omega_0\propto B$. Assuming $\omega-\omega_0=\omega_0$ we have from Eq. (12.12) $\delta(dI/dV)/dI/dV\sim 10^{-2}$. Expressed as a relative change of DOS of a superconductor $N(\omega)=N_0\omega/\Delta$ the effect is

$$\delta\frac{dI}{dV}\Big/\frac{dI}{dV}\sim \delta N(\mathbf{r}=0,\omega)/N(\omega_0)\sim 10^{-2}\frac{\omega-\omega_0}{\omega_0}\Theta(\omega-\omega_0). \tag{12.13}$$

It is of the same order as the observed vibrational modes of localized molecules in inelastic electron-tunneling spectroscopy STM, IETS-STM (Stipe *et al.*, 1998; Hahn and Ho, 2001). The satellites at $\Delta+\omega_0$ produce an order unity effect and are clearly seen even for small coupling.

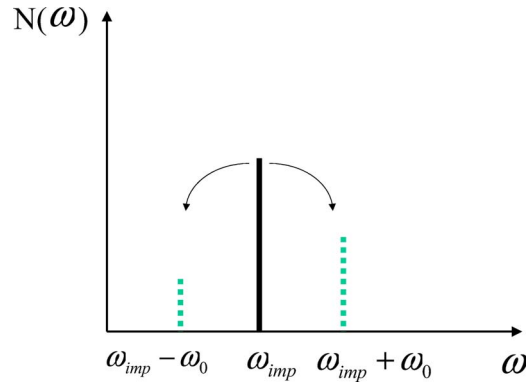

FIG. 32. (Color online) Satellite peaks for an impurity resonance ω_{imp} at $\omega_{\mathrm{imp}}\pm\omega_0$ shown schematically. The satellites have different spectral weight. If an electron with energy $\omega_{\mathrm{imp}}+\omega_0$ is injected into the system, it can excite a local mode and form the bound state at ω_{imp}. Similarly, an injected electron at energy $\omega_{\mathrm{imp}}-\omega_0$ can absorb local mode energy to reach ω_{imp}. For the latter process to occur, the mode has to be excited, and hence this peak has very low weight at low T. The two processes have different matrix elements. Relative weight of the side peaks is proportional to $J^2N_0^2$, which we assumed to be small. For magnetic scattering ($\omega_0=g\mu_BB$), the splitting is tunable by the field. From Balatsky *et al.*, 2003.

The important difference with phonons is that for a localized spin scattering the kink in DOS is tunable with magnetic field, which makes its detection easier.

The proposed extension of inelastic tunneling spectroscopy on strongly correlated electron states, such as d-wave superconductor and pseudogap normal states, opens the possibilities for studying the dynamics of local spin and vibrational excitations. The DOS in these systems often has power-law energy dependence, $N(\omega)\sim\omega^\gamma$, $\gamma>0$, resulting in weaker features than in normal metals. This technique allows for Zeeman-level spectroscopy of a single magnetic center, thus allowing, in principle, single-spin detection. The feature in $dI/dV\sim(\omega-\omega_0)^{\gamma-1}\Theta(\omega-\omega_0)$ near the threshold energy ω_0 is due to inelastic scattering. One also finds strong satellite features near the gap edge due to the coherence peak for a superconducting case. The singularity in the derivative of the conductance is of a power-law type and qualitatively different from the results for metallic DOS (Stipe *et al.*, 1998; Hahn and Ho, 2001). For the relevant values of parameters for high-T_c materials, the feature is expected to be on the order of several percent and should be observable. Similar predictions are also applicable to local vibrational modes in which ω_0 is the mode frequency.

C. Interplay between collective modes and impurities in *d*-wave superconductors

We have focused so far on the IETS for local modes in which inelastic scattering occurs only on one site. Here we extend the discussion to the case of a collective mode. In real systems this may be a spin mode (Norman and Ding, 1998; Campuzano *et al.*, 1999; Eschrig and

Norman, 2000; Abanov *et al.*, 2002; Kee *et al.*, 2002) or lattice mode (Damascelli *et al.*, 2003; Gweon *et al.*, 2004; Lanzara *et al.*, 2004).

We are motivated by the possible connection between the kink in the quasiparticle dispersion found in ARPES data on cuprates and phonon modes (and, possibly, interactions that lead to superconductivity) (Damascelli *et al.*, 2003; Gweon *et al.*, 2004; Lanzara *et al.*, 2004). Efforts to relate the data from ARPES, STM, and transport measurements in cuprates have recently intensified (Scalapino *et al.*, 2004; Zhu, Hirschnfeld and Scalapino, 2004). It has also been suggested that the full Eliashberg function in frequency and momentum space may be extracted from ARPES (Vekhter and Varma, 2003), and the challenge is to design a similar procedure to use with IETS STM.

At first glance it seems that local probes have poor momentum resolution since they couple to LDOS, which is summed over all momenta, and cannot identify the momentum dependence of collective modes. We argue that this is a misconception, and the FT IETS can provide the momentum spectroscopy of modes that produce inelastic scattering.

The elastic FT STM can identify Fermi wave vectors because of Friedel oscillations in the electron density due to impurities; see Sec. IX.D. For FT IETS, we need impurity scattering to produce interference waves in real space. Hence we look at features arising from the interplay between dynamic scattering off the collective mode and static disorder. We use the Fourier transform of the LDOS as a tool to investigate characteristic momentum and energy features containing fingerprints of bosonic excitations (Zhu, Sun, *et al.*, 2004).

We call this approach the Fourier-transformed inelastic electron-tunneling spectroscopy STM (FT IETS STM). The central object in this technique is the Fourier transform of the second derivative of the tunneling current $d^2I/dV^2(\mathbf{q},eV)$. The energy signatures of the quasiparticle interaction with the collective mode, and the real-space pattern of the scattering of the same quasiparticles from a local impurity, combine to produce features containing information on the energy and momentum of the mode in $d^2I/dV^2(\mathbf{r},eV)$. A Fourier-transform map of this quantity could help to uncover the characteristic momenta of the mode, just as conventional Friedel oscillations encode the Fermi wave vector in $d^2I/dV^2(\mathbf{r},E)$; see Sec. XII.B.

To illustrate this idea consider a spin-resonance mode, such as that revealed by neutron scattering in cuprates (Norman and Ding, 1998; Campuzano *et al.*, 1999; Eschrig and Norman, 2000; Abanov *et al.*, 2002; Kee *et al.*, 2002). To detect this mode, it has been proposed that STM be used (Zhu, Sun, *et al.*, 2004). We limit consideration to the example of a sharp mode at wave vector $\mathbf{Q}=(\pi,\pi)$ with energy $\omega_0=42$ meV. This assumption allows us to highlight the effect, but the formalism presented here is equally applicable to the case in which the mode spectral density is distributed in energy and momentum.

We have to keep track of self-energy effects as a function of energy as well as momentum. Inelastic scattering of quasiparticles requires considering off-shell excitations, up to energies $\Delta+\Omega_0\sim 70$ meV. At these energies Fermi-surface effects, typical wave vectors of the collective mode and typical wave vectors of the impurity potential all determine the momentum dependence of the inelastic tunneling features seen in FT IETS STM.[11]

We start with a model Hamiltonian describing two-dimensional electrons coupled to a collective spin mode and in the presence of disorder,

$$\mathcal{H}=\mathcal{H}_{\mathrm{BCS}}+\mathcal{H}_{\mathrm{sp}}+\mathcal{H}_{\mathrm{imp}}. \tag{12.14}$$

Here the BCS-type Hamiltonian is given by $\mathcal{H}_{\mathrm{BCS}}=\Sigma_{\mathbf{k},\sigma}(\varepsilon_{\mathbf{k}}-\mu)c^{\dagger}_{\mathbf{k}\sigma}c_{\mathbf{k}\sigma}+\Sigma_{\mathbf{k}}(\Delta_{\mathbf{k}}c^{\dagger}_{\mathbf{k}\uparrow}c^{\dagger}_{-\mathbf{k}\downarrow}+\Delta^{*}_{\mathbf{k}}c_{-\mathbf{k}\downarrow}c_{\mathbf{k}\uparrow})$, where $\varepsilon_{\mathbf{k}}$ is the normal-state dispersion, μ is the chemical potential, and $\Delta_{\mathbf{k}}=(\Delta_0/2)(\cos k_x-\cos k_y)$ is the d-wave superconducting energy gap. The coupling between electrons and the resonance mode is modeled by $\mathcal{H}_{\mathrm{sp}}=g\Sigma_i\mathbf{S}_i\cdot\mathbf{s}_i$, where g, $\mathbf{s}_i$, and $\mathbf{S}_i$ are the coupling strength, the electron-spin operator at site i, and the operator for the collective spin degrees of freedom, respectively. The dynamics of the collective mode is specified by spin $\mathbf{S}$ susceptibility $\chi_{ij}(\tau)$, defined below. Quasiparticle scattering from impurities in the Hamiltonian is given by $H_{\mathrm{imp}}=\Sigma_{i\sigma}U_ic^{\dagger}_{i\sigma}c_{i\sigma}$, where U_i is the strength of the impurity potential, and we consider weak (Born) scattering. One of the interesting findings is that characteristic wave vectors of the impurity potential $U_{\mathbf{q}}=\Sigma_iU_i\exp(i\mathbf{q}\cdot\mathbf{r}_i)$ play a crucial role in defining characteristic wave vectors of the DOS modulation. For simplicity, we consider only nonmagnetic scattering.

By introducing a two-component Nambu spinor operator, $\Psi_i=(c_{i\uparrow},c^{\dagger}_{i\downarrow})^T$, one can define the matrix Green's function for the full Hamiltonian system, $\hat{G}(i,j;\tau,\tau')=-\langle T_{\tau}[\Psi_i(\tau)\otimes\Psi^{\dagger}_j(\tau')]\rangle$. Simple algebra leads to the full-electron Green's function with impurity scattering,

$$\begin{aligned}G(i,j;i\omega_n)=\tilde{G}^{(0)}(i,j;i\omega_n)+\sum_{j'}U_{j'}[&\tilde{G}^{(0)}(i,j';i\omega_n)\\&\times\tilde{G}(j',j;i\omega_n)-\tilde{F}^{(0)}(i,j';i\omega_n)\tilde{F}^{(0)}\\&\times(j',i;i\omega_n)].\end{aligned} \tag{12.15}$$

Here $\tilde{G}^{(0)},\tilde{F}^{(0)},\tilde{F}^{*(0)}$ are the dressed by scattering of the collective mode normal and anomalous Green's function, with its Fourier component given by 11, 12, and 21 components of the full-matrix Green's function,

[11]We limit ourselves to second-order scattering between carriers and bosonic excitations and at this level there is no conceptual difference in the method for spin or phonon bosonic mode.

$$[\hat{\tilde{G}}^{(0)}]^{-1}(\mathbf{k};i\omega_n)=\begin{pmatrix} i\omega_n-\xi_{\mathbf{k}}-\Sigma_{11} & -\Delta_{\mathbf{k}}-\Sigma_{12} \\ -\Delta_{\mathbf{k}}-\Sigma_{21} & i\omega_n+\xi_{\mathbf{k}}-\Sigma_{22}\end{pmatrix}, \tag{12.16}$$

where $\xi_{\mathbf{k}}=\varepsilon_{\mathbf{k}}-\mu$, $\omega_n=(2n+1)\pi T$ is the fermionic Matsubara frequency. When quasiparticles scatter inelastically off of the collective mode, the self-energy, to second order in the coupling constant, is

$$\hat{\Sigma}(\mathbf{k};i\omega_n)=\frac{3g^2T}{4}\sum_{\mathbf{q}}\sum_{\Omega_l}\chi(\mathbf{q};i\Omega_l)\hat{G}^{(0)}(\mathbf{k}-\mathbf{q};i\omega_n-i\Omega_l), \tag{12.17}$$

where $\chi(\mathbf{q};i\Omega_l)$ is the dynamical spin susceptibility $\chi_{ij}(\tau)=\langle T_\tau[S_i^x(\tau)S_j^x(0)]\rangle$, $\Omega_l=2l\pi T$ is the bosonic Matsubara frequency, $\hat{G}^{(0)}$ is the bare superconducting Green's function, and $\hat{\tilde{G}}^{(0)}$ is the superconducting Green's function, dressed by scattering of the collective mode, but without disorder. We assume that the d-wave pair potential is real. For a single-site impurity, the equation of motion for the full Green's function can be exactly solved; see above. For multiple impurities, and especially for the inhomogeneous situation, an approximation scheme for $\hat{\Sigma}$ is in order. In the Born limit, the normal Green's function G is found to be

$$G(i,j;i\omega_n)=\tilde{G}^{(0)}(i,j;i\omega_n)+\delta G(i,j;i\omega_n), \tag{12.18}$$

with

$$\delta G(i,j;i\omega_n)=\sum_{j'}U_{j'}[\tilde{G}^{(0)}(i,j';i\omega_n)\tilde{G}^{(0)}(j',j;i\omega_n) - \tilde{F}^{(0)}(i,j';i\omega)\tilde{F}^{*(0)}(j',j;i\omega_n)]. \tag{12.19}$$

The LDOS at site i, summed over spin components, is

$$\rho(\mathbf{r}_i,E)=-\frac{2}{\pi}\,\mathrm{Im}\,G(i,i;E+i\gamma), \tag{12.20}$$

where $\gamma=0^+$. We are especially interested in the correction to the LDOS from the impurity scattering,

$$\delta\rho(\mathbf{r}_i,E)=-\frac{2}{\pi}\,\mathrm{Im}\,\delta G(i,i;E+i\gamma), \tag{12.21}$$

and its Fourier transform,

$$\begin{aligned}\delta\rho(\mathbf{q},E)&=\sum_i\delta\rho(i,E)e^{-i\mathbf{q}\cdot\mathbf{r}_i}\\ &=-\frac{U_{\mathbf{q}}}{N\pi i}\sum_{\mathbf{k}}[\tilde{G}^{(0)}(\mathbf{k}+\mathbf{q};E+i\gamma)\tilde{G}^{(0)}(\mathbf{k};E+i\gamma)\\ &\quad-\tilde{G}^{(0)*}(\mathbf{k}-\mathbf{q};E+i\gamma)\tilde{G}^{(0)*}(\mathbf{k};E+i\gamma)\\ &\quad-\tilde{F}^{(0)}(\mathbf{k}+\mathbf{q};E+i\gamma)\tilde{F}^{*(0)}(\mathbf{k};E+i\gamma)\\ &\quad+\tilde{F}^{(0)*}(\mathbf{k}-\mathbf{q};E+i\gamma)\tilde{F}^{(0)}(\mathbf{k};E+i\gamma)].\end{aligned} \tag{12.22}$$

Here $U_{\mathbf{q}}=\Sigma_i U_i e^{-i\mathbf{q}\cdot\mathbf{r}_i}$ is the Fourier transform of the scattering potential. It multiplies the entire result and directly affects the FT IETS image. For example, if $U_{\mathbf{q}}$ has a strong peak at $\mathbf{q}=\mathbf{q}_0$, it will result in a spurious peak in the image, not related to the characteristic momenta for inelastic scattering. Detailed knowledge of impurity scattering is necessary for extracting the intrinsic scattering momenta from FT IETS STM.

The local density of states is proportional to the local differential tunneling conductance (i.e., dI/dV). In looking at the renormalization effect of collective bosonic excitations in the STM, we see that the energy derivative of the LDOS, corresponding to the derivative of the local differential tunneling conductance (i.e., d^2I/dV^2), is more favorable to signal enhancement. For a fixed value of energy, one first gets a set of $\delta\rho'(i,E)$ (the prime means the energy derivative) in real space and then performs the Fourier transform,

$$\delta\rho'(\mathbf{q},E)=\sum_i\delta\rho'(\mathbf{r}_i,E)e^{-i\mathbf{q}\cdot\mathbf{r}_i}, \tag{12.23}$$

to obtain a map of the Fourier spectrum in $\mathbf{q}$ space,

$$P(\mathbf{q},E)=|\delta\rho'(\mathbf{q},E)|. \tag{12.24}$$

Up to now discussion and formulation are quite general and can be used to study the effects of any dynamic mode once the susceptibility χ is known. For the specific case of a magnetic mode, we take a phenomenological form (based on inelastic neutron-scattering observations) (see, also, Eschrig and Norman, 2000),

$$\chi(\mathbf{q};i\Omega_l)=-\frac{f(\mathbf{q})}{2}\left[\frac{1}{i\Omega_l-\Omega_0}-\frac{1}{i\Omega_l+\Omega_0}\right]. \tag{12.25}$$

Here the spin-resonance-mode energy is also denoted by Ω_0. The quantity $f(\mathbf{q})$ describes the momentum dependence of the mode and is assumed to be enhanced at the $\mathbf{Q}=(\pi,\pi)$ point. Using the correlation length ξ_{sf} (chosen to be 2 here), it can be written as

$$f(\mathbf{q})=\frac{1}{1+4\xi_{sf}^2[\cos^2 q_x/2+\cos^2 q_y/2]}. \tag{12.26}$$

This form captures the essential feature of a resonant peak observed by neutron-scattering experiments in the superconducting state of cuprates (Zhu, Sun, *et al.*, 2004). Note that strong impurity scattering will shift the position and broaden the width of the (π,π) spin-resonance peak (Li *et al.*, 1998). However, in the Born limit, the above form of the susceptibility should still be valid for this discussion. For normal-state energy dispersion, we adopt a six-parameter fit to the band structure used previously for optimally doped Bi-2212 systems (Norman *et al.*, 1995) having the form

$$\begin{aligned}\xi_{\mathbf{k}}&=-2t_1(\cos k_x+\cos k_y)-4t_2\cos k_x\cos k_y\\ &\quad-2t_3(\cos 2k_x+\cos 2k_y)-4t_4(\cos 2k_x\cos k_y\\ &\quad+\cos k_x\cos 2k_y)-4t_5\cos 2k_x\cos 2k_y-\mu,\end{aligned} \tag{12.27}$$

where $t_1=1$, $t_2=-0.2749$, $t_3=0.0872$, $t_4=0.0938$, $t_5=-0.0857$, and $\mu=-0.8772$. Unless specified explicitly,

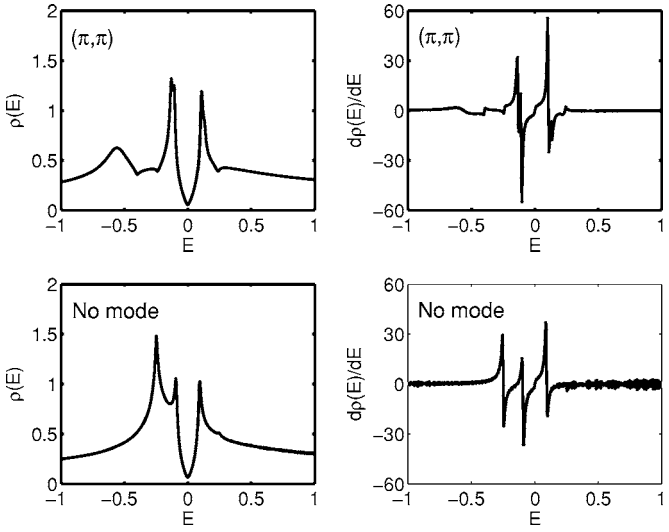

FIG. 33. Density of states (left column) and its energy derivative (right column) as a function of energy for a clean d-wave superconductor with the electronic coupling to the (π,π) spin-resonance mode ($g=2.30$). The case of no mode coupling ($g=0$) is also shown for comparison.

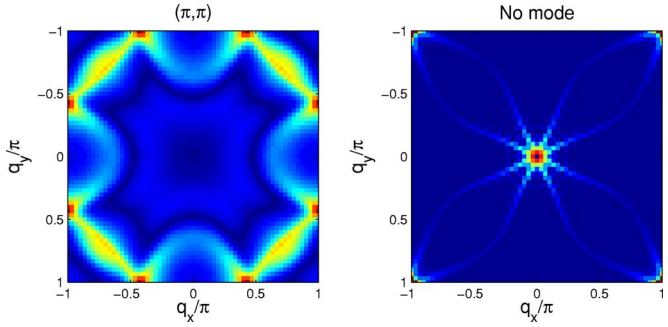

FIG. 34. (Color online) The Fourier spectral weight of the energy derivative of the LDOS at $E=-(\Delta_0+\Omega_0)$ for a d-wave superconductor with the electronic coupling to the spin-resonance modes ($g=2.30$). For comparison, the quantity is also shown for the case of no mode coupling ($g=0$).

the energy is measured in units of t_1 hereafter. Since the maximum energy gap for most of the cuprates at the optimal doping is about 30 meV, while the resonance-mode energy is in the range between 35 and 47 meV, we take $\Delta_0=0.1$ and $\Omega_0=0.15$ (i.e., $1.5\Delta_0$). To mimic the intrinsic lifetime broadening, in our numerical calculation we use $\gamma=0.005$ in Eq. (12.20). The system size is $N_x \times N_y=1024\times1024$.

We present in Fig. 33 the results of the DOS and its energy derivative as a function of energy for a clean (i.e., $U_0=0$) d-wave superconductor with electronic coupling to (π,π) spin-resonance modes. For comparison, the DOS for the case of no mode coupling is also shown. When there is no electron-mode coupling, there is a Van Hove singularity peak appearing outside the superconducting gap edge. When electrons are coupled to (π,π)-spin-resonance modes, the Van Hove singularity peak is strongly suppressed. Instead, one sees a dip structure following the coherent peak at the gap edge. The distance between this dip and the coherent peak defines the resonance energy Ω_0. These results, for the clean case, are consistent with earlier ARPES studies (Dessau *et al.*, 1991; Shen and Schrieffer, 1997; Norman and Ding, 1998; Campuzano *et al.*, 1999; Eschrig and Norman, 2000; Abanov *et al.*, 2002; Kee *et al.*, 2002) and DOS studies (Abanov and Chubukov, 2000). The shift of states due to inelastic scattering is also expected for scattering off the local mode; Sec. XII.B. Taking the second derivative d^2I/dV^2 emphasizes these features. As shown in the right column of Fig. 33, when electrons are coupled to spin-resonance modes there is a strong peak structure at $E=-(\Delta_0+\Omega_0)$ in the $\rho'(E)$ spectrum.

In Fig. 34, we show the Fourier spectrum of the derivative of the LDOS at the energy $-(\Delta_0+\Omega_0)$ (i.e., the peak position in d^2I/dV^2 in the presence of the mode coupling) with a structureless scattering potential $U_{\mathbf{q}}=U_0$, arising from a single-site impurity. In the absence of electron-mode coupling, the Fourier spectrum intensity is strongest at $\mathbf{q}=(0,0)$ and its equivalent points and has moderate weight along the edges of the square around $\mathbf{q}=(\pi,\pi)$. When the electron-spin mode coupling is present, as shown in Fig. 34, the spectrum has the strongest intensity at the diamonds around (π,π). Independent of the coupling to the collective mode, the spectrum has an intensity minimum $\mathbf{q}=(\pi,\pi)$. The Fourier-transformed image of d^2I/dV^2 is greatly affected in this case by the underlying band structure.

In this simple model, the inelastic feature is expected at $E_r=\Delta_0+\Omega_0\sim70$ meV for optimal doping. Since the observed gap is position dependent, so is E_r. The wave vectors in which inelastic features are most prominent depend on the momentum dependence of the disorder potential $U(\mathbf{q})$, doping, and the band structure. These combine to produce the "diamonds" seen in Fig. 34. In addition to structure at large momenta, there are features at small $\mathbf{q}$ in $d^2I(\mathbf{q},V)/dV^2$ (Zhu, Balatsky, *et al.*, 2005; Zhu, McElroy, *et al.*, 2005). Although we have focused on the spin mode, FT IETS STM is applicable to lattice (Zhu, Balatsky, *et al.*, 2005, Zhu, McElroy, *et al.*,2005) and local inelastic modes (Balatsky *et al.*, 2003; Morr and Nyberg, 2003).

The FT-IETS STM technique can be applied to a variety of systems, such as conventional and organic superconductors, and systems exhibiting charge- and spin-density waves. Disorder and "inelastic Friedel" oscillations produced by disorder are necessary ingredients of this new technique. The real potential of this technique can only be assessed when a comparison is made between experimental data and theoretical predictions on model systems. We are optimistic that this technique will be useful in the near future and refer the reader to recent literature on this rapidly developing field (Balatsky *et al.*, 2003; Morr and Nyberg, 2003; Zhu, Sun, *et al.*, 2004; Zhu, Balatsky, *et al.*, 2005; Zhu, McElroy, *et al.*, 2005).

XIII. AVERAGE DENSITY OF STATES IN SUPERCONDUCTORS WITH IMPURITIES

The Green's-function formalism is well suited to the analysis of the combined effect with many uncorrelated impurities in the bulk of a superconductor. The first treatment was given in a pioneering paper by Abrikosov and Gor'kov (1960). The basic assumptions underlying the calculations were given in Sec. III.C. After averaging over different impurity distributions following Eq. (3.14), the translational symmetry is restored, and the Green's function takes the form

$$\hat{G}^{-1}(\mathbf{k},\omega) = i\omega_n - \xi(\mathbf{k})\tau_3 - \Delta_0\sigma_2\tau_2 - \hat{\Sigma} \tag{13.1}$$

$$\equiv i\tilde{\omega} - \tilde{\varepsilon}(\mathbf{k})\tau_3 - \tilde{\Delta}\sigma_2\tau_2. \tag{13.2}$$

Here we have taken into account the matrix structure of the self-energy, $\hat{\Sigma}=\Sigma_i\hat{\tau}_i$, where sum over the index i is implied. The superconducting gap in the presence of impurities is determined by the self-consistency condition, Eq. (2.22), which reads here

$$\Delta(\hat{\Omega}) = \pi T N_0 \sum_{\omega_n} \int d\hat{\Omega}' V(\hat{\Omega},\hat{\Omega}') \frac{\tilde{\Delta}(\hat{\Omega}')}{\sqrt{\tilde{\omega}_n^2 + \Delta^2(\hat{\Omega}')}}. \tag{13.3}$$

T_c is the temperature at which a nontrivial solution of the self-consistency equation first appears. Equation (13.3) with the recipe for computing the self-energy form the basis for treating superconductors with impurities. We always ignore the contribution of Σ_3 as it simply renormalizes the chemical potential. This is justified in computing the density of states, although corrections may be relevant for some response functions (Hirschfeld *et al.*, 1988). In computing the self-energy, we neglect the interaction between spins on different impurity sites (Larkin *et al.*, 1971; Galitskii and Larkin, 2002) and interference effects of scattering on different impurities [of the order $(p_F l)^{-1}$, where l is the mean free path].

A. s-wave superconductors

1. Born approximation and Abrikosov-Gor'kov theory

We begin by reviewing the seminal results of Abrikosov and Gor'kov for impurity scattering in the Born limit (phase shift $\delta_0 \ll 1$). This sets the standard for comparison with theories going beyond the Born approximation. We follow the notations of Maki (1969).

Consider an impurity potential combining the potential and magnetic scattering,

$$\hat{U}_{\rm imp}(\mathbf{k}-\mathbf{k}') = U_{\rm pot}(\mathbf{k}-\mathbf{k}')\tau_3 + J(\mathbf{k}-\mathbf{k}')\boldsymbol{S}\cdot\boldsymbol{\alpha}, \tag{13.4}$$

where α is defined in Eq. (3.5). Abrikosov and Gor'kov considered the self-energy in the second-order (Born) approximation,

$$\hat{\Sigma}(\omega,\mathbf{k}) = n_{\rm imp}\int \frac{d\mathbf{k}'}{(2\pi)^3}\hat{U}_{\rm imp}(\mathbf{k}-\mathbf{k}')\hat{G}(\mathbf{k}',\omega) \times \hat{U}_{\rm imp}(\mathbf{k}'-\mathbf{k}). \tag{13.5}$$

Integrating over $\mathbf{k}'$ we find

$$\tilde{\omega} = \omega_n + \frac{1}{2}\left(\frac{1}{\tau_p}+\frac{1}{\tau_s}\right)\frac{\tilde{\omega}}{\sqrt{\tilde{\omega}_n^2+\Delta^2}}, \tag{13.6}$$

$$\tilde{\Delta} = \Delta + \left(\frac{1}{\tau_p}-\frac{1}{\tau_s}\right)\frac{\tilde{\Delta}}{\sqrt{\tilde{\omega}_n^2+\Delta^2}}. \tag{13.7}$$

The potential (τ_p) and spin-flip (τ_s) scattering times are

$$\frac{1}{\tau_p} = n_{\rm imp}N_0\int d\hat{\Omega}|U_{\rm pot}(\mathbf{k}-\mathbf{k}')|^2, \tag{13.8}$$

$$\frac{1}{\tau_s} = n_{\rm imp}N_0 S(S+1)\int d\hat{\Omega}|J(\mathbf{k}-\mathbf{k}')|^2, \tag{13.9}$$

and we averaged over directions of the impurity spin.

In the absence of spin-flip scattering both Δ and ω are renormalized identically, and it follows from Eq. (13.3) that the gap remains unchanged compared to the pure case. This is in accordance with Anderson's theorem. The spin-flip scattering violates the time-reversal symmetry, and τ_s enters the equations for $\tilde{\omega}$ and $\tilde{\Delta}$ with opposite sign. Introducing $u=\tilde{\omega}/\tilde{\Delta}$, we find

$$\frac{\omega}{\Delta} = u\left(1-\frac{(\Delta\tau_s)^{-1}}{\sqrt{1+u^2}}\right). \tag{13.10}$$

It follows that the gap in the single-particle spectrum is $E_{\rm gap}=\Delta[1-(\Delta\tau_s)^{-2/3}]^{3/2}$ for $\Delta\tau_s>1$ and vanishes for $\Delta\tau_s<1$. This gapless region starts at the value of the pair-breaking parameter α

$$\alpha' = \tau_s^{-1} = \Delta_{00}\exp(-\pi/4), \tag{13.11}$$

where Δ_{00} is the gap in the pure material at $T=0$.

The transition temperature is determined from

$$\psi\left(\frac{1}{2}+\frac{1}{2\pi\tau_s T_c}\right) - \psi\left(\frac{1}{2}\right) = \ln\frac{T_{c0}}{T_c}, \tag{13.12}$$

where $\psi(x)$ is the digamma function and T_{c0} is the transition temperature of the pure material. Consequently, superconductivity is destroyed ($T_c=0$) when

$$\alpha_c = \tau_s^{-1} = \pi T_{c0}/2\gamma = \Delta_{00}/2 > \alpha', \tag{13.13}$$

where $\gamma\approx 1.78$. As $\alpha'\approx 0.912\alpha_c$, Abrikosov and Gor'kov predicted that gapless superconductivity exists for a range of impurity scattering (Abrikosov and Gor'kov, 1960). This was later confirmed by experiment (Woolf and Reif, 1965).

The evolution of the density of states with increasing disorder was investigated in detail (Skalski *et al.*, 1964; Ambegaokar and Griffin, 1965; Gong and Cai, 1966) and is shown in Fig. 35. For $\alpha<\alpha'$ a hard gap in the single-particle spectrum persists up to the critical impurity con-

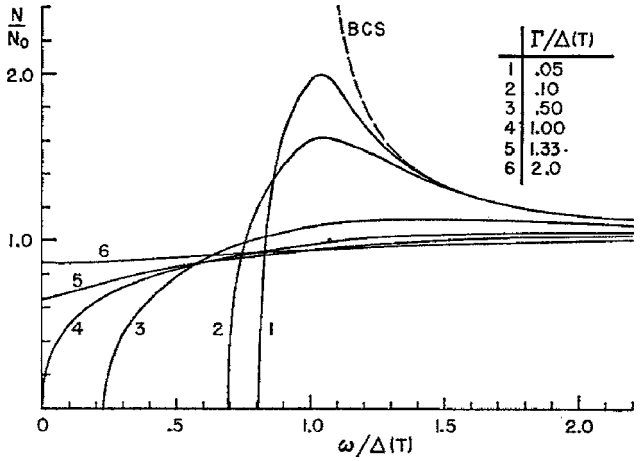

FIG. 35. Density of states in the Abrikosov-Gor'kov theory of magnetic impurities in superconductors. Here $\Gamma=\tau_s^{-1}$. Reproduced with permission from Skalski *et al.*, 1964.

centration, as shown in Fig. 36. This result is clearly at odds with our discussion in Sec. VI, which shows that even a single magnetic impurity creates a localized state in the superconducting gap.

2. Shiba impurity bands

In the Abrikosov-Gor'kov theory the impurity concentration and strength of the exchange coupling contribute to the suppression of superconductivity as a single pair-breaking parameter, $\alpha=\tau_s^{-1}=(2n_{\rm imp}/\pi N_0)\sin^2\delta_0 \propto n_{\rm imp}J^2S(S+1)$ for isotropic exchange; see Eq. (13.9). This is a result of the Born approximation; in general, the phase shift δ_0 and concentration of impurities $n_{\rm imp}$ are separate variables that control different aspects of impurity scattering. For example, in the limit of dilute concentration with strong magnetic impurities, the Abrikosov-Gor'kov approach yields a small scattering rate and a single-particle spectral gap virtually identical to that in a pure limit. On the other hand, we have learned that in this regime each impurity is accompanied by a bound state with an energy below the gap, and therefore we expect a finite number of these subgap states to exist in a superconductor. This section addresses this dichotomy.

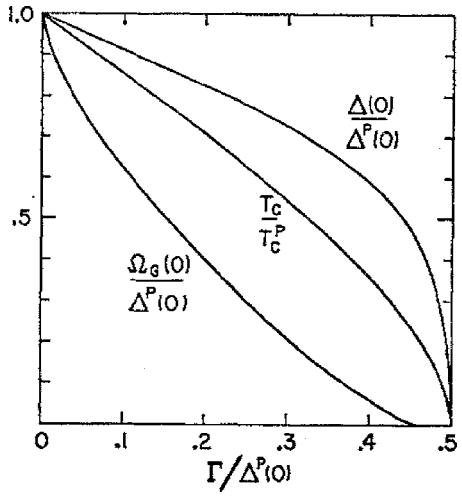

FIG. 36. Plot of the dependence of the order parameter Δ, transition temperature T_c, and the single-particle spectral gap Ω_G, here on the scattering rate $\Gamma=\tau_s^{-1}$. Reproduced with permission from Skalski *et al.*, 1964.

Analysis of the strong-scattering regime requires use of the self-consistent T-matrix approach (Hirschfeld *et al.*, 1986; Schmitt-Rink *et al.*, 1986), where the self-energy $\hat{\Sigma}(\mathbf{p},\omega)=n_{\rm imp}\hat{T}_{\mathbf{p},\mathbf{p}}$ and

$$\hat{T}_{\mathbf{p},\mathbf{p}'}=\hat{U}_{\mathbf{p},\mathbf{p}'}+\int d\mathbf{p}_1\hat{U}_{\mathbf{p},\mathbf{p}_1}\hat{G}(\mathbf{p}_1,\omega)\hat{T}_{\mathbf{p}_1,\mathbf{p}'}. \tag{13.14}$$

Following the treatment described in Sec. VI, we analyze the pair breaking in different angular momentum channels. The effective pair-breaking parameter in the lth channel is $\alpha_l=n_{\rm imp}(1-\epsilon_l^2)/(2\pi N_0)$, where ϵ_l is the position of the corresponding bound state; see Eq. (6.10). In analogy with the Abrikosov-Gor'kov treatment, we find that the ratio $u_n=\tilde{\omega}_n/\tilde{\Delta}(\omega_n)$ satisfies the equation (Rusinov, 1969; Chaba and Nagi, 1972)

$$\frac{\omega_n}{\Delta}=u_n\left[1-\sum_{l=0}^{\infty}(2l+1)\frac{\alpha_l}{\Delta}\frac{\sqrt{1+u_n^2}}{\epsilon_l^2+u_n^2}\right], \tag{13.15}$$

where the gap is determined self-consistently from

$$\Delta=2\pi TN_0g\sum_n(1+u_n^2)^{-1/2}. \tag{13.16}$$

This equation should be contrasted with Eq. (13.10). The pair-breaking parameter α_l now depends separately on the position of the single-impurity resonance state ϵ_l and the impurity concentration, in contrast to the Abrikosov-Gor'kov theory.

The growth of the impurity band was investigated for the spherically symmetric case of purely magnetic scattering (Shiba, 1968; Rusinov, 1969; Chaba and Nagi, 1972). The critical concentration of impurities at which the transition temperature vanishes is obtained by setting $T_c=0$ in the gap equation,

$$\ln(T_{c0}/T_c)=\psi(1/2+\alpha/2\pi T_c)-\psi(1/2), \tag{13.17}$$

where now (Ginzberg, 1979)

$$\alpha=\sum_l(2l+1)\alpha_l. \tag{13.18}$$

Since the gap equation is identical to that considered by Abrikosov and Gor'kov, the critical pair-breaking parameter is $\alpha_{\rm cr}=\Delta_0/2$. However, now the critical concentration of impurities depends on the phase shift of scattering by individual impurities and on the position of the single-impurity resonance; see Fig. 37,

$$n_{\rm cr}=\pi N_0\Delta_0\left[\sum_l(2l+1)(1-\epsilon_l^2)\right]^{-1}. \tag{13.19}$$

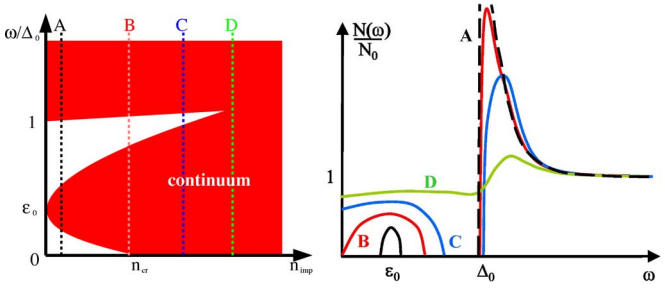

FIG. 37. (Color online) Evolution of the spectral gaps and density of states for strong magnetic impurities ($\epsilon_0 \ll \Delta_0$). Left panel: Available states (shaded) as a function of the impurity concentration. Right panel: Qualitative features of the DOS for different impurity concentrations; following cuts A, B, C, D on the left. Critical concentration corresponds to line B, when the impurity band touches $\omega=0$. The spectral gap between the top of the impurity band and the bottom of the continuum persists to higher impurity concentration (line D).

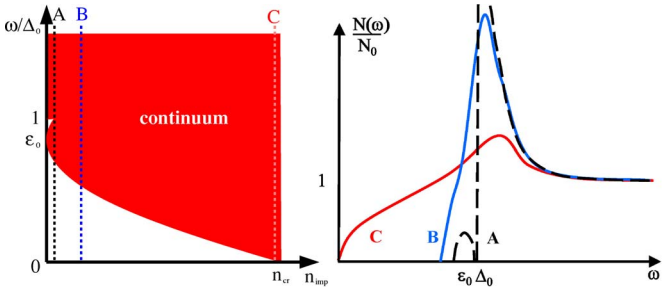

FIG. 38. (Color online) Evolution of the spectral gaps and density of states for weak magnetic impurities ($\epsilon_0 \lesssim \Delta_0$). Left panel: Available states (shaded) as a function of the impurity concentration. Right panel: Qualitative features of the DOS for different impurity concentrations; following cuts A, B, C on the left. The impurity band and the continuum merge at a low impurity concentration (line B), and further evolution of the DOS is very close to the predictions of the Abrikosov-Gor'kov theory. At the critical concentration (line C) gapless superconductivity sets in.

The width of the gapless regime depends on the details of scattering. For $l=0$ the gap vanishes when the pair-breaking parameter exceeds the value (Shiba, 1968; Rusinov, 1969)

$$\alpha'/\alpha_{\rm cr} = 2\epsilon_0^2 \exp[-\pi\epsilon_0^2/2(1+\epsilon_0)]. \tag{13.20}$$

In the Born approximation the bound state moves to the gap edge, $\epsilon_0=1$, and we regain the result of Abrikosov and Gor'kov. For stronger scattering, $\epsilon_0<1$, the realm of gapless superconductivity is enhanced compared to the Abrikosov-Gor'kov theory. As higher-order harmonics are included, the threshold at which the density of states at the Fermi energy becomes nonzero shifts even lower (Ginzberg, 1979). This behavior is modified by inclusion of Kondo screening (see the next section), but the overall shape of the DOS observed in planar tunneling measurements (Dumoulin *et al.*, 1975, 1977; Bauriedl *et al.*, 1981) is in agreement with these expectations.

For $l=0$ in the limit $\alpha_0 \ll \Delta$ the width of the impurity band around E_0 is estimated to be $W=(8\alpha_0\Delta)^{1/2}(1-\epsilon_0)^{1/4}$ and therefore varies as $n_{\rm imp}^{1/2}$ (Shiba, 1968). Therefore if the resonance state at E_0 is sufficiently close to the gap edge, the concentration c_0 at which the top of the impurity band merges with the continuum above Δ is smaller than the critical concentration c' at which the bottom of the impurity band reaches the Fermi surface and the superconductor becomes gapless (Shiba, 1968); see Fig. 38. The Abrikosov-Gor'kov result is an extreme example of this behavior when states due to individual impurities are infinitely close to the gap edge, and therefore upon increasing impurity concentration the gap decreases until the onset of gapless behavior.

3. Quantum spins and density of states

In the quantum treatment of the impurity spin, Sec. XI, we have discussed the competition between gapping the density of states due to superconductivity and the onset of Kondo screening of the impurity moment. We have concluded that, in contrast to classical spin, the position of the bound state is not simply given by the value of the bare exchange coupling but depends on the ratio T_K/T_c. Once the position of the bound state is established, for independent impurities the growth of the impurity band is analogous to that in the previous section. As discussed above, for ferromagnetic coupling of the impurity to the conduction electrons the bound state is always close to the gap edge, the scattering is weak, and the Abrikosov-Gor'kov theory gives correct results.

The behavior of the density of states and transition temperature for antiferromagnetic coupling when Kondo screening is effective was studied in the 1970s (Müller-Hartmann and Zittartz, 1971; Zittartz *et al.*, 1972; Müller-Hartmann, 1973; Schuh and Müller-Hartmann, 1978). The appearance of the predicted subgap band of localized states (qualitatively similar to the Shiba-Rusinov band above) was confirmed experimentally (Dumoulin *et al.*, 1975, 1977; Bauriedl *et al.*, 1981). The main new result was the prediction of the reentrant behavior for small $T_K/T_c \lesssim 1$. In that case the phase shift of the scattering increases upon lowering temperature but remains moderate at T_c enabling the transition to the superconducting state. Upon further decrease in temperature, scattering becomes stronger and suppresses superconductivity in a range of the phase diagram of Fig. 39. Finally, at temperatures below T_K, the system reenters the local Fermi-liquid regime and superconductivity may reappear. While further work (Matsuura *et al.*, 1977; Jarrell, 1990) cast doubt on the existence of the third transition, a region of two solutions for $T_c(n_{\rm imp})$ was confirmed by theoretical studies. In particular, a combination of the quantum Monte Carlo technique with Eliashberg equations gave the dependence of the reentrance transition on the electron-phonon coupling constant, while accounting nonperturbatively for the Kondo effect (Jarrell, 1990); see Fig. 39. Moreover, the initial decrease of T_c with increasing impurity concentration is fast (Müller-Hartmann and Zittartz, 1971; Jarrell, 1990) and depends on the coupling strength (Jar-

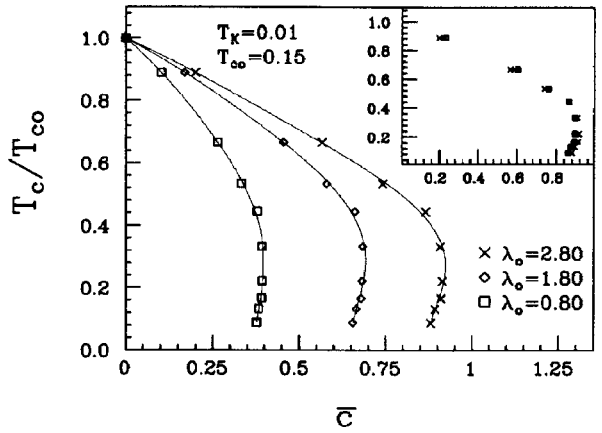

FIG. 39. Reduced transition temperature normalized to a pure system as a function of the impurity concentration for different electron-phonon coupling λ_0. The impurity concentration is $\bar{c} = n_{\rm imp}/(2\pi)^2 N_0 T_{c0}$. From Jarrell, 1990.

rell, 1990). The behavior of the density of states in this limit was investigated in detail (Bickers and Zwicknagl, 1987; Jarrell *et al.*, 1990). The overall shape of the transition temperature as a function of impurity concentration with reentrant transition was observed in the $(LaCe)Al_2$ alloy series (Maple, 1973).

B. *d*-wave superconductors

As mentioned above, scalar (nonmagnetic) impurities are pair breakers for any nonconventional superconductor and substantially change the low-energy quasiparticle spectrum. This problem was addressed with the self-consistent T-matrix approximation (Gor'kov and Kalugin, 1985; Hirschfeld *et al.*, 1986, 1988; Schmitt-Rink *et al.*, 1986; Hirschfeld and Goldenfeld, 1993; Lee, 1993; Balatsky *et al.*, 1994), which gives a finite density of states at the Fermi level. Here we briefly review only the main results; see Sec. I.D for details.

The self-consistent Green's function, averaged over impurity positions, is

$$\hat{G}^{-1}(\mathbf{k},\omega) = \hat{G}_0^{-1}(\mathbf{k},\omega) - \hat{\Sigma}(\omega), \tag{13.21}$$

with $\hat{\Sigma}(\omega) = n_{\rm imp}\hat{T}(\omega)$. For particle-hole symmetry (Hirschfeld *et al.*, 1988) and an unconventional gap (defined as having a zero average over the Fermi surface; see Sec. I), the only nonvanishing component of the T matrix is proportional to τ_0,

$$T_0(\omega) = \frac{g_0(\omega)}{c^2 - g_0(\omega)}. \tag{13.22}$$

The T matrix has to be determined self-consistently with $g_0(\omega) = (2\pi N_0)^{-1}\Sigma_{\mathbf{k}}{\rm Tr}\hat{G}(\mathbf{k},\omega)\hat{\tau}_0$. Solution of this equation leads to a finite density of states at the Fermi level. This result was first obtained for Born scattering (Gor'kov and Kalugin, 1985; Ueda and Rice, 1985), leading to an exponentially small $N(0)/N_0 \approx 4\tau^2\Delta_0^2 \exp(-2\Delta_0\tau)$, where τ is the normal-state scattering rate. The results are more dramatic for unitarity scattering ($c=0$) (Hirschfeld *et al.*, 1986; Schmitt-Rink *et al.*, 1986) when

$$\gamma \simeq \sqrt{n_{\rm imp}(\Delta_0/\pi N_0)}, \tag{13.23}$$

where $\gamma = -{\rm Im}\,\Sigma(\omega \to 0)$ is the scattering rate for low-energy quasiparticles. For $\omega \lesssim \gamma$, the density of states is determined by impurities and is finite: $N_{\rm imp}(0)/N_0 = 2\gamma/\pi\Delta_0$. The characteristic width of the impurity-dominated region is $\omega^* \simeq \gamma \propto \sqrt{n_{\rm imp}}$.

The origin of the finite DOS is the impurity band, growing from impurity-induced states. Scaling of the impurity bandwidth $\gamma \propto \sqrt{n_{\rm imp}}$ was found for paramagnetic impurities in an *s*-wave superconductor (Shiba, 1968). The fact that $\gamma \propto \sqrt{n_{\rm imp}}$ is valid for a *d*-wave superconductor is consistent with the picture of low-energy states formed from the bound states at finite impurity concentration. Many questions about localization of low-energy quasiparticles in unconventional superconductors remain unanswered; see Sec. I.

The results above are for isotropic impurity scattering. Anisotropic impurities may preferentially scatter electrons between regions with the same, or close, values of the gap so that scattering is inefficient in suppressing T_c. For general impurity phase shifts this has been considered by Haran and Nagi (1996, 1998), Choi (1999), Golubov and Mazin (1999), and Kulic and Dolgov (1999), while for a model with dominant small-angle scattering in cuprates (Abrahams and Varma, 2000) the effect was analyzed by Kee (2001).

XIV. OPTIMAL FLUCTUATION

A. Introduction

So far we have discussed the effect of a single impurity on its immediate surrounding and the combined effect of an ensemble of scattering centers on spatially averaged properties of a superconductor. In the case of a single pair-breaking impurity the characteristic length is simply the superconducting coherence length ξ_0. In the Abrikosov-Gor'kov approach, the gap is assumed to be uniformly suppressed, after averaging over all possible configurations of impurity atoms at the mean-field level (Abrikosov *et al.*, 1963).

It is clear, however, that some physics is missing in such an approach. Among the realizations of the impurity distribution in a sample of size L_0 there exist regions where the local impurity concentration, on some characteristic scale $L \ll L_0$, differs significantly from the average concentration n_i. If the local impurity concentration is sufficiently high, for $L > \xi_0$ superconductivity may be locally destroyed or sufficiently suppressed to generate a bound quasiparticle state at an energy $E \ll \Delta_0$.

Of course, such regions are rare. There is a high entropy cost to create an impurity droplet with a concentration significantly different from the average, hence the probability of finding these regions is small. However, states localized in such droplets make a nonperturbative contribution to the density of states averaged

over the entire sample, $N(E)$, and qualitatively modify its behavior compared to the mean-field (Abrikosov-Gor'kov and Shiba) treatment. Quite dramatically, they make any *s*-wave superconductor with a small concentration of magnetic impurities ($\Delta\tau_s \gg 1$) gapless (Balatsky and Trugman, 1997). It is due to such a dramatic modification that the interest in these "tail" states stretching below the mean-field gap edge has peaked in recent years.

The problem of tail states did not originate in the study of superconductivity. The contribution of regions of anomalous impurity concentration to the net density of states below the gap edge was first considered in doped semiconductors by Lifshitz (1964a, 1964b, 1967). He showed that such rare impurity configurations create a local profile in the Coulomb potential that can have bound states and therefore give rise to the nonvanishing density of states below the bottom of the band E_g. Henceforth states localized in droplets of impurities have become known as *Lifshitz tails* and have been extensively studied (Halperin and Lax, 1966; Zittartz and Langer, 1966; Van Mieghem, 1992).

While in retrospect it seems natural that inhomogeneities would lead to a low-energy tail in the density of states in superconductors in much the same way, little attention was paid to this problem until the paper by Balatsky and Trugman (1997). Their study was stimulated by experimental observations that the tunneling density of states in *s*-wave superconductors with magnetic impurities is far greater at low energies than the Abrikosov-Gor'kov theory suggests (Woolf and Reif, 1965; Edelstein, 1967; Bader *et al.*, 1975). A number of theoretical studies of the tail states followed, and this topic is now a subject of active interest.

Below, we review the physical picture of tail states in semiconductors and then apply it to the subgap states in superconductors.

B. Tail states in semiconductors and optimal fluctuation

We distinguish between heavily and lightly doped semiconductors. In the former case a localized tail state with energy $E < E_g$ forms in the impurity-rich region, and the extent of its wave function greatly exceeds the average distance between individual shallow sites. Therefore the exact impurity potential can be replaced by a smooth function, averaged over regions containing many impurities. The probability of realizing the potential with the "right" energy of the bound state among all impurity distributions determines its contribution to the DOS. In the latter case the number of impurity sites needed to form a bound state depends on how deep below the band edge the energy of such a state is. For example, if each impurity binds an electron at energy E_1, while E_2 is the energy of the state bound by two impurities on neighboring lattice sites, to obtain a localized state below E_1 but above E_2 one simply needs to find a region where the two impurities are at a particular finite distance from each other. The probability of finding such an impurity pair determines the density of states (Lifshitz, 1964b, 1967). As we go to energies below E_2, we need to position three impurities, etc.

For energy E the most probable (albeit still rare) configuration of impurities that creates a potential U, such that $[H_{\text{band}}+U]\psi=\mathcal{E}[U]\psi$, with $\mathcal{E}[U]=E$, and therefore contributes the most to $N(E)$, is called the optimal fluctuation. Given the probability density for the potential $P[U]$ and the density of states in it,

$$N(E) = \int \mathcal{D}U P[U]\delta(E - \mathcal{E}[U]), \tag{14.1}$$

the optimal fluctuation is obtained by using the saddle-point approximation and minimizing the resulting functional with respect to U. This approach finds the entropically cheapest impurity potential that creates a bound state at E. Therefore it optimizes the nonuniform impurity distribution (fluctuation from the uniform average) to the given energy, hence the name. The technical difficulty of minimization lies in its essential nonlinearity: the optimal potential depends on the wave function of the particle in this potential.

Consider many uncorrelated shallow impurity centers forming an extended potential. It is described by the Gaussian probability density,

$$P[U] \propto \exp\left[-\frac{1}{2U_0}\int d^d\mathbf{r}\, U^2(\mathbf{r})\right]. \tag{14.2}$$

The saddle-point approximation for Eq. (14.1) gives

$$\ln\frac{N(E)}{N_0} \approx -\mathcal{S}[U_{\text{opt}}], \tag{14.3}$$

where the optimal fluctuation is obtained by minimizing the functional

$$\mathcal{S}[U] = \frac{1}{2U_0^2}\int d^d\mathbf{r}\, U^2(\mathbf{r}) + \lambda(\mathcal{E}[U] - E) \tag{14.4}$$

with respect to the potential U and the Lagrange multiplier λ. At the simplest level it is sufficient to consider only potentials where $\mathcal{E}[U]=E$ is the lowest energy state in the potential U; fluctuations where E coincides with higher eigenstates are exponentially less probable. In a semiconductor the kinetic energy of quasiparticle is $p^2/2m^*$, where m^* is the effective mass. Consequently, in a potential well of depth U (all energies are measured from the band edge) and size L the energy of the localized state is of the order of $U+1/(mL^2)=E$ ($\hbar=1$). In the optimal fluctuation $E \sim U \sim L^{-2}$, so that the action is $\mathcal{S}[U] \approx L^d U^2/U_0^2$, or $\ln[N(E)/N_0] \approx -|E|^{2-d/2}/U_0^2$ (Lifshitz 1964b; Halperin and Lax, 1966). Importantly, the size of the optimal fluctuation, $L \propto |E|^{-1/2}$, increases as the energy approaches the band edge, while its depth, $|U| \sim |E|$, decreases.

More formally, since the energy of the bound state is the expectation value of the Hamiltonian over the wave function of the bound state $\psi(\mathbf{r})$, we have

$$\mathcal{E}[U] = \langle \hat{H} \rangle = \langle \psi | \frac{\mathbf{p}^2}{2m^*} + U | \psi \rangle = E. \tag{14.5}$$

Minimization in Eq. (14.4) with respect to U dictates that

$$U(x) = -\lambda U_0^2 \langle \psi | \frac{\delta \hat{H}}{\delta U} | \psi \rangle = -\lambda U_0^2 \psi^2(x), \tag{14.6}$$

while minimization with respect to λ requires that the bound state is at energy E, i.e. (setting $m^*=1$),

$$\left[-\tfrac{1}{2}\nabla^2 - \lambda U_0^2 \psi^2(\mathbf{r}) \right] \psi(\mathbf{r}) = E\psi(\mathbf{r}). \tag{14.7}$$

In one dimension this equation is exactly solved to give (Halperin and Lax, 1966)

$$\psi(x) = \sqrt{\frac{\kappa}{2}}\ \mathrm{sech}\ \kappa x, \tag{14.8}$$

$$\lambda U_0^2 = 8\kappa, \tag{14.9}$$

with $E=-\kappa^2/2$. Therefore the "optimal action" is $\mathcal{S}(U_{\mathrm{opt}}) \simeq \kappa^2/U_0^2 \sim |E|^{3/2}$ as expected.

In higher dimensions the corresponding equation is not solvable. However, one can extract the energy dependence of the action by assuming a spherically symmetric optimal fluctuation and an exponentially decaying (at large distances) bound state to find the Lifshitz tail $N(E) \propto \exp(-|E|^{2-d/2})$ (Lifshitz, 1964b; Lifshitz *et al.*, 1988). To obtain the preexponential factor, one needs to consider all wave functions in the potential, and this analysis has only been carried out in low dimensions (Halperin and Lax, 1966).

C. *s*-wave superconductors

1. Magnetic and nonmagnetic disorder

The effect of tails is most dramatic for fully gapped superconductors with magnetic impurities. The general route is similar to the above approach: Given the probability density of different impurity configurations, we find the most probable configuration of impurities that gives rise to a state at a given energy within the gap. Technical implementations of this algorithm vary depending on the specifics of the problem at hand; see below.

There are important differences between the physics of the optimal fluctuation in a superconductor and a semiconductor. First, since the superconducting quasiparticles consist of electron pairs close to the Fermi surface, their kinetic energy is not simply that of a band particle, but is given instead by the Hamiltonian

$$\hat{H} = \hat{\xi}\tau_3 + \Delta(\mathbf{r})\tau_1\sigma_2. \tag{14.10}$$

Here we use Nambu notation with τ_i and σ_i the Pauli matrices in the particle-hole and spin space, respectively. Therefore while the envelope of the tail-state wave function still varies smoothly over the length scale of inhomogeneities in the impurity distribution, there are also rapid oscillations on the atomic scale due to the Fermi surface. As shown below, these considerations substantially modify the behavior of the tail states.

Second, the scattering potential is a matrix in particle-hole and spin space,

$$\hat{\mathbf{U}}(\mathbf{r}) = \sum_i \left[U_0\tau_3\delta(\mathbf{r}-\mathbf{r}_i) + J(\mathbf{r}-\mathbf{r}_i)\mathbf{S}_i \cdot \boldsymbol{\alpha} \right]. \tag{14.11}$$

The potential part of the scattering U_0 is not pair breaking in accordance with Anderson's theorem. However, since the size of the optimal fluctuation is large compared to the correlation length, it is necessary to distinguish between cases where the motion of quasiparticles within the optimal fluctuation is diffusive (strong potential scattering $\Delta\tau \ll 1$, $\tau \ll \tau_s$, where τ is the transport lifetime) and ballistic (weak potential scattering $\tau \gg \tau_s$). Moreover, we also distinguish between strong and weak magnetic scattering: If magnetic scattering is strong there are resonance (Shiba-Rusinov) states in the gap, and tails states stretch not from the mean-field gap edge but from the localized impurity band. If magnetic scattering can be treated in the self-consistent Born approximation, tail states emerge below the Abrikosov-Gor'kov renormalized single-particle spectral gap, $\Delta_0 = \Delta[1 - (\Delta\tau_s)^{-2/3}]^{3/2}$, where Δ is the superconducting order parameter. In the Abrikosov-Gor'kov limit the probability density for the magnetic impurity potential is Gaussian, as it is averaged over a large number of impurity sites. In contrast, in the unitarity limit there are subgap states localized on one or a few impurities; consequently, the Poisson density distribution is appropriate. These possibilities provide for a rich variety of behavior that is still a subject of active interest.

All models ignore interactions between the impurity spins: this is justified as discussed in Sec. III.C. The models also treat impurity spins as classical, and therefore do not account for the Kondo effect. This is justified either when the Kondo temperature $T_K \ll T_c$ (and depletion of states at the Fermi level prevents screening of the local moment) or in the opposite limit, $T_K \gg T_c$, when the moments are already quenched in the normal state (Müller-Hartmann and Zittartz, 1971).

To our knowledge, the first discussion of the influence of nonuniform impurity distribution on the transition temperature appeared in 1968 (Kulik and Itskovich, 1968). These authors found that, in the limit of average impurity concentration $n \ll n_{\mathrm{cr}}$ of the Abrikosov-Gor'kov theory, there are localized regions that become superconducting at a temperature $T_c' > T_c(n)$, where $T_c(n)$ is the corresponding Abrikosov-Gor'kov transition temperature. The difference between the two was evaluated for parabolic one-dimensional variations of the effective impurity potential. Kulik and Itskovich (1968) noted that their results are modified if there is nonmagnetic as well as magnetic scattering, but did not address this further.

2. Diffusive limit, weak magnetic scattering

If the scattering on individual magnetic impurities is weak, the optimal fluctuation is created by large droplets of these scattering centers. Since impurities are uncorre-

lated, the probability density for the impurity potential is Gaussian, which greatly simplifies the analysis.

Historically, most of the studies have been carried out in the diffusive limit. Larkin and Ovchinnikov (1972) investigated the smearing of the gap edge due to local fluctuations in the effective interaction between electrons. If the correlation length of the inhomogeneities, $r_c \gg \xi$, where $\xi \sim (D/\Delta)^{1/2}$ is the coherence length of the dirty superconductor and D is the diffusion constant, the order parameter simply locally adjusts to the local value of the interaction. In that case the density of states is determined by the local gap amplitude,

$$N(E) = \int_0^\infty N(E,\Delta) P(\Delta) d\Delta, \tag{14.12}$$

where $P(\Delta)$ is the probability density of the gap.

In the opposite limit of short-range correlations in the pairing interaction, the finite density of states below the mean-field gap edge is due to states spatially localized in correlated droplets of size $r_0 \sim \xi[(\Delta_0 - E)/\Delta]^{-1/4}$ (increasing rapidly as $E \to \Delta_0$ as in a semiconductor), which leads to $N(E) \propto \exp\{-[(\Delta_0 - E)/\Delta]^{5/4}\}$ in $d=3$. As in semiconductors, the high entropy cost of a large droplet is offset by the lowering of the kinetic energy of the bound state. Indeed, in a clean system with $\Delta\tau_s \gg 1$, and therefore $\Delta_0 \approx \Delta$, we find the characteristic kinetic energy $D/r_0^2 \simeq \sqrt{\Delta_0^2 - E^2}$.

Recently, it was argued that the above result is flawed since it does not properly account for rapid oscillations of the bound-state wave function on the Fermi wavelength scale (Meyer and Simons, 2001). These authors used a field-theoretical approach that maps the disordered superconducting system onto a nonlinear σ model [for a review, see Altland *et al.* (2000)] to show that while the droplet size for the optimal fluctuation is identical to that obtained by Larkin and Ovchinnikov, the subgap density of states is $N(E) \propto \exp\{-[(\Delta_0 - E)/\Delta]^{(6-d)/4}\}$, which gives the exponent $3/4$, rather than $5/4$, for $d=3$.

The paper that brought the investigation of subgap states in superconductors into the limelight after a quarter-century-long hiatus was the study of the density of states due to regions where the impurity concentration is sufficient to locally destroy superconductivity (Balatsky and Trugman, 1997). The fluctuation region spectrum is similar to that of a disordered metallic grain of the same size L and depends on the mean level spacing δ_L. The average density of states was obtained in two steps. First, an average over all realizations of disorder for grains of size L yielded $N_L(E) \sim \delta_L^{-1}$. Second, the probability of finding a fluctuation region of size L with the critical concentration of impurities n_c for a given average impurity concentration n, $P_L(n_c;n)$, was used to define the average DOS, $N(E) \sim \int dV P_L(n_c;n) N_L(E)$. This integral was estimated to give

$$N(E) \sim \delta_{L_0}^{-1} \exp\{-L_0^d [n_c \ln(n_c/n) - n_c + n]\}, \tag{14.13}$$

as $E \to 0$. Here $L_0 = (\xi_0 l)^{1/2}$ is of the order of the coherence length in a dirty superconductor with $l \ll \xi_0$.

At energies closer to the gap edge it is not necessary to destroy superconductivity completely to generate tail states. Using the instanton approach for the nonlinear σ model, Lamacraft and Simons (2000, 2001) demonstrated how these states arise out of inhomogeneous instanton configurations for the action. The resulting optimal action reads

$$S_0 = a_d (\Delta\tau_s)^{2/3} [1 - (\Delta\tau_s)^{-2/3}]^{-(2+d)/8} \left(\frac{\Delta_0 - E}{\Delta}\right)^{(6-d)/4} \tag{14.14}$$

and the DOS varies as $N(E) \sim \exp[-4\pi g (\xi/L)^{d-2} S_0] \sim \exp\{-[(\Delta_0 - E)/\Delta]^{(6-d)/4}\}$. Here g is the bare conductance and $a_d \sim 1$.

The same approach was used to derive (Lamacraft and Simons, 2001) universal gap fluctuations in small metallic grains, first obtained using random-matrix theory (Vavilov *et al.*, 2001), namely $N(E) \sim \exp[-(\Delta_0 - E)^{3/2}]$, valid for $\Delta_0 - E \ll \Delta_0$. In this regime, the spatial extent of the optimal fluctuation is greater than the size of the grain, so that effectively we are in dimension $d=0$, and the exponent $3/2$ agrees with the general result of Lamacraft and Simons, $(6-d)/4$. In the same $d=0$ limit, but at $E \ll \Delta_0$, the random-matrix theory gives $N(E) \sim (|E|/\delta^{3/2}\Delta^{1/2}) \exp[-\pi\tau_s(\Delta_0 - E)^2/\delta]$, where δ is the mean level spacing in the grain (Beloborodov *et al.*, 2000).

3. Diffusive limit, strong scattering

Recently, the field-theoretical treatment has been extended to the case of strong scatterers (Marchetti and Simons, 2002). When the probability distribution of the scattering strength is Poissonian rather than Gaussian, the action cannot be expanded to second order in the magnetic potential, as done for the weak potential. Marchetti and Simons circumvented this difficulty by considering the dominant contribution of droplets densely populated by magnetic impurities, so that $\xi \ll l_s \ll l$. As shown above, an impurity band already emerges within the superconducting gap in the limit of near-unitary scattering at the level of the mean-field theory. Consequently, tail states extend from the edge of the continuum above Δ_0 as well as from the top and bottom of the impurity band; see Fig. 41. According to Marchetti and Simons in these cases the density of states varies as $N(E) \propto \exp[-(|E - E_i|/\Delta)^{(6-d)/4}]$, where E_i is the appropriate band edge. The exponent of the action is identical to that found above in the diffusive limit.

4. Ballistic limit, weak scattering

It was noticed early on that in some systems magnetic scattering is dominant: Upon increasing the concentration of impurities, the increase in the residual resistivity ratio correlates with the suppression of the superconducting transition temperature (Edelstein, 1967). Since both magnetic and nonmagnetic scattering contribute to the resistivity, but only the magnetic part suppresses T_c, this is an indication of almost purely spin-dependent

scattering. Shytov *et al.* (2003) considered subgap states in this clean ($l \gg \xi_0$ or $\Delta\tau_s \gg 1$) limit, when the spectral gap obtained in the self-consistent Born approximation nearly coincides with the order parameter, $\Delta_0 \approx \Delta$.

Once again, since impurities are weak, the optimal fluctuation is large and shallow, and the spin-dependent potential has Gaussian probability density. When the size of the optimal fluctuation is much greater than the coherence length, $l \gg L \gg \xi_0$, the motion of the quasiparticles in this potential is ballistic. As a result, mapping on the nonlinear σ model is not feasible, and the problem requires a quantum-mechanical treatment akin to that in a semiconductor.

We first consider the one-dimensional problem as shown above. An important assumption (discussed below) is that a ferromagnetic fluctuation maximizes the effect of the impurity potential. Choosing the direction of the impurity spins along the y axis and performing the rotation $\sigma_2 \to \sigma_3$, we remove the vector character of the slowly varying potential $\mathbf{U}$ and consider the Hamiltonian

$$\hat{H}_{\pm} = \hat{\xi}\tau_3 \pm \Delta_0\tau_1 \pm U(\mathbf{r}). \tag{14.15}$$

The Hamiltonian, however, still remains a matrix in particle-hole space, and the wave functions of the optimal fluctuation are the Nambu spinors Ψ.

Let us discuss the physical behavior qualitatively. We linearize the kinetic energy near the Fermi surface, so that the typical kinetic energy in an optimal fluctuation of size L is $\xi \simeq v_F/L$. Then the energy of a quasiparticle in the optimal fluctuation (measured from the Fermi energy) is $E \simeq U + \sqrt{\Delta_0^2 + v_F^2/L^2}$. For energies close to the superconducting gap, $(\Delta_0 - E)/\Delta_0 \ll 1$, the optimal fluctuation is large ($L \gg \xi_0 = v_F/\Delta_0$) and shallow ($|U|/\Delta_0 \ll 1$), so that $E - \Delta_0 \approx U + v_F^2/\Delta_0 L^2$. Introducing the dimensionless energy $\epsilon = E/\Delta_0$, we obtain, in analogy with above arguments, $|U|/\Delta_0 \simeq \xi_0^2/L^2 \simeq 1 - \epsilon$. Notice that the size of the fluctuation is $L \simeq \xi_0/\sqrt{1-\epsilon} \gg \xi_0$. As a result, we find [see Eq. (14.4)] $\mathcal{S}[U] \approx LU^2/U_0^2 = \Delta_0^2 \xi_0 (1-\epsilon)^{3/2}/U_0^2$. From the definition of U_0,

$$-\ln \frac{N(E)}{N_0} \approx \mathcal{S}[U_{\text{opt}}] \simeq (\Delta_0\tau_s)(1-\epsilon)^{3/2}. \tag{14.16}$$

The energy dependence in Eq. (14.16) is identical to the result of Lifshitz in $d=1$, despite the linear, rather than quadratic, dependence of the kinetic energy on the size of the droplet. This follows from the smallness of this energy compared to the gap: even though $\xi \propto 1/L$, the expansion is in ξ^2.

The minimization of the saddle-point action proceeds exactly as in Sec. XIV.B. For spin-up particles, $\mathcal{E}_+[U] = \langle \Psi | \hat{H}_+ | \Psi \rangle$. Minimization with respect to U gives

$$U(x) = -\lambda U_0^2 \langle \Psi | \frac{\delta \hat{H}_+}{\delta U} | \Psi \rangle. \tag{14.17}$$

In principle this variational derivative includes the effect of the self-consistent suppression of the gap. However, this effect is small (Shytov *et al.*, 2003). Then, in exact analogy with the semiconductor problem, $U(x) = -\lambda U_0^2 [\Psi^\star(x)\Psi(x)]$, where $(\Psi^\star\Psi)$ denotes the scalar product in particle-hole space. In turn, the Schrödinger equation takes the form

$$\left[-iv_F \frac{\partial}{\partial x}\tau_3 + \Delta_0\tau_1 - \lambda U_0^2 (\Psi^\star\Psi) \right] \Psi = E\Psi. \tag{14.18}$$

This equation is solved by introducing bilinear forms $R_i = \Psi^\star(x)\hat{\tau}_i\Psi(x)$, which play the role of the Halperin-Lax wave function in Nambu space. We find

$$R_0 = \frac{1-\epsilon^2}{\xi_0 \arccos \epsilon} \frac{1}{\epsilon + \cosh(2x\sqrt{1-\epsilon^2}/\xi_0)}, \tag{14.19}$$

$$R_1 = R_0(\epsilon + \xi_0 R_0 \arccos \epsilon), \tag{14.20}$$

$$R_2 = \sqrt{R_0^2 - R_1^2}, \tag{14.21}$$

and $R_3 = 0$ (Shytov *et al.*, 2004). The physical potential of the optimal fluctuation is (Shytov *et al.*, 2003)

$$\frac{U(x)}{2\Delta_0} = -\frac{1-\epsilon^2}{\epsilon + \cosh(2x\sqrt{1-\epsilon^2}/\xi_0)}, \tag{14.22}$$

which corresponds to the value of the action

$$\mathcal{S}[U] = 8\pi(\Delta_0\tau_s)[\sqrt{1-\epsilon^2} - \epsilon \arccos \epsilon]. \tag{14.23}$$

For $\epsilon \approx 1$ the length scale of the optimal fluctuation is $\xi_0/\sqrt{1-\epsilon^2}$, its depth is $U \sim \Delta_0(1-\epsilon^2)$, and the density of states is $N(E) \sim \exp[-(1-\epsilon^2)^{3/2}]$, in complete agreement with qualitative estimates.

The most important observation of Shytov *et al.* (2003) is that in higher dimensions the optimal fluctuation is strongly anisotropic, in contrast to both conventional semiconductors and superconductors in the diffusive limit. This is a direct consequence of the composite nature of superconducting quasiparticles: they are made out of objects that move with Fermi velocity. The wave function of the subgap state is concentrated along the quasiclassical trajectory, which is a chord in a potential of any shape. Consequently, there is little energy cost in reducing the size of the optimal fluctuation in the "transverse" direction, while the smaller volume makes such fluctuations more probable; see Fig. 40. As a result, the

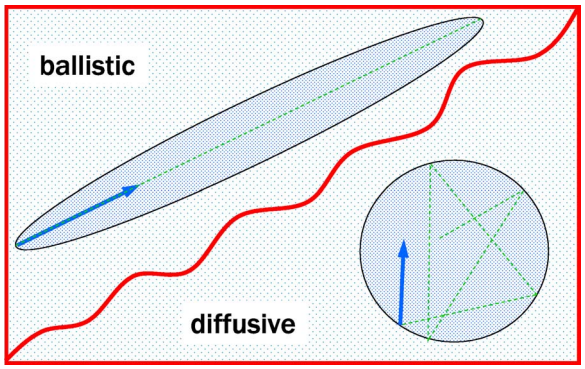

FIG. 40. (Color online) The spatial structure of the optimal fluctuation in the ballistic and diffusive limits.

optimal fluctuation is strongly elongated in one (x) direction. The wave function of the bound state can be written as $\mathbf{\Psi}(x,\mathbf{y})=\exp(ik_F x)\Phi(x,\mathbf{y})$, where $\mathbf{y}$ denotes the transverse $d-1$ coordinates and Φ is a slowly varying function. The kinetic energy of the quasiparticle is

$$\hat{\xi}\Psi \approx -e^{ik_F x}\left(iv_F\frac{\partial}{\partial x}+\frac{\nabla_y^2}{2m}\right)\Phi \sim \left(\frac{v_F}{L_x}+\frac{1}{mL_y^2}\right)\Psi. \tag{14.24}$$

The transverse size of the fluctuation can therefore be reduced until the second term becomes comparable to the first, i.e., $L_y \simeq (\lambda_F L_x)^{1/2}$, where $\lambda_F \simeq k_F^{-1}$ is the Fermi wavelength. Consequently, $|U|/\Delta_0 \sim 1-\epsilon$ and $L_x \sim \xi_0/\sqrt{1-\epsilon}$, and

$$\mathcal{S}[U_{\rm opt}] \simeq L_x L_y^{d-1}\frac{U^2}{U_0^2} \simeq (\Delta_0\tau_s)\left(\frac{E_F}{\Delta_0}\right)^{(d-1)/2}(1-\epsilon)^{(7-d)/4}, \tag{14.25}$$

where E_F is the Fermi energy. Consequently, the density of states is given by $N(E)\sim\exp[-(1-\epsilon)^{(7-d)/4}]$. The action for this anisotropic fluctuation is smaller than that for an isotropic droplet with the same energy of the bound state, by a factor of $(E_F/\Delta_0)^{(d-1)/2}(1-\epsilon)^{-(d-1)/4}$, so that the corresponding DOS is exponentially higher.

Since the optimal fluctuation is a result of a saddle-point approximation for the functional integral, Eq. (14.1), it is only valid when $\mathcal{S}[U_{\rm opt}]\gg 1$, or

$$1-\epsilon \gg (\Delta_0\tau_s)^{4/(d-7)}\left(\frac{\Delta_0}{E_F}\right)^{[2(d-1)]/(7-d)}. \tag{14.26}$$

For $d=1$ this condition is $1-\epsilon \gg (\Delta_0\tau_s)^{-2/3}$, while for $d=3$ it does not depend on the gap, $1-\epsilon \gg (k_F l)^{-1}$.

It is possible to compare the DOS given by different approaches at the crossover scale between the diffusive and ballistic regimes (Vekhter *et al.*, 2003). A transition to the diffusive regime occurs when the size of the optimal fluctuation $L \geqslant v_F\tau_s$, or $1-\epsilon \leqslant (\Delta_0\tau_s)^{-2}$. The result of Lamacraft and Simons (2000) for $\Delta_0\tau_s \gg 1$ was $S_D=(\Delta_0\tau_s)^{5/3}(E_F/\Delta_0)^{d-1}(1-\epsilon)^{(6-d)/4}$. Consequently, at the crossover point the action from Eq. (14.25) is smaller, $S_D/S_0 \simeq (E_F/\Delta_0)^{(d-1)/2}(\Delta_0\tau_s)^{7/6} \gg 1$, and the optimal fluctuation found by Shytov *et al.* (2003) corresponds to a greater DOS. Therefore the structure of the optimal fluctuation near the crossover between the ballistic and diffusive regimes still closely resembles that given above. As the size of the optimal fluctuation increases even further, the anisotropic fluctuation becomes insupportable due to diffusive motion.

Balatsky and Trugman (1997) considered the DOS at $E=0$ due to the suppression of superconductivity by the paramagnetic impurity potential. They needed a large volume fluctuation, $V \geqslant \xi^d$, which is less probable and yields lower DOS than that of Eq. (14.25). Vekhter *et al.* (2003) have checked whether local suppression of the gap from Δ_0 to E due to a large number of impurities with uncorrelated spins (as opposed to a ferromagnetic optimal fluctuation above) is advantageous. For $1-\epsilon \ll 1$ the local pair-breaking rate γ needed to reduce the gap to E is $\gamma\tau_s \approx 1+(1-\epsilon)(\Delta_0\tau_s)^{2/3}$, and the volume of the region has to be at least equal to that of the anisotropic optimal fluctuation to avoid high kinetic-energy cost (this is an underestimate since it ignores proximity coupling to bulk). In that case the optimal action $S_{\rm BT}/S_0 \approx (\Delta_0\tau_s)^{1/3}(E_F/\Delta_0)\bar{c}$, where $\bar{c}=n_{\rm imp}\lambda_F^d$ is the atomic concentration of impurity atoms. As a result, for realistic values of $\bar{c}$ and clean samples $S_{\rm BT} \gg S_0$, the DOS given by the action in Eq. (14.25) is higher. Therefore the ballistic limit of the action obtained by Shytov *et al.* (2003) is expected to be valid up to the crossover to the diffusive regime.

5. Ballistic regime, strong scattering

As of today, we are not aware of any investigations of the optimal fluctuation structure in the ballistic regime when there exist bound states on individual magnetic impurities. It is reasonable to assume that the result differs from the standard Lifshitz formula for the same reason as above: The wave functions of the states localized on magnetic impurities in superconductors oscillate with the Fermi wavelength; see Sec. VI. As a result, in the dilute impurity limit the shift of the energy level localized on, for example, two impurities located at distance $R \gg p_F^{-1}$ will be suppressed by the typical factor $\exp(-R/\xi_0)$ (Rusinov, 1968). Consequently, states significantly below the impurity band must be created by a large number of impurities or impurities located on neighboring lattice sites. This problem still awaits further investigation.

6. Summary

In s-wave superconductors with magnetic impurities, the density of states does not vanish irrespective of the concentration and nature of the impurity scattering. The tails of the density of states extend into the mean-field gap. Therefore, all superconductors with magnetic impurities are gapless. This behavior is illustrated in Fig. 41.

XV. SUMMARY AND OUTLOOK

While considering the role of impurities in conventional and unconventional superconductors, this review has focused on theoretical and experimental results that highlight the physics beyond the standard Abrikosov-Gor'kov theory, the Anderson theorem, and average lifetime effects. Studies of disorder in s-wave superconductors were carried out in detail in the 1960s. We have discussed more recent results in this field. Our main emphasis has been on how individual impurities influence local electronic states in their immediate vicinity and on deviations from the standard Abrikosov-Gor'skov theory on mesoscopic scales. This focus is dictated by advances in experimental techniques, NMR methods and STS measurements for probing electronic states with atomic spatial resolution at the scales where impu-

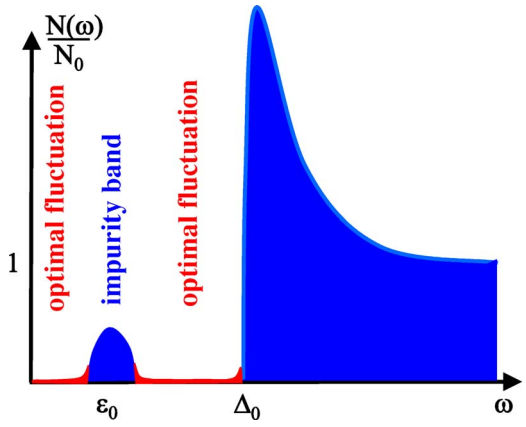

FIG. 41. (Color online) Sketch of the density of states in an *s*-wave superconductor with magnetic impurities. The (blue) dome at ε_0 and the area beyond Δ_0 are regions where the mean-field density of states is finite. The thick (red) lines within the range $[0,\Delta_0]$ signifies the finite but exponentially small DOS induced by the fluctuations in the local impurity distribution. If impurities are weak, the impurity band is absent and the tail extends from the mean-field gap edge.

rities perturb their surrounding (Fischer *et al.*, 2005), and the concomitant development of new theoretical approaches.

The stimulus for such extensive studies is that impurities are markers that allow us to reveal the nature of correlations and pairing of the state where impurities are placed. Indeed, the particular pattern of impurity-induced electronic states is closely connected to the symmetry of the superconducting gap and to the underlying electronic band structure and helps us to understand the nature of superconducting pairing. If strong electronic correlations in the ground state are present, they also are reflected in details of impurity-induced states. Therefore watching the waves created by throwing a pebble in the pond of correlated electrons helps us understand the properties of the underlying electronic liquid.

We have kept the discussion general in order to allow applications to other systems and materials. For instance, this was our rationale for employing the BCS state to describe superconductivity. We believe that it is a good approximation in heavy-fermion systems, organic superconductors, and $SrRuO_4$, at very low energy. At the same time, deviations from this mean-field picture may provide additional details on the underlying physics of the particular material. The majority of the data at the moment are obtained in high-T_c materials. It is clear that similar local effects are present around impurities in other unconventional superconductors, e.g., in $Na_xCoO_2 \cdot yH_2O$ superconductors (Wang and Wang, 2004), although we are not aware of any data on single-impurity states in these materials. Given the importance of the impurity states, this field will undoubtedly be extended to other systems by future experiments.

New ideas and directions continue to emerge in electronic properties induced by impurities. The suite of new experimental tools that address local electronic effects, such as STM, will help to clarify the role of interference between several impurities and pave the way towards connecting the microscopic local states with average properties. Recent theoretical work addressed some aspects of this subject (Andersen, 2003; Atkinson *et al.* 2003; Morr and Balatsky, 2003; Morr and Stavropoulos, 2003b; Zhu *et al.*, 2003; Zhu, Atkinson, and Hirschfeld, 2004) and is awaiting direct comparison with experiment.

Another promising avenue is combining the spatial resolution of STM-STS with the time resolution. The subject is still in its infancy, both theoretically and experimentally, but holds immense promise for the future. Section XI reviewed some recent work in this direction. Temporal and spatial characterization of states generated by dynamical impurities allows exploration of correlations inside the electronic state in which the impurity is placed. One obvious example in which such characterization is crucial is the Kondo effect in a superconducting state. It is desirable to have time-resolved measurements that allow us to visualize the Kondo effect in a superconductor. Another interesting problem that needs further elaboration is the role of collective modes in impurity-induced states. We are only starting to investigate these questions, as discussed in Sec. XII.C.

Real progress on these problems will be made when we have real data. As usual, one should expect that the data will have surprises that were not anticipated in simple theoretical models. This will motivate further theoretical studies, stimulate more measurements, and therefore will lead to a further rapid development of the field. They can provide a space- (and time-) resolved window into the intimate workings of correlated electron matter. We have every reason to be enthusiastic and optimistic about the future of the field of impurity states in superconductors and in other correlated electron systems.

ACKNOWLEDGMENTS

We would like to thank many of our colleagues for useful discussions. We are especially grateful to our collaborators over many years who were instrumental in our work on the subjects that are reviewed here. Without their insights and knowledge this work would have been impossible. We thank Ar. Abanov, E. Abrahams, H. Alloul, B. Altshuler, K. Bedell, A. R. Bishop, D. Bonn, P. Bourges, C. Capan, J. Carbotte, A. H. Castro Neto, S. Chakravarty, N. Curro, J. C. Davis, D. Eigler, M. Franz, C. D. Gong, L. P. Gor'kov, M. J. Graf, I. A. Gruzberg, W. Hardy, P. J. Hirschfeld, W. Ho, C. R. Hu, A. Kapitulnik, S. Kivelson, T. K. Lee, I. Martin, D. K. Morr, S.H. Pan, D. Pines, A. Rosengren, M. I. Salkola, J. Sarrao, J. A. Sauls, D. J. Scalapino, K. Scharnberg, J. R. Schrieffer, A. V. Shytov, Q. Si, J.D. Thompson, C. S. Ting, M. Vojta, Z. D. Wang, A. Yazdani, and J. Zaanen for fruitful discussions. This work was supported by the U.S. Department of Energy (A.V.B. and J.X.Z.) and by the Board of Regents of Louisiana (I.V.).

LIST OF SYMBOLS

Quantity	Explanation
a	Lattice parameter
b ($b^\dagger$)	Bosonic annihilation (creation) operators
c ($c^\dagger$)	Fermionic annihilation (creation) operators
d	Spatial dimension
D	Half-energy bandwidth
Δ_0	Superconducting energy gap
Δ_k	Momentum-dependent superconducting energy gap
$\phi_n(\mathbf{r})$	Electron eigenfunction
E_F	Electron Fermi energy
$G(\tau,\tau'), G(\tau,\mathbf{r})$	Electron Green's function in coordinate space
$G(\omega_n,\mathbf{k}), G(\mathbf{k},\omega_n)$	Electron Green's function in Matsubara frequency and momentum space
$H,\mathcal{H},H_{\rm int}$	Hamiltonian
J,J_0,J_c	Exchange coupling
L	Linear dimension of a system
μ	Chemical potential
$N(\epsilon)$	Electron density of states
$N(\epsilon,\mathbf{r}), N(E,i)$	Electron local density of states
$\psi(\mathbf{r})[\psi^\dagger(\mathbf{r})]$	Fermionic field operators in continuum space
$\lvert\Psi\rangle, \lvert\Psi_0\rangle$	BCS variational wave function
$\lvert\Psi_{-1}\rangle, \lvert\Phi_{-1}\rangle$	Excited variational wave function with single-particle excitation present
$\mathbf{r}$	Spatial coordinates
$\boldsymbol{\sigma}$	Pauli matrices in spin space
$\boldsymbol{\tau}$	Pauli matrices in Nambu space
$V_{\alpha\beta\gamma\delta}, \tilde{V}_{\alpha\beta}$	Superconducting pairing interaction
$\mathbf{S}$	Local spin operator
t,t'	Electron hopping integral
u	Electronlike Bogoliubov quasiparticle wave-function amplititude
$T(\omega)$	T matrix
T	Temperature
v	Holelike Bogoliubov quasiparticle wave-function amplitude
U	Hubbard on-site electron-electron interaction
U_0	Impurity scattering potential
W	Energy bandwidth
$W_{\mathbf{k}}$	d-density-wave order parameter
ξ_0	BCS superconducting coherence length at low temperatures
$\xi(T)$	BCS temperature-dependent coherence length

REFERENCES

Abanov, A., and A. V. Chubukov, 2000, Phys. Rev. B **61**, R9241.

Abanov, A., A. V. Chubukov, M. Eschrig, M. R. Norman, and J. Schmalian, 2002, Phys. Rev. Lett. **89**, 177002.

Abrahams, E., and C. M. Varma, 2000, Proc. Natl. Acad. Sci. U.S.A. **97**, 5714.

Abrikosov, A. A., and L. P. Gor'kov, 1960, Zh. Eksp. Teor. Fiz. **39**, 1781 [Sov. Phys. JETP **12**, 1243 (1961)].

Abrikosov, A. A., L. P. Gor'kov, and I. E. Dzyaloshinski, 1963, *Methods of Quantum Field Theory in Statistical Physics* (Dover, New York).

Adagideli, I., P. M. Goldbart, A. Shnirman, and A. Yazdani, 1999, Phys. Rev. Lett. **83**, 5571.

Affleck, I., and J. B. Marston, 1988, Phys. Rev. B **37**, 3774.

Alloul, H., P. Mendels, H. Casalta, J.-F. Marucco, and J. Arabski, 1991, Phys. Rev. Lett. **67**, 3140.

Altland, A., B. D. Simons, and D. Taras-Semchuk, 2000, Adv. Phys. **49**, 321.

Altland, A., B. D. Simons, and M. R. Zirnbauer, 2002, Phys. Rep. **359**, 283.

Altland, A., and M. Zirnbauer, 1997, Phys. Rev. B **55**, 1142.

Altshuler, B. L., 1985, Pis'ma Zh. Eksp. Teor. Fiz. **51**, 530 [JETP Lett. **41**, 648 (1985)].

Ambegaokar, V., and A. Griffin, 1965, Phys. Rev. **137**, A1151.

Andersen, B. M., 2003, Phys. Rev. B **68**, 094518.

Andersen, B. M., and P. Hedegård, 2003, Phys. Rev. B **67**, 172505.

Andersen, O. K., A. I. Lichtenstein, O. Jepsen, and F. Paulsen, 1995, J. Phys. Chem. Solids **56**, 1573.

Anderson, P. W., 1959, Phys. Rev. Lett. **3**, 325.

Anderson, P. W., 1970, J. Phys. C **3**, 2436.

Anderson, P. W., G. Yuval, and D. R. Hamann, 1970, Phys. Rev. B **1**, 4464.

Andrei, N., 1980, Phys. Rev. Lett. **45**, 379.

Annett, J., 1990, Adv. Phys. **39**, 83.

Aprili, M., M. Covington, E. Paraoanu, B. Niedermeier, and L. H. Greene, 1998, Phys. Rev. B **57**, R8139.

Arfi, B., H. Bahlouli, C. Pethick, and D. Pines, 1988, Phys. Rev. Lett. **60**, 2206.

Aristov, D. N., and A. G. Yashenkin, 1998, Phys. Rev. Lett. **80**, 1116.

Atkinson, W. A., and P. J. Hirschfeld, 2002, Phys. Rev. Lett. **88**, 187003.

Atkinson, W. A., P. J. Hirschfeld, A. H. MacDonald, and K. Ziegler, 2000, Phys. Rev. Lett. **85**, 3926.

Atkinson, W. A., P. J. Hirschfeld, and L. Zhu, 2003, Phys. Rev. B **68**, 054501.

Bader, S. D., N. E. Phillips, M. B. Maple, and C. A. Luengo, 1975, Solid State Commun. **16**, 1263.

Balatsky, A., 1998, Phys. Rev. Lett. **80**, 1972.

Balatsky, A., 2000, Phys. Rev. B **61**, 6940.

Balatsky, A., and E. Abrahams, 1992, Phys. Rev. B **45**, 13125.

Balatsky, A. V., A. Abanov, and J.-X. Zhu, 2003, Phys. Rev. B **68**, 214506.

Balatsky, A. V., A. Rosengren, and B. L. Altshuler, 1994, Phys. Rev. Lett. **73**, 720.

Balatsky, A. V., and M. I. Salkola, 1998, Phys. Rev. Lett. **80**, 1117.

Balatsky, A. V., M. I. Salkola, and A. Rosengren, 1995, Phys. Rev. B **51**, 15547.

Balatsky, A. V., and S. A. Trugman, 1997, Phys. Rev. Lett. **79**, 3767.

Barash, Y. S., A. Grishin, and M. Sigrist, 1997, Zh. Eksp. Teor. Fiz. **112**, 304 [JETP **85**, 168 (1997)].

Barash, Y. S., M. S. Kalenkov, and J. Kurkijrvi, 2000, Phys. Rev. B **62**, 6665.

Bauriedl, W., P. Ziemann, and W. Buckel, 1981, Phys. Rev.

Lett. **47**, 1163.
Beloborodov, I. S., B. N. Narozhny, and I. L. Aleiner, 2000, Phys. Rev. Lett. **85**, 816.
Berezinskii, V., 1974, Phys. Rev. Lett. **20**, 628 [JETP Lett. **20**, 287 (1974)].
Berlinsky, A. J., D. A. Bonn, R. Harris, and C. Kallin, 2000, Phys. Rev. B **61**, 9088.
Bhaseen, M. J., J. S. Caux, I. I. Kogan, and A. M. Tsvelik, 2001, Nucl. Phys. B **618**, 465.
Bickers, N. E., and G. E. Zwicknagl, 1987, Phys. Rev. B **36**, 6746.
Blonder, G. E., M. Tinkham, and T. M. Klapwijk, 1982, Phys. Rev. B **25**, 4515.
Blount, E. I., 1985, Phys. Rev. B **32**, 2935.
Bobroff, J., H. Alloul, W. MacFarlane, P. Mendels, N. Blanchard, G. Collin, and J. Marucco, 2001, Phys. Rev. Lett. **86**, 4116.
Borkowski, L. S., and P. J. Hirschfeld, 1992, Phys. Rev. B **46**, 9274.
Borkowski, L. S., and P. J. Hirschfeld, 1994, J. Low Temp. Phys. **96**, 185.
Brandt, U., 1970, J. Low Temp. Phys. **2**, 573.
Buchholtz, L. J., and G. Zwicknagl, 1981, Phys. Rev. B **23**, 5788.
Bulaevskii, L., V. Kuzii, and A. Sobyanin, 1977, Pis'ma Zh. Eksp. Teor. Fiz. **25**, 314 [JETP Lett. **25**, 290 (1977)].
Bulla, R., M. T. Glossop, D. E. Logan, and T. Pruschke, 2000, J. Phys.: Condens. Matter **12**, 4899.
Bulla, R., T. Pruschke, and A. C. Hewson, 1997, J. Phys.: Condens. Matter **9**, 10463.
Buzdin, A. I., 2005, Rev. Mod. Phys. **77**, 935.
Buzdin, A., L. Bulaevskii, and S. Panyukov, 1982, J. Phys.: Condens. Matter **35**, 147 [JETP Lett. **35**, 178 (1982)].
Byers, J. M., M. E. Flatté, and D. J. Scalapino, 1993, Phys. Rev. Lett. **71**, 3363.
Campuzano, J. C., M. R. Norman, and M. Randeria, 2004, *Physics of Superconductors* (Springer, Berlin), Vol. II, p. 167.
Campuzano, J. C., *et al.*, 1999, Phys. Rev. Lett. **83**, 3709.
Capriotti, L., D. J. Scalapino, and R. D. Sedgewick, 2003, Phys. Rev. B **68**, 014508.
Carbotte, J. P., 1990, Rev. Mod. Phys. **62**, 1027.
Carr, G. L., R. P. S. M. Lobo, J. LaVeigne, D. H. Reitze, and D. B. Tanner, 2000, Phys. Rev. Lett. **85**, 3001.
Cassanello, C. R., and E. Fradkin, 1996, Phys. Rev. B **53**, 15079.
Cassanello, C. R., and E. Fradkin, 1997, Phys. Rev. B **56**, 11246.
Chaba, A. N., and A. D. S. Nagi, 1972, Can. J. Phys. **50**, 1736.
Chakravarty, S., R. B. Laughlin, D. K. Morr, and C. Nayak, 2001, Phys. Rev. B **63**, 094503.
Chamon, C., and C. Mudry, 2001, Phys. Rev. B **63**, 100503.
Chen, D. C., D. Rainer, and J. Sauls, 1998, in *Proceedings of the International Conference on Quasiclassical Methods in Superconductivity and Superfluidity*, Verditz 1996, edited by D. Rainer and J. A. Sauls (University Bayreuth, Bayreuth, Germany).
Chen, H.-D., J.-P. Hu, S. Capponi, E. Arrigoni, and S.-C. Zhang, 2002, Phys. Rev. Lett. **89**, 137004.
Chen, H. Y., and C. S. Ting, 2003, Phys. Rev. B **68**, 212502.
Chen, K., and C. Jayaprakash, 1995, J. Phys.: Condens. Matter **7**, L491.
Chen, Q., I. Kosztin, B. Janko, and K. Levin, 1998, Phys. Rev. Lett. **81**, 4708.
Chen, Y., and C. S. Ting, 2004, Phys. Rev. Lett. **92**, 077203.
Chiao, M., R. W. Hill, C. Lupien, L. Taillefer, P. Lambert, R. Gagnon, and P. Fournier, 2000, Phys. Rev. B **62**, 3554.
Choi, C., and P. Muzikar, 1990, Phys. Rev. B **41**, 1812.
Choi, C. H., 1999, Phys. Rev. B **60**, 6884.
Chubukov, A. V., A. Abanov, and D. N. Basov, 2003, Phys. Rev. B **68**, 024504.
Coleman, P., 1984, Phys. Rev. B **29**, 3035.
Coleman, P., 1985, J. Magn. Magn. Mater. **47**, 323.
Corson, J., J. Orenstein, S. Oh, J. O'Donnell, and J. N. Eckstein, 2000, Phys. Rev. Lett. **85**, 2569.
Covington, M., M. Aprili, E. Paraoanu, L. H. Greene, F. Xu, J. Zhu, and C. A. Mirkin, 1997, Phys. Rev. Lett. **79**, 277; **79**, 2598(E) (1997).
Cox, D. L., and A. Zawadowski, 1998, Adv. Phys. **47**, 599.
Damascelli, A., Z. Hussain, and Z.-X. Shen, 2003, Rev. Mod. Phys. **75**, 473.
de Gennes, P. G., 1989, *Superconductivity of Metals and Alloys* (Addison-Wesley, New York).
Dessau, D. S., B. O. Wells, Z. Shen, W. E. Spicer, A. J. Arko, R. S. List, D. B. Mitzi, and A. Kapitulnik, 1991, Phys. Rev. Lett. **66**, 2160.
Duffy, D., P. J. Hirschfeld, and D. J. Scalapino, 2001, Phys. Rev. B **64**, 224522.
Dumoulin, L., E. Guyon, and P. Nedellec, 1975, Phys. Rev. Lett. **34**, 264.
Dumoulin, L., E. Guyon, and P. Nedellec, 1977, Phys. Rev. B **16**, 1086.
Edelstein, A. S., 1967, Phys. Rev. Lett. **19**, 1184.
Elliott, R. J., 1954, Phys. Rev. **96**, 266.
Emery, V. J., and S. A. Kivelson, 1995, Nature (London) **374**, 434.
Eschrig, M., and M. R. Norman, 2000, Phys. Rev. Lett. **85**, 3261.
Fetter, A. L., 1965, Phys. Rev. **140**, A1921.
Fetter, A. L., and J. D. Walecka, 1971, *Quantum Theory of Many-Particle Systems* (McGraw-Hill, New York).
Fischer, O., M. Kugler, I. Maggio-Aprile, C. Berthod, and C. Renner, 2005, Rev. Mod. Phys. (unpublished).
Flatté, M. E., and J. M. Byers, 1997a, Phys. Rev. Lett. **78**, 3761.
Flatté, M. E., and J. M. Byers, 1997b, Phys. Rev. B **56**, 11213.
Flatte, M. E., and J. M. Byers, 1998, Phys. Rev. Lett. **80**, 4546.
Flatté, M. E., and J. M. Byers, 1999, Solid State Phys. **52**, 137.
Fogelström, M., D. Rainer, and J. A. Sauls, 1997, Phys. Rev. Lett. **79**, 281.
Franz, M., C. Kallin, and A. J. Berlinsky, 1996, Phys. Rev. B **54**, R6897.
Franz, M., D. E. Sheehy, and Z. Tešanović, 2002, Phys. Rev. Lett. **88**, 257005.
Franz, M., and Z. Tešanović, 1998, Phys. Rev. Lett. **80**, 4763.
Galitskii, V. M., and A. I. Larkin, 2002, Phys. Rev. B **66**, 064526.
Ghosal, A., and H. Y. Kee, 2004, Phys. Rev. B **69**, 224513.
Ghosal, A., M. Randeria, and N. Trivedi, 1998, Phys. Rev. Lett. **81**, 3940.
Ginzberg, D. M., 1979, Phys. Rev. B **20**, 960.
Glazman, L., and K. Matveev, 1989, Pis'ma Zh. Eksp. Teor. Fiz. **49**, 570 [JETP Lett. **49**, 660 (1989)].
Golubov, A. A., and I. I. Mazin, 1999, Phys. Rev. B **55**, 15146.
Gong, C.-D., and J.-H. Cai, 1966, J. Phys., (China) **22**, 381.
Gonzalez-Buxton, C., and K. Ingersent, 1998, Phys. Rev. B **57**, 15254.
Gor'kov, L. P., and P. A. Kalugin, 1985, Pis'ma Zh. Eksp. Teor.

Fiz. **41**, 208 [JETP Lett. **41**, 253 (1985)].
Graf, M., A. Balatsky, and J. Sauls, 2000, Phys. Rev. B **61**, 3255.
Graf, M. J., J. Sauls, and D. Rainer, 1995, Phys. Rev. B **52**, 10588.
Graf, M. J., S.-K. Yip, J. A. Sauls, and D. Rainer, 1996, Phys. Rev. B **53**, 15147.
Grimaldi, C., 1999, Europhys. Lett. **48**, 306.
Grimaldi, C., 2002, Phys. Rev. B **65**, 094502.
Gweon, G.-H., T. Sasagawa, S. Y. Zhou, J. Graf, H. Takagi, D.-H. Lee, and A. Lanzara, 2004, Nature (London) **430**, 187.
Hahn, J. R., and W. Ho, 2001, Phys. Rev. Lett. **87**, 166102.
Halperin, B. I., and M. Lax, 1966, Phys. Rev. **148**, 722.
Hamann, D. R., 1967, Phys. Rev. **158**, 570.
Han, Q., Z. D. Wang, X.-G. Li, and L. Y. Zhang, 2002, Phys. Rev. B **66**, 104502.
Han, Q., T. Xia, Z. D. Wang, and X.-G. Li, 2004, Phys. Rev. B **69**, 224512.
Haran, G., and A. D. S. Nagi, 1996, Phys. Rev. B **54**, 15463.
Haran, G., and A. D. S. Nagi, 1998, Phys. Rev. B **58**, 12441.
Harlingen, D. J. V., 1995, Rev. Mod. Phys. **67**, 515.
Heinrichs, J., 1968, Phys. Rev. **168**, 451.
Hettler, M. H., and P. J. Hirschfeld, 1999, Phys. Rev. B **59**, 9606.
Hewson, A. C., 1993, *The Kondo Problem to Heavy Fermions* (Cambridge University Press, Cambridge).
Hill, R. W., C. Lupien, M. Sutherland, E. Boaknin, D. G. Hawthorn, C. Proust, F. Ronning, L. Taillefer, R. Liang, D. A. Bonn, and W. N. Hardy, 2004, Phys. Rev. Lett. **92**, 027001.
Hirschfeld, P. J., and W. A. Atkinson, 2002, J. Low Temp. Phys. **126**, 881.
Hirschfeld, P. J., and N. Goldenfeld, 1993, Phys. Rev. B **48**, 4219.
Hirschfeld, P. J., W. O. Putikka, and D. J. Scalapino, 1994, Phys. Rev. B **50**, 10250.
Hirschfeld, P. J., S. M. Quinlan, and D. J. Scalapino, 1997, Phys. Rev. B **55**, 12742.
Hirschfeld, P. J., P. Wölfle, D. Einzel, J. A. Sauls, and W. O. Putikka, 1989, Phys. Rev. B **40**, 6695.
Hirschfeld, P. J., P. Wölfle, and D. Vollhard, 1986, Solid State Commun. **59**, 111.
Hirschfeld, P. J., P. W. Wölfle, and D. Einzel, 1988, Phys. Rev. B **37**, 83.
Hoffman, J. E., E. W. Hudson, K. M. Lang, V. Madhavan, H. Eisaki, S. Uchida, and J. C. Davis, 2002, Science **295**, 466.
Hoffman, J. E., K. McElroy, D.-H. Lee, K. M. Lang, H. Eisaki, S. Uchida, and J. C. Davis, 2002, Science **297**, 1148.
Hosseini, A., R. Harris, S. Kamal, P. Dosanjh, J. Preston, R. Liang, W. N. Hardy, and D. A. Bonn, 1999, Phys. Rev. B **60**, 1349.
Hotta, T., 1993, J. Phys. Soc. Jpn. **62**, 274.
Howald, C., H. Eisaki, N. Kaneko, M. Greven, and A. Kapitulnik, 2003, Phys. Rev. B **67**, 014533.
Howald, C., P. Fournier, and A. Kapitulnik, 2001, Phys. Rev. B **64**, 100504.
Howell, P. C., A. Rosch, and P. J. Hirschfeld, 2004, Phys. Rev. Lett. **92**, 037003.
Hsu, T. C., J. B. Marston, and I. Affleck, 1991, Phys. Rev. B **43**, 2866.
Hu, C.-R., 1994, Phys. Rev. Lett. **72**, 1526.
Hudson, E. W., K. M. Lang, V. Madhavan, S. H. Pan, H. Eisaki, S. Uchida, and J. C. Davis, 2001, Nature (London) **411**, 920.
Hudson, E. W., S. H. Pan, A. K. Gupta, K.-W. Ng, and J. C. Davis, 1999, Science **285**, 88.
Hussey, N. E., 2002, Adv. Phys. **51**, 1685.
Ingersent, K., 1996, Phys. Rev. B **54**, 11936.
Ingersent, K., and Q. Si, 1998, e-print cond-mat/9810226.
Ishida, K., Y. Kitaoka, N. Ogata, T. Kamino, K. Asayama, J. R. Cooper, and N. Athanassopoulou, 1993, J. Phys. Soc. Jpn. **63**, 2803.
Ishida, K., Y. Kitaoka, K. Yamazoe, K. Asayama, and Y. Yamada, 1996, Phys. Rev. Lett. **76**, 531.
Ishida, K., Y. Kitaoka, T. Yoshitomi, N. Ogata, T. Kamino, and K. Asayama, 1991, Physica C **179**, 29.
Itoh, Y., 1993, J. Phys. Soc. Jpn. **62**, 2184.
Janko, B., I. Kosztin, K. Levin, M. Norman, and D. Scalapino, 1999, Phys. Rev. Lett. **82**, 4304.
Jarrell, M., 1990, Phys. Rev. B **41**, 4815.
Jarrell, M., D. S. Silva, and B. Patton, 1990, Phys. Rev. B **42**, 4804.
Joynt, R., 1997, J. Low Temp. Phys. **109**, 811.
Kampf, A. P., and T. P. Devereaux, 1997, Phys. Rev. B **56**, 2360.
Kashiwaya, S., and Y. Tanaka, 2000, Rep. Prog. Phys. **63**, 1641.
Kee, H. Y., 2001, Phys. Rev. B **64**, 012506.
Kee, H.-Y., S. A. Kivelson, and G. Aeppli, 2002, Phys. Rev. Lett. **88**, 257002.
Ketterson, J. B., and S. N. Song, 1999, *Superconductivity* (Cambridge University Press, Cambridge).
Khaykovich, B., Y. S. Lee, R. W. Erwin, S. H. Lee, S. Wakimoto, K. J. Thomas, M. A. Kastner, and R. J. Birgeneau, 2002, Phys. Rev. B **66**, 014528.
Kim, H., and P. Muzikar, 1993, Phys. Rev. B **48**, 39332.
Kivelson, S. A., I. P. Bindloss, E. Fradkin, V. Oganesyan, J. M. Tranquada, A. Kapitulnik, and C. Howald, 2003, Rev. Mod. Phys. **75**, 1201.
Koga, M., and M. Matsumoto, 2002a, J. Phys. Soc. Jpn. **71**, 943.
Koga, M., and M. Matsumoto, 2002b, Phys. Rev. B **65**, 094434.
Kondo, J., 1964, Prog. Theor. Phys. **32**, 37.
Kosterlitz, J. M., and D. J. Thouless, 1973, J. Phys. C **6**, 1181.
Kosterlitz, J. M., and D. J. Thouless, 1974, J. Phys. C **7**, 1046.
Krasnov, V. M., A. Yurgens, D. Winkler, P. Delsing, and T. Claeson, 2000, Phys. Rev. Lett. **84**, 5860.
Kruis, H. V., I. Martin, and A. V. Balatsky, 2001, Phys. Rev. B **64**, 054501.
Kuboki, K., and M. Sigrist, 1998, J. Phys. Soc. Jpn. **67**, 2873.
Kulic, M. L., and O. V. Dolgov, 1999, Phys. Rev. B **60**, 13062.
Kulik, I. O., and O. Y. Itskovich, 1968, Zh. Eksp. Teor. Fiz. **55**, 193 [Sov. Phys. JETP **28**, 102 (1969)].
Lake, B., G. Aeppli, K. N. Clause, D. F. McMorrow, K. Lefmann, N. E. Hussey, N. Mangkorntong, M. Nohara, H. Takagi, T. E. Mason, and A. Schröder, 2001, Science **291**, 1759.
Lake, B., *et al.*, 2002, Nature (London) **415**, 299.
Lamacraft, A., and B. D. Simons, 2000, Phys. Rev. Lett. **85**, 4783.
Lamacraft, A., and B. D. Simons, 2001, Phys. Rev. B **64**, 014514.
Landau, L., and E. Lifshitz, 2000, *Quantum Mechanics* (Butterworth-Heinemann, Oxford), Vol. 3.
Lang, K. M., V. Madhavan, J. E. Hoffman, E. W. Hudson, H. Eisaki, S. Uchida, and J. C. Davis, 2002, Nature (London) **415**, 412.
Lanzara, A., *et al.*, 2004, Nature (London) **430**, 187.
Larkin, A., 1965, JETP Lett. **2**, 130.
Larkin, A. I., V. I. Mel'nikov, and D. E. Khmelnitskii, 1971,

Sov. Phys. JETP **33**, 458.
Larkin, A. I., and Y. N. Ovchinnikov, 1972, Sov. Phys. JETP **34**, 1144.
Laughlin, R. B., 1998, Phys. Rev. Lett. **80**, 5188.
Lee, P. A., 1993, Phys. Rev. Lett. **71**, 1887.
Lee, P. A., and T. V. Ramakrishnan, 1985, Rev. Mod. Phys. **57**, 287.
Lee, Y.-S., K. Segawa, Y. Ando, and D. N. Basov, 2004, Phys. Rev. B **70**, 014518.
Li, J.-X., W.-G. Yin, and C.-D. Gong, 1998, Phys. Rev. B **58**, 2895.
Liang, S. D., and T. K. Lee, 2002, Phys. Rev. B **65**, 214529.
Lifshitz, I. M., 1964a, Adv. Phys. **13**, 483.
Lifshitz, I. M., 1964b, Usp. Fiz. Nauk **83**, 617 [Sov. Phys. Usp. **7**, 549 (1965)].
Lifshitz, I. M., 1967, Zh. Eksp. Teor. Fiz. **53**, 743 [Sov. Phys. JETP **26**, 462 (1968)].
Lifshitz, I. M., S. A. Gredeskul, and L. A. Pastur, 1988, *Introduction to the Theory of Disordered Systems* (Wiley, New York).
Logan, D. E., and M. T. Glossop, 2000, J. Phys.: Condens. Matter **12**, 985.
Loktev, V. M., and Y. Pogorelov, 2002, Europhys. Lett. **60**, 757.
Loram, J. W., J. L. Luo, J. R. Cooper, W. Y. Liang, and J. L. Tallon, 2000, Physica C **341-348**, 831.
Ma, M., and P. A. Lee, 1985, Phys. Rev. B **32**, 5658.
Machida, K., and F. Shibata, 1972, Prog. Theor. Phys. **47**, 1817.
Mackenzie, A. P., K. Haselwimmer, A. Tyler, G. Lonzarich, Y. Mori, S. Nishizaki, and Y. Maeno, 1998, Phys. Rev. Lett. **80**, 161.
Mackenzie, A. P., and Y. Maeno, 2003, Rev. Mod. Phys. **75**, 657.
Mahajan, A. V., H. Alloul, G. Collin, and J.-F. Marucco, 1994, Phys. Rev. Lett. **72**, 3100.
Mahajan, A. V., H. Alloul, G. Collin, and J.-F. Marucco, 2000, Eur. Phys. J. B **13**, 457.
Mahan, G. D., 2000, *Many-Particle Physics*, 3rd ed. (Kluwer Academic/Plenum, New York).
Maki, K., 1969, in *Superconductivity*, edited by R. D. Parks (Dekker, New York), p. 1035.
Maple, M. B., 1973, in *Magnetism*, edited by H. Suhl (Academic, New York), Vol. V, p. 289.
Marchetti, F. M., and B. D. Simons, 2002, J. Phys. A **35**, 4201.
Markowitz, D., and L. P. Kadanoff, 1963, Phys. Rev. **131**, 563.
Marston, J. B., and I. Affleck, 1989, Phys. Rev. B **39**, 11538.
Martin, I., and A. V. Balatsky, 2000, Phys. Rev. B **62**, 6124.
Martin, I., A. V. Balatsky, and J. Zaanen, 2002, Phys. Rev. Lett. **88**, 097003.
Martinez-Samper, P., H. Suderow, S. Vieira, J. P. Brison, N. Luchier, P. Lejay, and P. C. Canfield, 2003, Phys. Rev. B **67**, 014526.
Matsumoto, M., and M. Koga, 2002, Phys. Rev. B **65**, 024508.
Matsuura, T., 1977, Prog. Theor. Phys. **57**, 1823.
Matsuura, T., S. Ichinose, and Y. Nagaoka, 1977, Prog. Theor. Phys. **57**, 713.
McElroy, K., R. W. Simmonds, J. E. Hoffman, D. H. Lee, J. Orenstein, H. Eisaki, S. Uchida, and J. C. Davis, 2003, Nature (London) **422**, 592.
Mendels, P., J. Bobroff, G. Collin, H. Alloul, M. Gabay, J.-F. Marucco, N. Blanchard, and B. Grenier, 1999, Europhys. Lett. **46**, 678.
Meyer, J. S., and B. D. Simons, 2001, Phys. Rev. B **64**, 134516.
Millis, A. J., 2003, Solid State Commun. **126**, 3.
Misra, S., S. Oh, D. J. Hornbaker, T. DiLuccio, J. N. Eckstein, and A. Yazdani, 2002, Phys. Rev. Lett. **89**, 087002.
Moradian, R., J. F. Annett, B. L. Gyorffy, and G. Litak, 2001, Phys. Rev. B **63**, 024501.
Morr, D. K., 2002, Phys. Rev. Lett. **89**, 106401.
Morr, D. K., and A. V. Balatsky, 2003, Phys. Rev. Lett. **90**, 067005.
Morr, D. K., and R. H. Nyberg, 2003, Phys. Rev. B **68**, 060505.
Morr, D. K., and N. A. Stavropoulos, 2002, Phys. Rev. B **66**, 140508.
Morr, D. K., and N. A. Stavropoulos, 2003a, Phys. Rev. B **68**, 094518.
Morr, D. K., and N. A. Stavropoulos, 2003b, Phys. Rev. B **67**, 020502.
Movshovich, R., M. A. Hubbard, M. B. Salamon, A. V. Balatsky, R. Yoshizaki, J. L. Sarrao, and M. Jaime, 1998, Phys. Rev. Lett. **80**, 1968.
Müller-Hartmann, E., 1973, in *Magnetism*, edited by H. Suhl (Academic, New York), Vol. V, p. 353.
Müller-Hartmann, E., and J. Zittartz, 1971, Phys. Rev. Lett. **26**, 428.
Nagaoka, Y., 1965, Phys. Rev. **138**, A1112.
Nagaoka, Y., 1967, Prog. Theor. Phys. **37**, 13.
Neils, W. K., and D. J. V. Harlingen, 2002, Phys. Rev. Lett. **88**, 047001.
Nersesyan, A., and A. Tsvelik, 1997, Phys. Rev. Lett. **78**, 3981.
Nersesyan, A., A. Tsvelik, and F. Wenger, 1995, Nucl. Phys. B **438**, 561.
Nicol, E. J., and J. P. Carbotte, 2003, Phys. Rev. B **67**, 214506.
Norman, M. R., and H. Ding, 1998, Phys. Rev. B **57**, 11089.
Norman, M. R., H. Ding, M. Randeria, J. C. Campuzano, T. Yokoya, T. Takeuchi, T. Takahashi, T. Mochiku, K. Kadowaki, P. Guptasarma, and D. G. Hinks, 1998, Nature (London) **392**, 157.
Norman, M. R., M. Randeria, H. Ding, and J. C. Campuzano, 1995, Phys. Rev. B **52**, 615.
Ogura, J., and T. Saso, 1993, J. Phys. Soc. Jpn. **62**, 4364.
Okabe, Y., and A. D. S. Nagi, 1983, Phys. Rev. B **28**, 1320.
Pan, S., E. W. Hudson, and J. Davis, 1998, Appl. Phys. Lett. **73**, 2992.
Pan, S. H., E. W. Hudson, A. K. Gupta, K.-W. Ng, H. Eisaki, S. Uchida, and J. C. Davis, 2000, Phys. Rev. Lett. **85**, 1536.
Pan, S. H., E. W. Hudson, K. M. Lang, H. Eisaki, S. Uchida, and J. C. Davis, 2000, Nature (London) **403**, 746.
Pan, S. H., *et al.*, 2001, Nature (London) **413**, 282.
Pepin, C., and P. A. Lee, 1998, Phys. Rev. Lett. **81**, 2779.
Pepin, C., and P. A. Lee, 2001, Phys. Rev. B **63**, 054502.
Petersen, L., P. T. Sprunger, P. Hoffmann, E. Lægsgaard, B. G. Briner, M. Doering, H.-P. Rust, A. M. Bradshaw, F. Besenbacher, and E. W. Plummer, 1998, Phys. Rev. B **57**, R6858.
Pethick, C. J., and D. Pines, 1986, Phys. Rev. Lett. **57**, 118.
Podolsky, D., E. Demler, K. Damle, and B. I. Halperin, 2003, Phys. Rev. B **67**, 094514.
Pogorelov, Y., 1994, Physica C **235-240**, 2279.
Polkovnikov, A., 2002, Phys. Rev. B **65**, 064503.
Polkovnikov, A., S. Sachdev, and M. Vojta, 2001, Phys. Rev. Lett. **86**, 296.
Polkovnikov, A., S. Sachdev, and M. Vojta, 2003, Physica C **388-389**, 19.
Quinlan, S. M., P. J. Hirschfeld, and D. J. Scalapino, 1996, Phys. Rev. B **53**, 8575.
Quinlan, S. M., D. J. Scalapino, and N. Bulut, 1994, Phys. Rev. B **49**, 1470.

Rainer, D., and M. Vuorio, 1977, J. Phys. C **10**, 3093.
Read, N., 1985, J. Phys. C **18**, 2651.
Read, N., and D. M. Newns, 1983a, J. Phys. C **16**, 3273.
Read, N., and D. M. Newns, 1983b, J. Phys. C **16**, L1055.
Renner, C., B. Revaz, J.-Y. Genoud, K. Kadowaki, and Ø. Fischer, 1998, Phys. Rev. Lett. **80**, 149.
Rusinov, A. I., 1968, Zh. Eksp. Teor. Fiz. Pis'ma Red. **9**, 146 [JETP Lett. **9**, 85 (1969)].
Rusinov, A. I., 1969, Zh. Eksp. Teor. Fiz. **56**, 2047 [Sov. Phys. JETP **29**, 1101 (1969)].
Sakai, O., Y. Shimizu, H. Shiba, and K. Satori, 1993, J. Phys. Soc. Jpn. **62**, 3181.
Sakurai, A., 1970, Prog. Theor. Phys. **44**, 1472.
Salkola, M. I., A. V. Balatsky, and D. J. Scalapino, 1996, Phys. Rev. Lett. **77**, 1841.
Salkola, M. I., A. V. Balatsky, and J. R. Schrieffer, 1997, Phys. Rev. B **55**, 12648.
Samokhin, K., and M. Walker, 2001, Phys. Rev. B **64**, 024507.
Satori, K., H. Shiba, O. Sakai, and Y. Shimizu, 1992, J. Phys. Soc. Jpn. **61**, 3239.
Saxena, S. S., *et al.*, 2000, Nature (London) **406**, 587.
Scalapino, D. J., P. J. Hirschfeld, and T. Nunner, 2004, Proceedings of SNS-2004 (Sitges) (unpublished).
Schachinger, E., 1982, Z. Phys. B: Condens. Matter **47**, 217.
Schachinger, E., and J. P. Carbotte, 1984, Phys. Rev. B **29**, 165.
Schachinger, E., J. M. Daams, and J. P. Carbotte, 1980, Phys. Rev. B **22**, 3194.
Schlottmann, P., 1976, Phys. Rev. B **13**, 1.
Schmitt-Rink, S., K. Miyake, and C. M. Varma, 1986, Phys. Rev. Lett. **57**, 2575.
Schrieffer, J. R., 1964, *The Theory of Superconductivity* (Benjamin, New York).
Schuh, B., and E. Müller-Hartmann, 1978, Z. Phys. B **29**, 39.
Segre, G. P., N. Gedik, J. Orenstein, D. A. Bonn, R. Liang, and W. N. Hardy, 2002, Phys. Rev. Lett. **88**, 137001.
Senthil, T., and M. P. A. Fisher, 1999, Phys. Rev. B **60**, 6893.
Senthil, T., and M. P. A. Fisher, 2000, Phys. Rev. B **61**, 9690.
Senthil, T., M. P. A. Fisher, L. Balents, and C. Nayak, 1998, Phys. Rev. Lett. **81**, 4704.
Sheehy, D. E., I. Adagideli, P. M. Goldbart, and A. Yazdani, 2001, Phys. Rev. B **64**, 224518.
Shen, Z. X., and J. R. Schrieffer, 1997, Phys. Rev. Lett. **78**, 1991.
Shiba, H., 1968, Prog. Theor. Phys. **40**, 435.
Shiba, H., 1973, Prog. Theor. Phys. **50**, 50.
Shnirman, A., I. Adagideli, P. M. Goldbart, and A. Yazdani, 1999, Phys. Rev. B **63**, 7517.
Shytov, A. V., I. Vekhter, I. A. Gruzberg, and A. V. Balatsky, 2003, Phys. Rev. Lett. **90**, 147002.
Shytov, A. V., I. Vekhter, I. A. Gruzberg, and A. V. Balatsky, 2004, unpublished.
Sidorov, V. A., M. Nicklas, P. G. Pagliuso, J. L. Sarrao, Y. Bang, A. V. Balatsky, and J. D. Thompson, 2002, Phys. Rev. Lett. **89**, 157004.
Sigrist, M., and K. Ueda, 1991, Rev. Mod. Phys. **63**, 239.
Simon, M. E., and C. M. Varma, 1999, Phys. Rev. B **60**, 9744.
Skalski, S., O. Betbeder-Matibet, and P. R. Weiss, 1964, Phys. Rev. **136**, A1500.
Soda, T., T. Matsuura, and Y. Nagaoka, 1967, Prog. Theor. Phys. **38**, 551.
Spivak, B., and S. Kivelson, 1991, Phys. Rev. B **43**, 3740.
Sprunger, P. T., L. Petersen, E. W. Plummer, E. Lægsgaard, and F. Besenbacher, 1997, Science **275**, 1764.
Stamp, P. C. E., 1987, J. Magn. Magn. Mater. **63-64**, 429.
Stipe, B., M. Rezaei, and W. Ho, 1998, Science **280**, 1732.
Suderow, H., P. Martinez-Samper, N. Luchier, J. P. Brison, S. Vieira, and P. C. Canfield, 2001, Phys. Rev. B **64**, 020503.
Takegahara, K., Y. Shimizu, and O. Sakai, 1992, J. Phys. Soc. Jpn. **61**, 3443.
Takigawa, M., M. Ichioka, and K. Machida, 2003, Phys. Rev. Lett. **90**, 047001.
Tanaka, K., and F. Marsiglio, 2000, Phys. Rev. B **62**, 5345.
Tanuma, Y., Y. Tanaka, M. Ogata, and S. Kashiwaya, 1998, J. Phys. Soc. Jpn. **67**, 1118.
Timusk, T., 2003, e-print cond-mat/0303383.
Timusk, T., and B. Statt, 1999, Rep. Prog. Phys. **62**, 61.
Tinkham, M., 1996, *Introduction to Superconductivity*, 2nd ed. (McGraw-Hill, New York).
Tsai, S.-W., and P. J. Hirschfeld, 2002, Phys. Rev. Lett. **89**, 147004.
Tsuchiura, H., Y. Tanaka, M. Ogata, and S. Kashiwaya, 2000, Phys. Rev. Lett. **84**, 3165.
Tsuei, C. C., and J. R. Kirtley, 2000, Rev. Mod. Phys. **72**, 969.
Tsuneto, T., 1962, Prog. Theor. Phys. **28**, 857.
Tu, J. J., C. C. Homes, G. D. Gu, D. N. Basov, and M. Strongin, 2002, Phys. Rev. B **66**, 144514.
Turner, P. J., *et al.*, 2003, Phys. Rev. Lett. **90**, 237005.
Ueda, K., and M. Rice, 1985, in *Theory of Heavy Fermions and Valence Fluctuations*, edited by T. Kasuya and T. Saso (Springer-Verlag, Berlin).
Van Mieghem, P., 1992, Rev. Mod. Phys. **64**, 755.
Varma, C. M., 1999, Phys. Rev. Lett. **83**, 3538.
Vavilov, M. G., P. W. Brouwer, V. Ambegaokar, and C. W. J. Beenakker, 2001, Phys. Rev. Lett. **86**, 874.
Vekhter, I., A. V. Shytov, I. A. Gruzberg, and A. V. Balatsky, 2003, Physica B **329–333**, 1446.
Vekhter, I., and C. M. Varma, 2003, Phys. Rev. Lett. **90**, 237003.
Vershinin, M., S. Misra, S. Ono, Y. Abe, Y. Ando, and A. Yazdani, 2004, Science **303**, 1995.
Vishveshwara, S., T. Senthil, and M. P. A. Fisher, 2000, Phys. Rev. B **61**, 6966.
Vojta, M., 2001, Phys. Rev. Lett. **87**, 097202.
Vojta, M., and R. Bulla, 2001, Phys. Rev. B **65**, 014511.
Volovik, G. E., and L. P. Gor'kov, 1984, JETP Lett. **39**, 550.
Walter, H., W. Prusseit, R. Semerad, H. Kinder, W. Assmann, H. Huber, H. Burkhardt, D. Rainer, and J. A. Sauls, 1998, Phys. Rev. Lett. **80**, 3598.
Wang, Q., and C.-R. Hu, 2004, Phys. Rev. B **70**, 092505.
Wang, Q.-H., 2002, Phys. Rev. Lett. **88**, 057002.
Wang, Q.-H., and D.-H. Lee, 2003, Phys. Rev. B **67**, 020511.
Wang, Q.-H., and Z. D. Wang, 2004, Phys. Rev. B **69**, 092502.
Wiegmann, P. B., 1980, JETP Lett. **31**, 367.
Wilson, K. G., 1975, Rev. Mod. Phys. **47**, 773.
Withoff, D., and E. Fradkin, 1990, Phys. Rev. Lett. **64**, 1835.
Woolf, M. A., and F. Reif, 1965, Phys. Rev. **137**, A557.
Wu, C., T. Xiang, and Z.-B. Su, 2000, Phys. Rev. B **62**, 14427.
Xiang, T., Y. H. Su, C. Panagopoulos, Z. B. Su, and L. Yu, 2002, Phys. Rev. B **66**, 174504.
Xiang, T., and J. M. Wheatley, 1995, Phys. Rev. B **51**, 11721.
Yafet, Y., 1963, Solid State Phys. **14**, 1.
Yashenkin, A. G., W. A. Atkinson, I. V. Gornyi, P. J. Hirschfeld, and D. V. Khveshchenko, 2001, Phys. Rev. Lett. **86**, 5982.
Yazdani, A., C. M. Howald, C. P. Lutz, A. Kapitulnik, and D. M. Eigler, 1999, Phys. Rev. Lett. **83**, 176.

Yazdani, A., B. A. Jones, C. P. Lutz, M. F. Crommie, and D. M. Eigler, 1997, Science **275**, 1767.
Yoshioka, T., and Y. Ohashi, 1998, J. Phys. Soc. Jpn. **67**, 1332.
Yoshioka, T., and Y. Ohashi, 2000, J. Phys. Soc. Jpn. **69**, 1812.
Yu, L., 1965, Acta Phys. Sin. **21**, 75.
Zhang, D., and C. S. Ting, 2003, Phys. Rev. B **67**, 100506.
Zhang, D., and C. S. Ting, 2004, Phys. Rev. B **69**, 012501.
Zhang, G.-M., H. Hu, and L. Yu, 2001, Phys. Rev. Lett. **86**, 704.
Zhang, G.-M., H. Hu, and L. Yu, 2002, Phys. Rev. B **66**, 104511.
Zhu, J.-X., and A. Balatsky, 2002, Phys. Rev. B **65**, 132502.
Zhu, J.-X., A. V. Balatsky, T. P. Devereaux, Q. Si, J. Lee, K. McElroy, and J. C. Davis, 2005, e-print cond-mat/0507610.
Zhu, J.-X., W. Kim, C. S. Ting, and J. P. Carbotte, 2001, Phys. Rev. Lett. **87**, 197001.
Zhu, J.-X., T. K. Lee, C. R. Hu, and C. S. Ting, 2000, Phys. Rev. B **61**, 8667.
Zhu, J.-X., I. Martin, and A. R. Bishop, 2002, Phys. Rev. Lett. **89**, 067003.
Zhu, J.-X., K. McElroy, J. Lee, T. P. Devereaux, Q. Si, J. C. Davis, and A. V. Balatsky, 2005, e-print cond-mat/0507621.
Zhu, J.-X., D. N. Sheng, and C. S. Ting, 2000, Phys. Rev. Lett. **85**, 4944.
Zhu, J.-X., J. Sun, Q. Si, and A. V. Balatsky, 2004, Phys. Rev. Lett. **92**, 017002.
Zhu, J.-X., and C. S. Ting, 2001a, Phys. Rev. B **63**, 020506.
Zhu, J.-X., and C. S. Ting, 2001b, Phys. Rev. B **64**, 060501.
Zhu, J.-X., and C. S. Ting, 2001c, Phys. Rev. Lett. **87**, 147002.
Zhu, J.-X., C. S. Ting, and C. R. Hu, 2000, Phys. Rev. B **62**, 6027.
Zhu, L., W. A. Atkinson, and P. J. Hirschfeld, 2003, Phys. Rev. B **67**, 094508.
Zhu, L., W. A. Atkinson, and P. J. Hirschfeld, 2004, Phys. Rev. B **69**, 060503.
Zhu, L., P. J. Hirschfeld, and D. J. Scalapino, 2004, Phys. Rev. B **70**, 214503.
Ziegler, K., 1996, Phys. Rev. B **53**, 9653.
Ziegler, K., M. H. Hettler, and P. J. Hirschfeld, 1996, Phys. Rev. Lett. **77**, 3013.
Zittartz, J., A. Bringer, and E. Müller-Hartmann, 1972, Solid State Commun. **10**, 513.
Zittartz, J., and J. S. Langer, 1966, Phys. Rev. **148**, 741.
Zittartz, J., and E. Müller-Hartmann, 1970, Z. Phys. **232**, 11.